Supplementary File 1

Year-by-Year Analyses of Diabetes-Related ED Visits (Binary)

Contents

List of Figures

Part I: Overall Effect Analysis

The overall analysis evaluates how NO_2 or $PM_{2.5}$ exposure influences ED visits while accounting for temporal variations in temperature, relative humidity, precipitation, and wildfire impact for $PM_{2.5}$. Each patient serves as their control, with control periods defined as one to four weeks before the assessment. This design minimizes confounding by individual-level factors such as age, sex, and comorbidities, ensuring a precise evaluation of exposure-outcome relationships. By incorporating lag periods (0–3 days) into the model, the analysis captures both immediate and delayed effects of exposure. Acute effects may manifest within hours, while systemic or inflammatory responses may require additional time.

Diabetes population trend analysis

The increase in the diabetic population of Type 2 in California from around 500,000 in 2010 to nearly 1,000,000 in 2019 (Figure 1) can largely be attributed to healthcare expansion under the Affordable Care Act (ACA), which improved access to screening and diagnosis through Medi-Cal and subsidized insurance plans, leading to the identification of previously undiagnosed cases. Additionally, population growth and the aging of the "baby boomer" generation, individuals born between 1946 and 1964, who are at higher risk for Type 2 diabetes, might have contributed significantly to the rise. As this population aged, their vulnerability to air pollution-related health effects, such as those from NO_2 and $PM_{2.5}$ exposure, likely increased. Rising obesity rates, driven by sedentary lifestyles and poor dietary habits, further exacerbated the diabetes burden. Improved data collection and reporting during this period may have also played a role. The slight decline in 2019 suggests potential stabilization of obesity rates due to prevention efforts or variability in diagnosis rates.

NO_2 effect analysis

In 2010, NO_2 exposure was relatively low across Type 2 diabetic patients. The economic slowdown following the Great Recession (2007-2009) played a role in lowering pollution levels at and before 2010. This economic contraction likely resulted in a temporary dip in pollution levels, particularly in urban areas where transportation emissions are a major source of NO_2 and particulate matter. In addition, the wildfire activity in 2010 has been lower compared to other years. The relative calm in wildfire activity in 2010 likely prevented significant spikes in particulate pollution from that source. NO_2 exposure increased in 2011-2013, but after that, overall NO_2 concentrations and their SD continued to decline, which can be attributed to improvements in air quality driven by regulatory measures and cleaner technologies. Policies such as stricter vehicle emissions standards, industrial regulations, and adopting cleaner fuels have reduced overall emissions and a more uniform reduction in NO_2 levels, minimizing extreme pollution events that once contributed to higher variability. While the mean NO_2 concentrations and its SD continued to decline, the IQR of NO_2 exposure experienced an upward trend after 2016. A reduced SD alongside an increased IQR indicates that most data points became more

tightly clustered around the mean, but the spread within the middle portion of the data grew wider. This suggests a more stretched-out distribution of NO_2 levels, where values in the central range became more variable even as extreme outliers became less frequent.

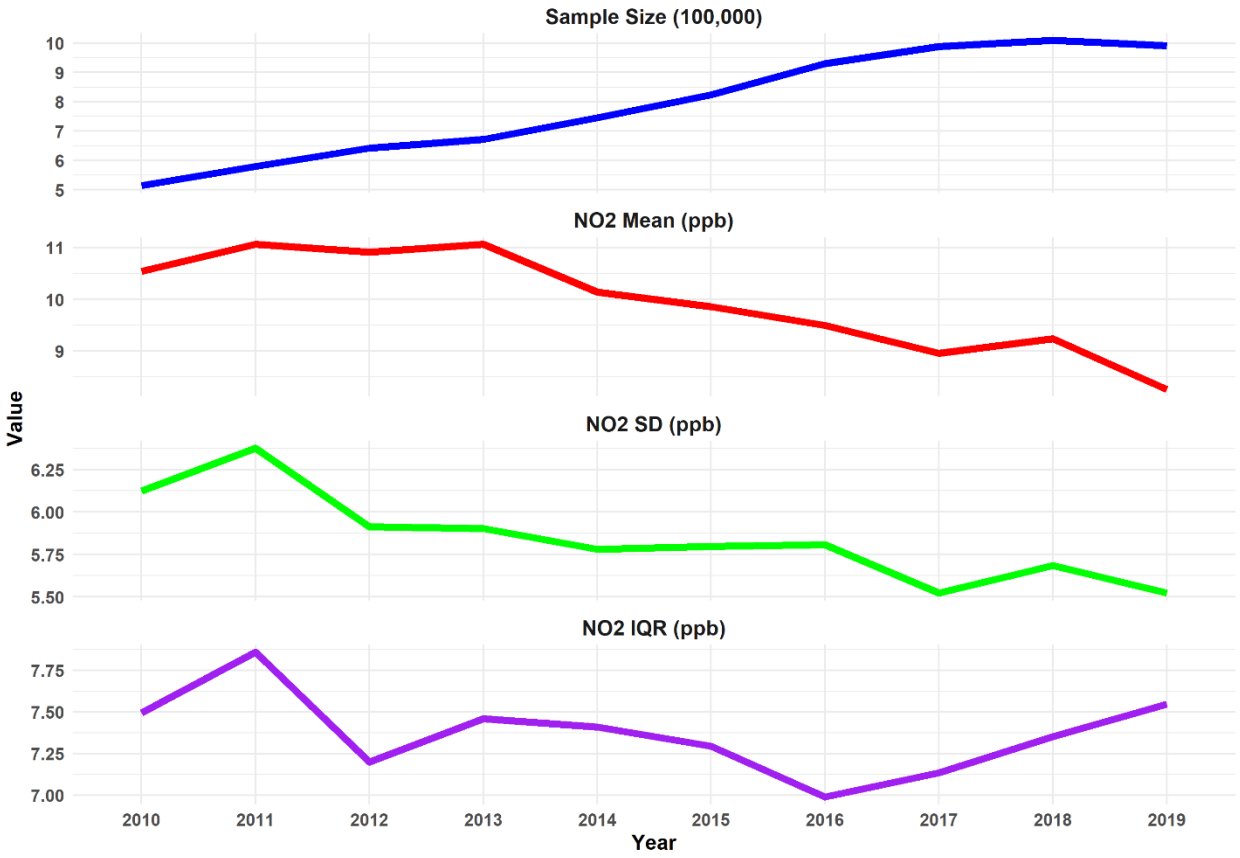

Figure 1. The temporal trend of the population in California diagnosed with diabetes and NO_2 exposure from 2010 to 2019.

The CR functions between NO_2 exposure and ED visits show a downward trend in effect estimates from 2010 to 2014, followed by an upward trend from 2014 to 2019 (Figure 2). This pattern can be linked to several critical factors. First, the Affordable Care Act (ACA), signed into law in 2010 and fully implemented by 2014, significantly expanded healthcare access, mainly through Medicaid for low-income populations and Medicare Part B for individuals over 65 (Figure 5). The increased access to healthcare likely improved disease management and preventative care, which reduced reliance on EDs for acute conditions. As a result, the impact of environmental exposures like NO_2 on ED visits declined from 2010 to 2014. After 2014, the stretched-out distribution of NO_2 levels could explain the renewed increase in its health impact on ED visits despite overall declines in concentration.

Regarding the lagged effect, the impact of NO_2 exposure remained largely consistent over the 0–2 day period. By day 3, the effect showed a slight decrease, suggesting a more transient nature of the exposure's impact or a diminishing short-term influence on ED visits. Regarding the control comparisons, the 1-to-1 control uses one week before the event as the reference, while the 4-to-1

control uses four weeks before. When the control period is further from the event day, we observed a greater effect of NO_2. This could be due to exposure levels in the control period becoming more diluted over time, making the event day exposure appear more elevated and thus resulting in a higher estimated effect. This observation emphasizes the sensitivity of the analysis to the temporal choice of control periods and highlights the need to account for variability in NO_2 exposure levels when interpreting these findings.

Overall, the impact of NO_2 on ED visits is statistically significant across the years 2010–2019, considering 0–3 days of lags and using one-week to four-weeks before the event as controls. This demonstrates the robustness of the association between NO_2 exposure and adverse health outcomes, regardless of the specific temporal framework or control strategy applied. The consistent significance highlights that short-term NO_2 exposure remains a critical driver of diabetic patients' ED visits, reinforcing the importance of monitoring and mitigating air pollution. The persistence of this association over nearly a decade further emphasizes the need for targeted interventions to address NO_2 exposure, particularly in vulnerable populations and high-risk areas.

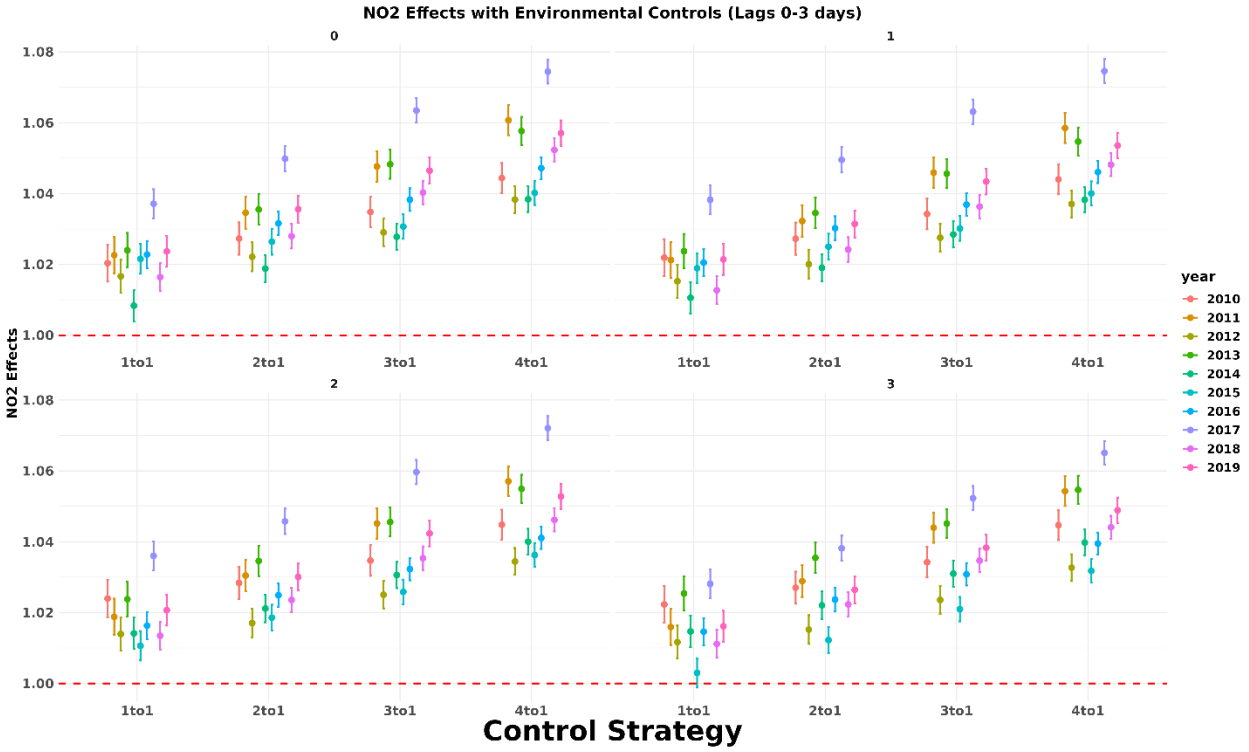

Figure 2. The association between NO_2 exposure and ED visits over 0–3 lag days across four control categories, modeled annually from 2010 to 2019.

$PM_{2.5}$ effect analysis

Similar to NO_2 exposure, $PM_{2.5}$ exposure was relatively low across Type 2 diabetic patients in 2010 (Figure 3). This could be attributed to economic slowdown following the Great Recession and lower wildfire activity compared to other years. After 2011, mean $PM_{2.5}$ concentrations

steadily declined, reflecting significant improvements in air quality driven by stricter environmental regulations and cleaner technologies. Policies such as enhanced vehicle emissions standards, industrial pollution controls, and adopting cleaner fuels played a pivotal role. The SD of $PM_{2.5}$ concentrations also decreased, indicating fewer extreme pollution events and more uniform improvements across regions. However, the IQR of $PM_{2.5}$ exposure began increasing after 2016, suggesting a growing variability in mid-range pollution levels. While extreme outliers in $PM_{2.5}$ exposure diminished, this widening spread within the central range may result from regional disparities in pollution control efforts or localized sources of $PM_{2.5}$.

The declining mean $PM_{2.5}$ levels and SD highlight the success of air quality interventions. However, in 2018, $PM_{2.5}$ levels spiked, largely due to the unprecedented wildfire activity that year. Major fires, including the Camp Fire in Northern California and the Woolsey Fire in Southern California, released vast amounts of fine particulate matter into the atmosphere, significantly impacting air quality across the state. These extreme wildfire events underscore the growing influence of climate change on air pollution trends, even as regulatory measures continue to reduce emissions from traditional sources. Further, the increasing IQR emphasizes the need for targeted, localized actions to address variability in mid-range exposures.

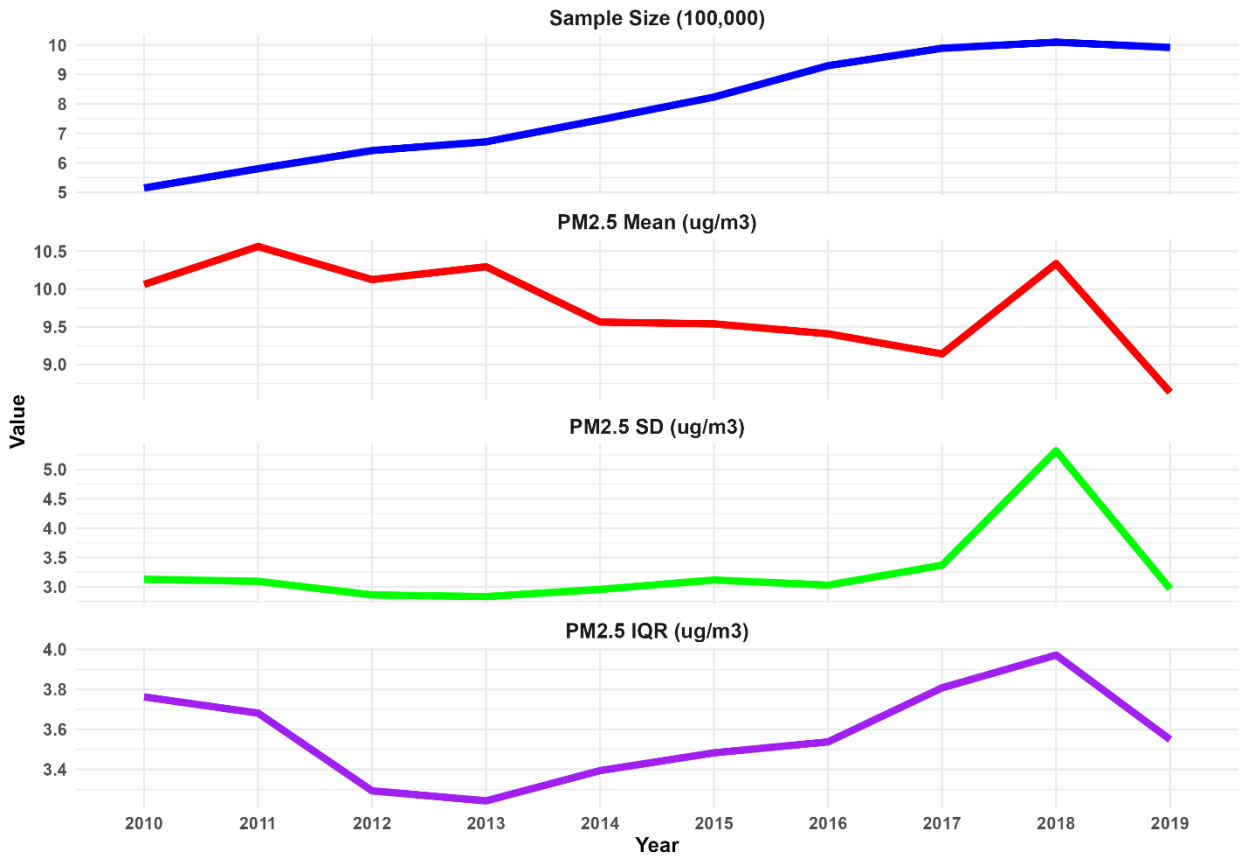

Figure 3. The temporal trend of the population in California diagnosed with diabetes and $PM_{2.5}$ exposure from 2010 to 2019.

The relationship between $PM_{2.5}$ exposure and ED visits demonstrates a notable pattern: a negative association in 2010, followed by positive but declining effect estimates from 2011 to 2014, and then a subsequent increase from 2014 to 2019 (Figure 4). This trend can be attributed to several key factors. The relatively low $PM_{2.5}$ level contributed to the negative impact in 2010. The full implementation of the Affordable Care Act (ACA) by 2014 significantly expanded healthcare access, primarily through Medicaid for low-income individuals and Medicare Part B for older adults (Figure 7). Improved access to healthcare likely facilitated better disease management and preventative care, reducing dependence on ED visits for acute conditions. As a result, the health impact of environmental exposures such as $PM_{2.5}$ diminished during 2011–2014. Conversely, the upward trend observed after 2014 may reflect shifts in exposure patterns and increased population vulnerability, with significant increase in middle level $PM_{2.5}$ exposures despite overall declines.

The growing influence of $PM_{2.5}$ on ED visits after 2014 may also stem from demographic changes, particularly the aging of the "baby boomer" generation. As older adults became more integrated into the healthcare system, their heightened sensitivity to air pollutants like $PM_{2.5}$ likely contributed to increased health impacts. Interestingly, despite the increase in $PM_{2.5}$ levels

in 2018, the impact on ED visits was relatively low for that year. This could be attributed to several factors. First, wildfire-related $PM_{2.5}$ episodes tend to be short-lived but intense, whereas chronic exposure to elevated air pollution from traffic and industrial sources has been more consistently linked to long-term health effects and increased healthcare utilization. Second, public awareness and protective measures, such as air quality alerts, widespread use of N95 masks, and recommendations to stay indoors during wildfires, may have mitigated acute health impacts. Additionally, the affected populations may have adapted by avoiding outdoor activities or using air filtration systems, reducing direct exposure. There may also be a lag in health effects, where the full impact of exposure is not immediately reflected in ED visit data. Finally, the control of wildfire-related $PM_{2.5}$ in the modeling process may have inadvertently over-controlled for its impact on ED visits, potentially underestimating the association between $PM_{2.5}$ exposure and health outcomes.

Regarding lagged effects, the influence of $PM_{2.5}$ exposure on ED visits remained relatively stable within the 0–2 day window, with a slight decline in effect by day 3. This suggests that the impact of $PM_{2.5}$ exposure is primarily short-term, with diminishing influence over time. Additionally, comparisons of control periods—using the 1-to-1 method (one week before the event) and the 4-to-1 method (four weeks before)—revealed an interesting trend: a stronger effect though less pronounced than NO_2 was observed when the control period was further from the event day. This could result from lower exposure levels during the control period, amplifying the relative impact of event-day exposure. These findings emphasize the importance of carefully selecting temporal control strategies to ensure accurate interpretation of results.

Overall, the impact of $PM_{2.5}$ on ED visits remains largely statistically significant from 2010 to 2019, regardless of lag periods (0–3 days) or control strategies (1-to-1 or 4-to-1). This consistent association underscores the critical role of short-term $PM_{2.5}$ exposure in driving diabetic patients' ED visits. The persistence of these trends over nearly a decade highlights the urgent need for targeted policies and interventions to reduce $PM_{2.5}$ exposure, particularly among vulnerable populations and in high-risk regions.

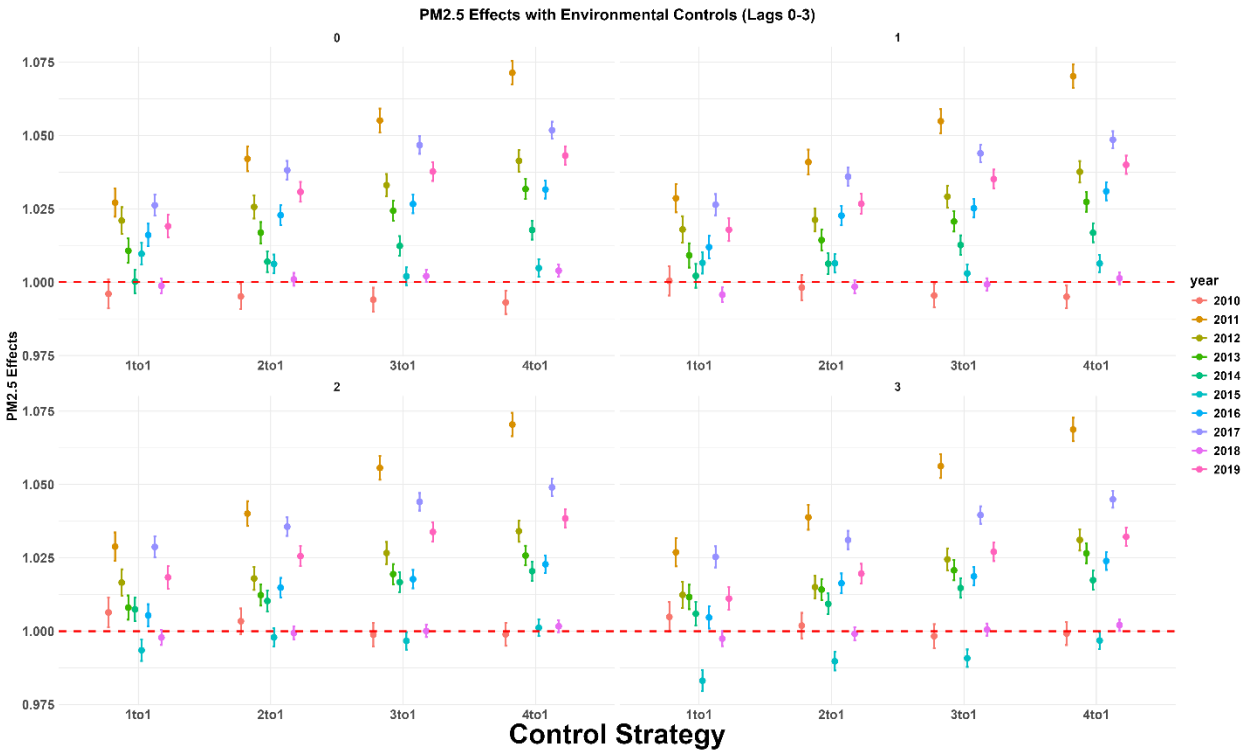

Figure 4.The association between $PM_{2.5}$ exposure and ED visits over 0–3 lag days across four control categories, modeled annually from 2010 to 2019.

Part II: Stratification Effect Analysis

The stratification analysis assesses how NO_2 or $PM_{2.5}$ exposure impacts ED visits across various subgroups while accounting for temperature, relative humidity, precipitation, and wildfire impact for $PM_{2.5}$. Similar to the overall analysis, each patient serves as their control, with control periods defined as one to four weeks before the assessment. The inclusion of lag periods (0–3 days) ensures both immediate and delayed effects are evaluated. The stratification analysis includes race-ethnicity, gender, age groups, primary language spoken, health insurance payer category, and study regions.

Health insurance payer type analysis

From 2010 to 2012, the percentage of individuals categorized by payer type remained relatively stable, with minimal changes observed across most groups (Figure 5). For example, Health Maintenance Organization (HMO) participants consistently accounted for about 21% of the population, while Medicaid (Medi-Cal) and Medicare Part B remained at around 27% and 14%, respectively. However, significant shifts occurred starting in 2013, with a noticeable increase in Medicaid and Medicare Part B participation. By 2019, Medicaid coverage rose to 32.9%, and Medicare Part B reached 24.1%. This rise is largely attributed to healthcare reforms under the ACA, which expanded Medicaid for low-income populations and Medicare Part B for seniors. In contrast, the percentage of self-pay individuals decreased dramatically during this

period, from 15.9% in 2010 to just 3.7% by 2019. This shift likely reflects a change from a largely uninsured population before 2014 to a group of wealthier individuals who may have maintained or transitioned to self-pay after 2015, as more individuals gained insurance coverage through Medicaid, Medicare, and other means.

Regarding NO_2 exposure, the mean levels for most payer categories showed a general decrease over the years. For instance, the Health Maintenance Organization (HMO) mean NO_2 level dropped from 10.8 ppb in 2010 to 8.7 ppb in 2019. Similarly, Medicaid saw its NO_2 mean exposure drop from 10.5 ppb in 2010 to 8.5 ppb in 2019, while Medicare Part B's NO_2 mean decreased from 10.2 ppb in 2010 to 7.4 ppb in 2019. We found that Medicare Part B patients had lower NO_2 exposure compared to other payer categories. Medicare Part B typically covers individuals aged 65 and older, and we believe the elderly population tends to live in suburban or rural areas where air pollution levels, including NO_2, may be lower compared to urban areas.

Despite the decrease in overall mean NO_2 values from 2010 to 2019, the IQR of NO_2 levels began to increase after 2016, suggesting a rise in variability or fluctuation of exposure in more recent years. This could indicate that while overall NO_2 levels decreased, some areas may have experienced more sporadic air quality issues, contributing to higher IQRs.

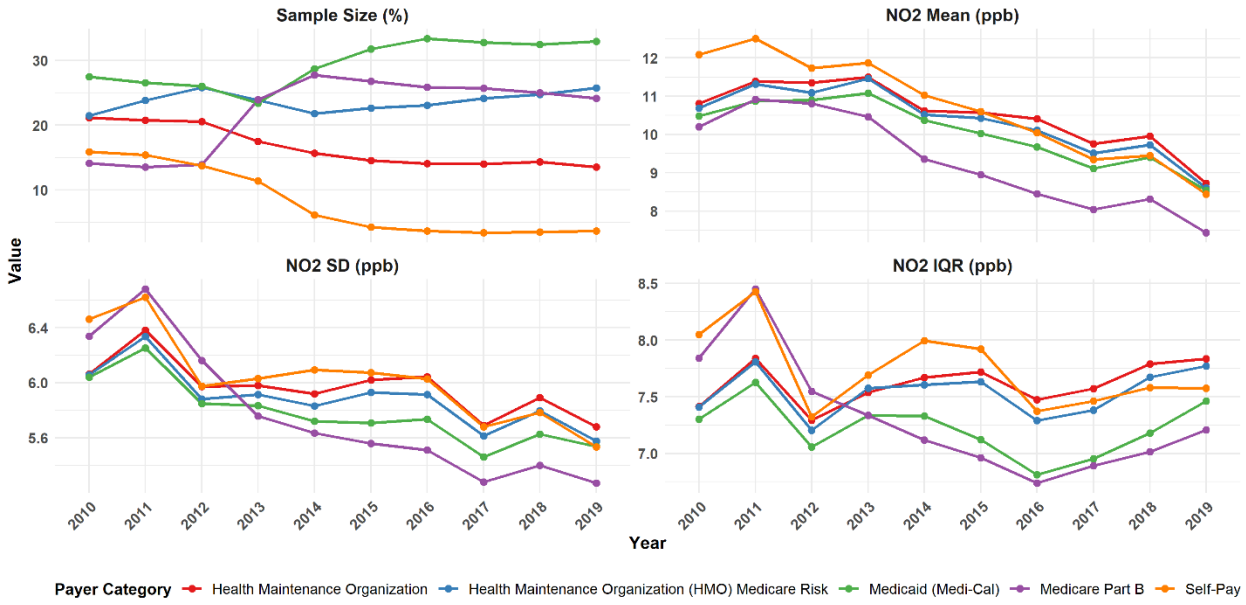

Figure 5. The temporal trend of the population, categorized by insurance coverage, in California diagnosed with diabetes and NO_2 exposure from 2010 to 2019.

For C-R functions, the self-pay category demonstrates the highest variability over time, particularly in the later years, from 2016 to 2019. Its consistent deviation from the baseline across all lag durations underscores its significant sensitivity and influence compared to other categories. In contrast, Medicaid exhibits the least variability, remaining consistently close to the

baseline throughout the years (Figure 6). The characteristics of self-payers may explain this disparity during this period, as they were predominantly uninsured individuals who were more vulnerable to the health effects of air pollution, such as exposure to NO_2.

Starting in 2012, the impact of NO_2 exposure on ED visits among self-payers declined, reaching its lowest point in 2015. This likely reflects a shift in the self-payer population, transitioning from primarily uninsured individuals to wealthier patients with better access to healthcare, who may have been less susceptible to the effects of NO_2 exposure. However, after 2015, the self-payer category experienced a notable rise in the impact of NO_2 exposure on ED visits. This category consistently exhibits the highest impact after 2015. This increase could be linked to changes in the self-payer population's increase in air pollution susceptibility, including individuals with higher health risks driven by aging, chronic conditions, lifestyle behaviors, or socioeconomic vulnerabilities that amplify sensitivity to pollution. The wider confidence intervals observed for self-payers suggest smaller sample sizes than other payer categories.

Regarding lag times, the effect of NO_2 exposure within each payer category was minimal, with a slight decrease in impact as the lag period extended from zero to 3 days, particularly from 2016-2019. When considering control periods, the smallest effect was observed when the control period was closest to the event. Conversely, the impact of NO_2 exposure increased as the control period extended from one to four weeks before the event (Figures S1, S2, S3).

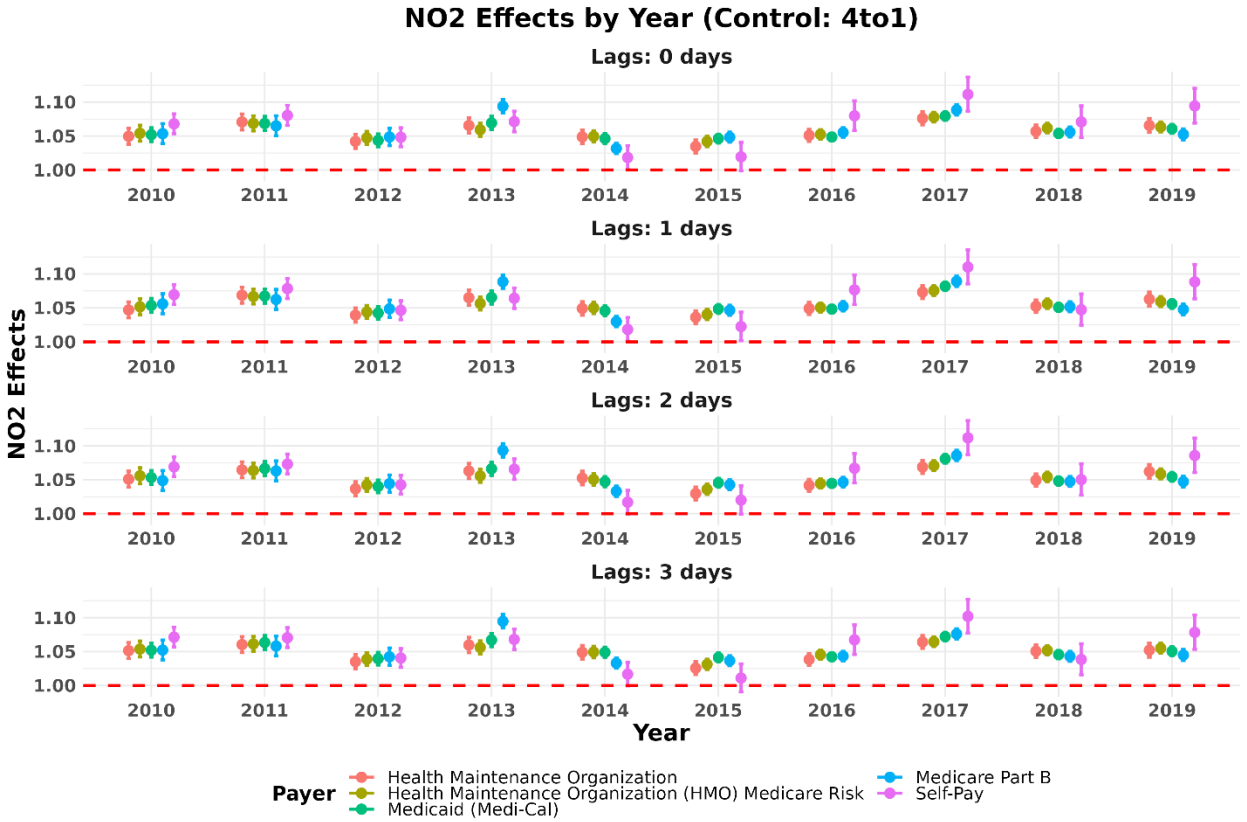

Figure 6. The associations between NO_2 exposure and ED visits for diabetic patients across different health insurance payer categories in California from 2010 to 2019.

On $PM_{2.5}$ exposure (Figure 7), mean levels declined across all payer categories over the study period. For instance, the mean $PM_{2.5}$ exposure for HMO participants decreased from 9.88 μg/m³ in 2010 to 8.5 μg/m³ in 2019. Similarly, mean levels for Medicaid and Medicare Part B beneficiaries fell from 10.27 μg/m³ and 8.86 μg/m³ in 2010 to 9.99 μg/m³ and 8.50 μg/m³, respectively, in 2019. Despite these reductions, the IQR of $PM_{2.5}$ exposure began to expand after 2012, indicating increased variability in exposure levels. This trend suggests that overall $PM_{2.5}$ concentrations have improved, but certain areas may still have faced localized air quality challenges, contributing to the broader IQR. This is especially true for Medicare Part B beneficiaries, who tend to live in suburban areas with less traffic. They had lower mean NO_2 levels as well as lower NO_2 variability (SD and IQR). $PM_{2.5}$, however, has both local and regional sources, including wildfires, long-range transport, and secondary formation. While suburban and rural areas may have lower direct emissions, they can still experience high variability due to episodic pollution events like wildfires, dust storms, or regional transport of $PM_{2.5}$. Consistent with the overall unstratified $PM_{2.5}$ exposure analysis, all payer categories experienced the highest $PM_{2.5}$ exposure in 2018.

For C-R functions, $PM_{2.5}$ exposure was negatively or non-significantly associated with ED visits across the payer categories in 2010. Like the unstratified analysis, this could be due to the lower level of $PM_{2.5}$ exposure. In 2011 and 2012, $PM_{2.5}$ exposure was significantly associated with ED visits across all payer categories, with self-payers experiencing the most pronounced effects (Figure 8). This heightened sensitivity among self-payers likely reflects the vulnerabilities of a largely uninsured population during this period. Starting from 2013, however, the impact of $PM_{2.5}$ exposure on ED visits for self-payers began to decline, reaching its lowest point in 2015. This decline coincided with a demographic shift in the self-payer population toward individuals with greater financial resources and improved access to healthcare, reducing their susceptibility to $PM_{2.5}$-related health effects. After 2015, the effect of $PM_{2.5}$ exposure on self-payers began to rise again, possibly due to an increased representation of individuals with higher health risks in this group. These could include aging populations, those with chronic conditions, or other vulnerable groups more sensitive to air pollution. The wider confidence intervals observed for self-payers suggest smaller sample sizes than other payer categories, contributing to greater uncertainty in the estimates. Among all categories, self-payers consistently exhibited the largest deviations from the baseline, particularly in 2016 and 2017. This category also displayed prominent fluctuations across all lag durations (0, 1, 2, and 3 days), with values exceeding 1.05 in several instances.

Similar to the unstratified analysis, the stratified analysis showed that despite the highest $PM_{2.5}$ exposure in 2018, its impact on ED visits remained relatively low across all payer categories.

The reasoning behind the overall unstratified analysis applies consistently to each payer category. Regarding lag times, the effect of $PM_{2.5}$ exposure across payer categories remained consistent over the 0–3 day period, with lagged effect being slightly smaller on the third day.

On control periods, the smallest effect was observed when the control was closest to the event. As the control period extended from one to four weeks before the event, the observed impact of $PM_{2.5}$ exposure increased (Figures S4, S5, S6). This likely reflects the dilution of exposure levels during the control period, making event-day exposure appear more pronounced. Overall, the significant association between $PM_{2.5}$ exposure and ED visits across payer categories underscores the pervasive vulnerability to $PM_{2.5}$ exposure. These findings highlight the need for targeted interventions to reduce exposure, particularly among high-risk populations, and to mitigate the broader public health impacts of air pollution.

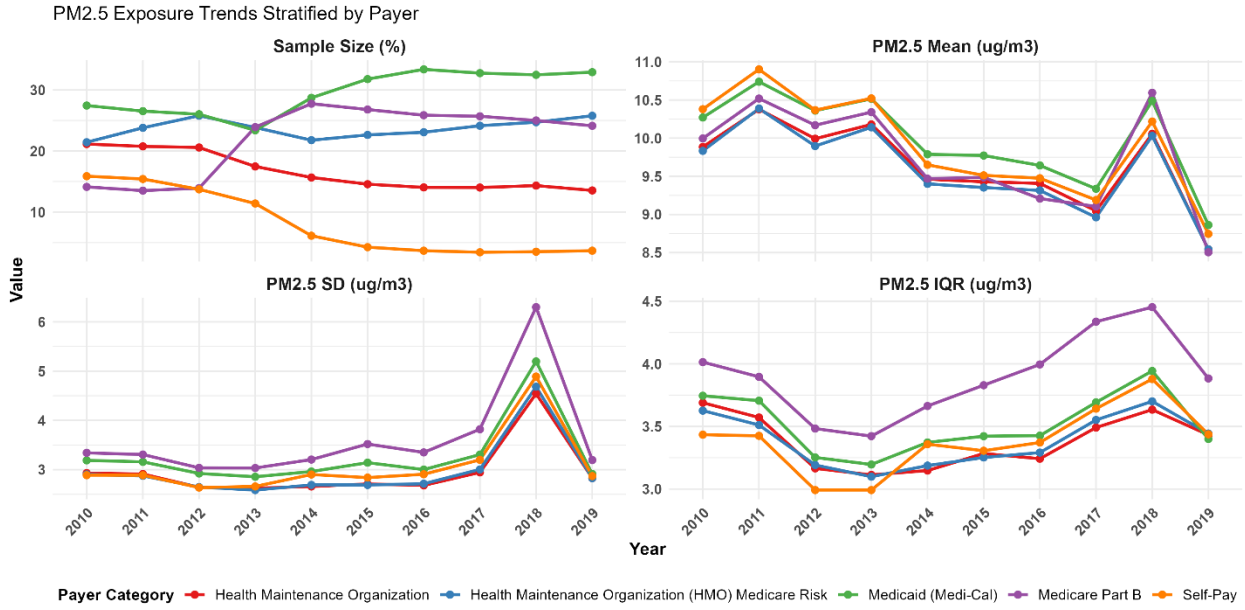

Figure 7. The temporal trend of the population, categorized by insurance coverage in California diagnosed with diabetes and $PM_{2.5}$ exposure from 2010 to 2019.

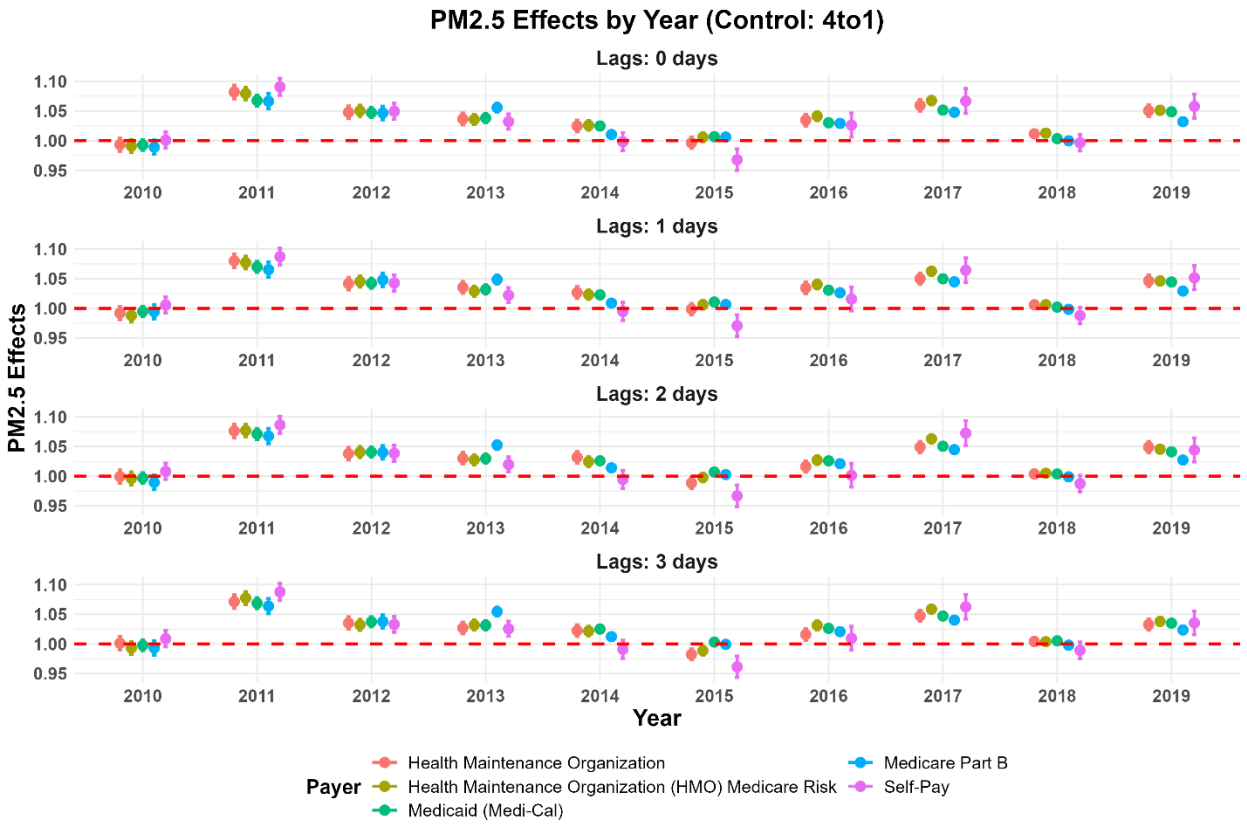

Figure 8.The associations between $PM_{2.5}$ exposure and ED visits for diabetic patients across different health insurance payer categories in California from 2010 to 2019.

Region analysis

From 2010 to 2019, California's regional distribution of Type 2 diabetic patients shifted gradually across the three main regions: the SF Bay Area, Southern California (SoCal), and the Central Valley (Figure 9). The SF Bay Area's population share gradually decreased from 25% to 16%, while SoCal experienced a steady increase from 60% in 2010 to 65% in 2019. In contrast, the Central Valley's representation gradually declined from 20% to 18.2%. These changes potentially reflected demographic shifts, migration patterns, or regional population growth.

Regarding NO_2 exposure, all regions experienced a reduction in mean levels over the study period. For example, the SF Bay Area declined from 8.12 ppb in 2010 to 5.90 ppb in 2019, while SoCal's mean exposure dropped from 13.49 ppb to 9.78 ppb during the same period. Similarly, the Central Valley observed a decrease from 7.75 ppb in 2010 to 6.45 ppb in 2019. Despite these overall reductions, the SDs and IQRs of NO_2 remained consistently flat across the period. This suggests that while NO_2 concentrations have decreased uniformly across all regions, the relative variability in exposure has not changed significantly. One possible explanation is that traffic and industrial sources continue to dominate NO2 emissions, meaning that areas with historically high NO_2 levels (such as major highways and industrial corridors) may still experience similar

fluctuations over time. Additionally, while statewide policies have contributed to an overall decline, localized sources of pollution may still create persistent spatial variability, keeping the SDs and IQRs stable over time. Overall, SoCal had the greatest mean, SD and IQR NO_2 exposure levels, followed by SF Bay and Central Valley.

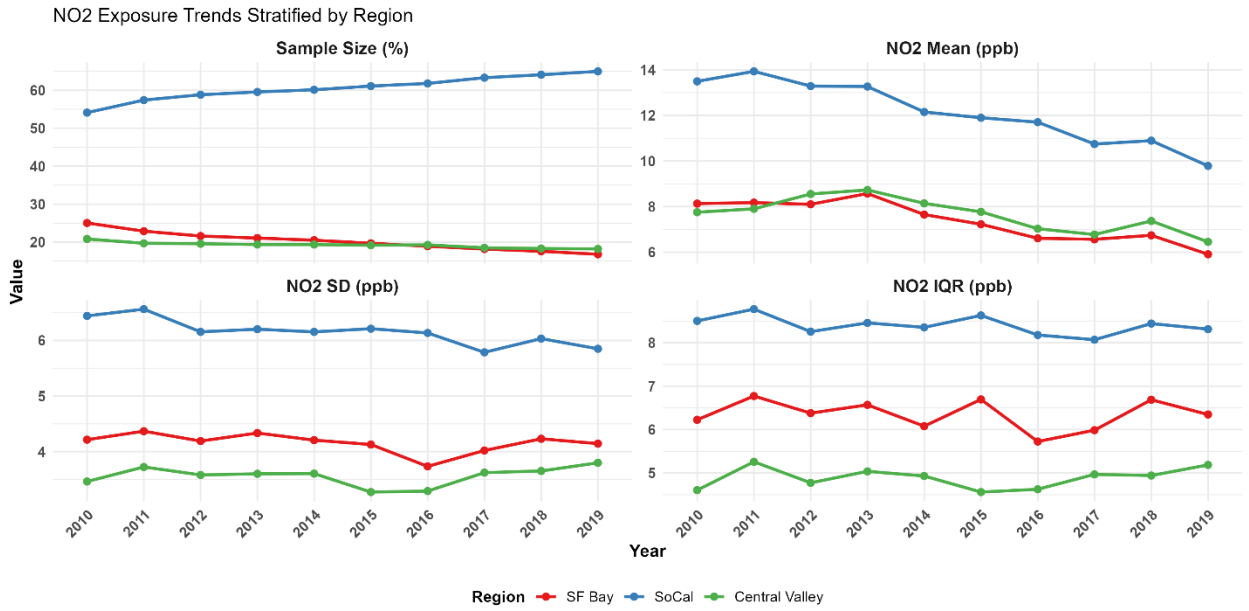

Figure 9. The temporal trend of the population, categorized by region, in California diagnosed with diabetes and NO_2 exposure from 2010 to 2019.

On NO_2 impact on ED visits, the Central Valley exhibits the most significant changes across multiple years, with some highs approaching 1.2 and lows being in verse relationship (Figure 10). Specifically, the effect increased from 2010 to 2011, reaching highs nearing 1.2. This might be due to the high sensitivity of diabetic patients in this region, which has a large proportion of seasonal workers, predominantly Mexican immigrants with low income and low educational attainment but high diabetic prevalence. Following 2012, the influence of NO_2 exposure on ED visits in the Central Valley began to decline, reaching its lowest levels around 2014. This period coincided with a significant increase in ACA enrollment, particularly among farm workers, a population historically characterized by limited healthcare access. With expanded healthcare coverage, many individuals in this group likely experienced improved disease management and greater access to preventative care, reducing their reliance on emergency departments for acute conditions. As a result, the overall impact of environmental exposures like NO_2 on ED visits diminished during this time, despite continued NO_2 emissions. However, after 2014, the impact of NO_2 exposure on ED visits began to rise again, even as NO_2 concentrations continued to

decline. This renewed increase in health impact suggests that changes in population susceptibility played a significant role such as aging of the baby boomers discussed above.

The effect started to decline in 2018 and 2019, likely due to continued improvements in air quality regulations, further reductions in NO_2 emissions from transportation and industry, and increased public awareness of air pollution-related health risks. Additionally, adaptation measures, such as increased use of air filtration systems, better access to preventive healthcare, and behavioral changes (e.g., staying indoors on high-pollution days), may have contributed to reducing the health impact of NO_2 exposure in the Central Valley.

Compared to the Central Valley, the SF Bay Area exhibited similar trends but with a much less pronounced effect, likely due to differences in population demographics, healthcare access, and baseline air pollution levels. The region's higher socioeconomic status and better access to healthcare may have contributed to a lower overall sensitivity to NO_2 exposure, resulting in a more stable impact on ED visits.

In contrast, the impact in the SoCal region remained even smaller, with effects largely unchanged throughout the years. This stability could be attributed to the consistently high population density and long-term exposure to NO_2, which may have led to a more adapted population with lower short-term sensitivity to pollution spikes. Regarding lag times, the effects of NO_2 exposure remained consistent across regions for a 0–2 day period, with a slight decrease observed by day 3, suggesting the transient nature of short-term exposure impacts. On control strategies, the smallest effects were noted when the control period was closest to the event, while more substantial impacts emerged as the control period extended from one to four weeks (Figures S7, S8, S9). This pattern underscores the importance of carefully selecting temporal reference periods to accurately estimate the health impacts of NO_2 exposure in epidemiological studies.

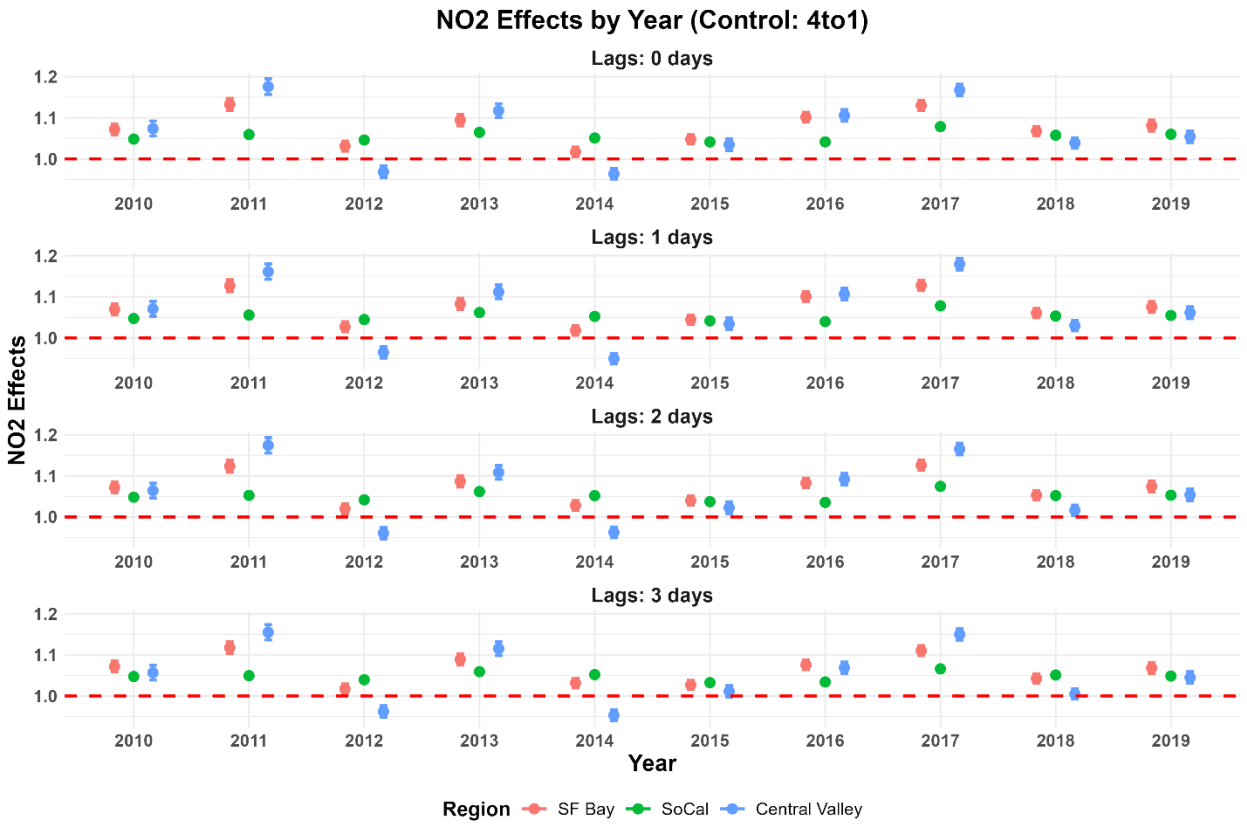

Figure 10. The associations between NO_2 exposure and ED visits for diabetic patients across regions in California from 2010 to 2019.

Regarding $PM_{2.5}$ exposure (Figure 11), all regions experienced a decrease, though smaller than those in NO_2, in mean levels over the study period. For instance, the Central Valley reduced average $PM_{2.5}$ exposure from 11.14 µg/m³ in 2010 to 9.88 µg/m³ in 2019. Similarly, the SF Bay Area's mean $PM_{2.5}$ levels declined from 8.74 µg/m³ to 7.09 µg/m³, while SoCal experienced a drop from 10.51 µg/m³ to 8.80 µg/m³ over the same timeframe. The SD and IQR of $PM_{2.5}$; however, remained flat before 2016. Despite the overall decline in mean $PM_{2.5}$ concentrations, levels rose significantly in 2018, accompanied by increases in both the SD and IQR. As previously discussed, this spike in $PM_{2.5}$ and its associated variability was likely driven by the surge in wildfire activity during 2018. The widespread and severe wildfires that year led to extreme air pollution events, causing sharp fluctuations in $PM_{2.5}$ levels across all three regions and contributing to the observed increase in SD and IQR.

On C-R functions, the effect of $PM_{2.5}$ on ED visits (Figure 12) followed a similar pattern to that of NO_2 across the three regions, though the magnitude of the effects appeared smaller. In most cases, $PM_{2.5}$ exposure was associated with an increase in ED visits over the years, with the positive impact in SoCal being consistent across the entire period. Further, SoCal exhibited the highest impact starting in 2016, suggesting a possible shift in population susceptibility or increase in wildfire pollution exposure patterns.

Regarding lag times, the effects of $PM_{2.5}$ exposure across regions remained relatively stable, with only a slight decrease observed as the lag extended from zero to three days. The smallest effects were noted when the control period was closest to the event. On control period, larger impacts were observed as the control period extended from one to four weeks prior (Figures S10, S11, S12). The Central Valley's behavior underscores its significant sensitivity compared to other regions, highlighting its unique challenges in managing air pollution impacts. These findings emphasize the importance of carefully selecting temporal frameworks to ensure accurate estimates of exposure effects.

Overall, the association between $PM_{2.5}$ exposure and ED visits remained significant across all regions from 2010 to 2019, regardless of lag times or control periods. These results underline the critical role of $PM_{2.5}$ in driving adverse health outcomes and emphasize the urgent need for sustained air quality improvements and healthcare interventions, particularly in vulnerable areas like the Central Valley.

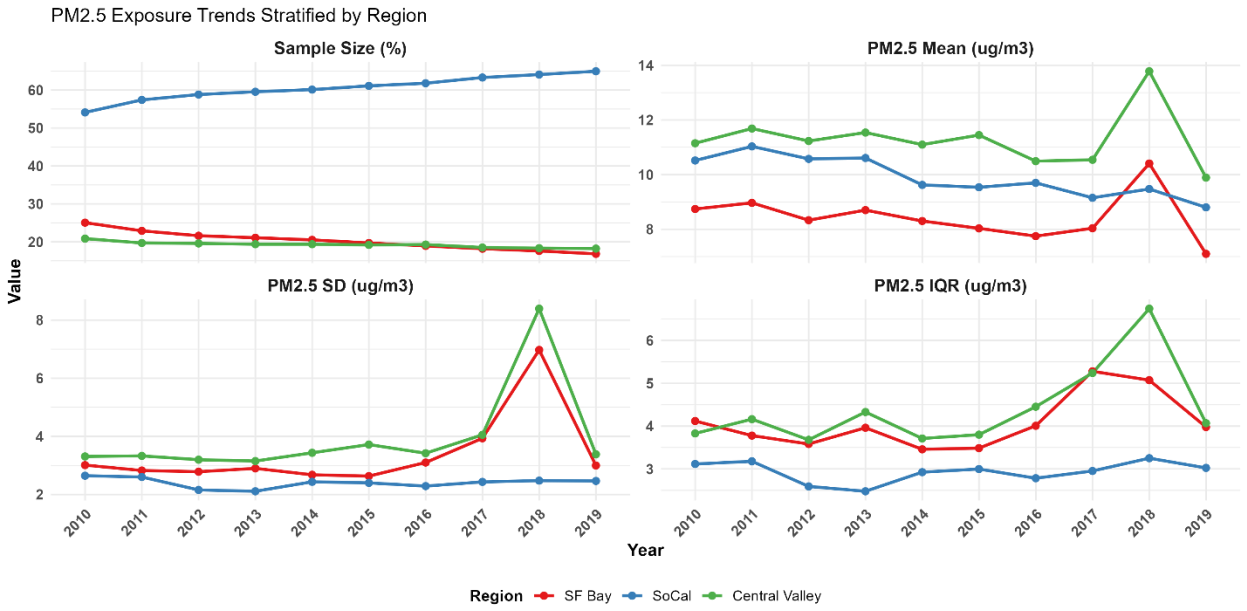

Figure 11. The temporal trend of the population, categorized by region, in California diagnosed with diabetes and $PM_{2.5}$ exposure from 2010 to 2019.

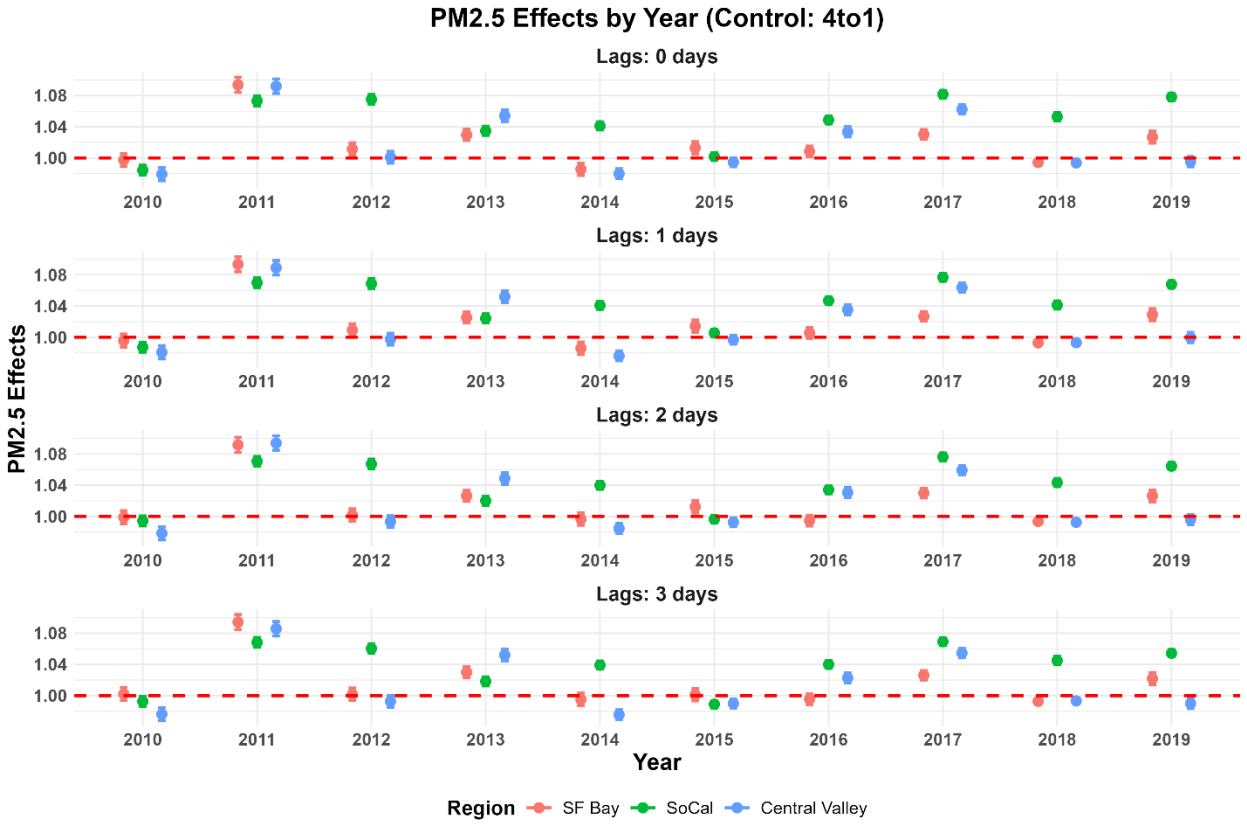

Figure 12. The associations between $PM_{2.5}$ exposure and ED visits for diabetic patients across regions in California from 2010 to 2019.

Language analysis

In 2010, the English, Other, and Spanish race-ethnicity categories in diabetic patients accounted for 40%, 50%, and 10% of the population, respectively; however, starting from 2011, their compositions shifted to 80%, 2%, and 18%. This dramatic change is largely attributable to improvements in data collection and classification. In earlier years, a significant portion of race-ethnicity information was missing, and patients with incomplete demographic data were categorized as "Other." As data reporting improved over time, many of these previously unclassified patients were reassigned to more accurate racial-ethnic categories, leading to a sharp decline in the "Other" category. From 2011 and 2019, the distribution of individuals categorized by primary language remained relatively stable, with slight decrease for English language speakers but slight increases for Hispanics and Other categories (Figure 13). From 2011 to 2019, the distribution of individuals categorized by primary language remained relatively stable, with only minor shifts observed over time. The proportion of English-language speakers experienced a slight decrease, suggesting probably a gradual diversification of the population. In contrast, the Hispanic and Other language categories saw slight increases, which may reflect demographic changes, such as an increase in Spanish-speaking immigrant populations. These trends may also be influenced by broader societal and policy changes, including healthcare access expansions, shifts in migration patterns, and efforts to provide linguistically inclusive healthcare services. The relatively stable overall distribution indicates that while minor fluctuations occurred, no dramatic shifts in language composition took place during this period.

On NO_2 exposure, average concentrations declined across all language groups throughout the study period. For example, English speakers experienced a reduction in mean NO_2 levels from 10.8 ppb in 2010 to 8.02 ppb in 2019, while Spanish speakers saw a similar decrease from 12.59 ppb to 9.11 ppb during the same timeframe. Despite these reductions, the IQR of NO_2 exposure widened after 2016, suggesting increased variability in exposure levels. This trend indicates that while overall air quality improved, certain areas experienced greater fluctuations in NO_2 levels, potentially linked to localized environmental or urban factors.

On C-R functions, the Spanish-speaking population exhibited the most significant changes, particularly in 2010, when its odds ratio exceeded 1.2, marking the largest deviation observed across all language categories and years. While the English-speaking group also experienced a notable impact from NO_2 exposure (odds ratio = 1.18), the Other language category showed a negative effect (odds ratio = 0.93) (Figure 14). Starting in 2011, this trend shifted significantly. The positive effects observed for Spanish- and English-speaking individuals declined substantially, while the negative effect seen in the Other language category reversed, becoming positive. This shift can largely be attributed to the reclassification of many individuals previously categorized under the Other language group into the English- and Spanish-speaking groups. As data collection and classification improved, more accurate language categorization likely led to a

redistribution of individuals, altering the observed NO_2-health effect associations within each language category.

Between 2012 and 2015, the effect of NO_2 exposure on ED visits among non-English speakers declined, likely due to improved healthcare access and the introduction of preventive measures during this period. However, beginning in 2016, the impact increased again, potentially driven by factors such as an aging population, persistent socioeconomic vulnerabilities, or unresolved disparities in healthcare access. Regarding lag effects, NO_2 exposure had the most pronounced influence within the 0- to 2-day lag periods, with effects slightly diminishing by day 3. This pattern suggests that the health impacts of short-term NO_2 exposure are immediate but transient. Additionally, the impact of NO_2 exposure appeared more pronounced when the control period extended further from the event day, such as one to four weeks prior (Figures S13, S14, S15). These findings underscore the importance of selecting appropriate temporal control periods when assessing the relationship between NO_2 exposure and health outcomes. The strong association between NO_2 exposure and ED visits across language groups underscores the widespread health risks posed by air pollution, particularly for vulnerable and underserved populations – the Other language category. These results highlight the need for targeted interventions to improve air quality and address health disparities in linguistically diverse communities.

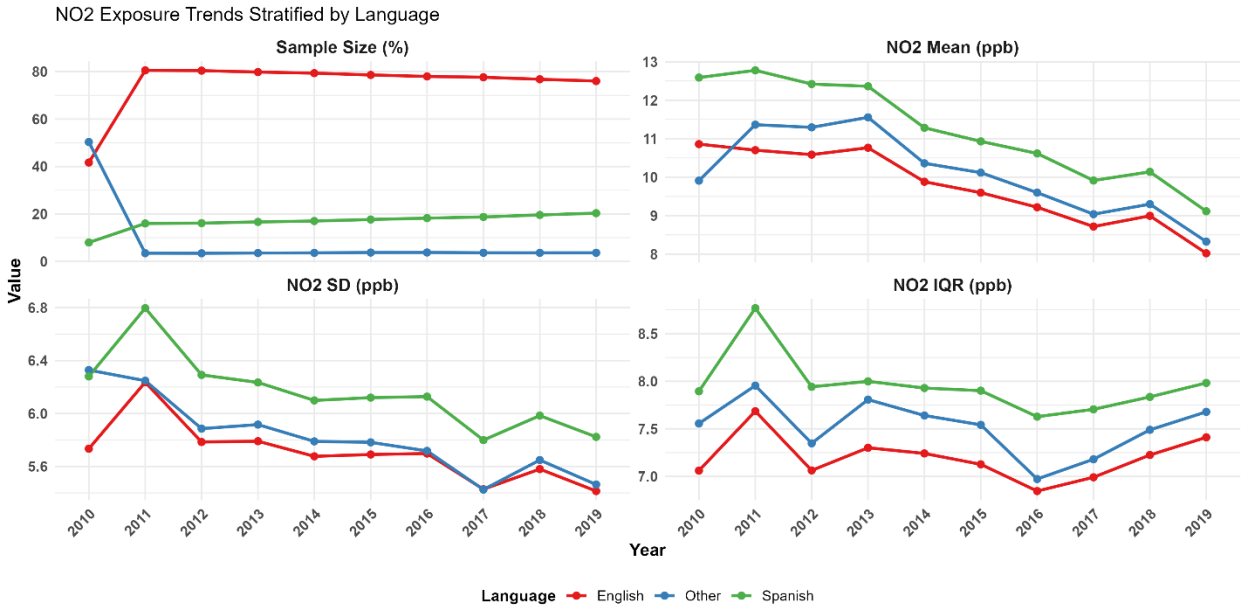

Figure 13. The temporal trend of the population, categorized by language, in California diagnosed with diabetes and NO_2 exposure from 2010 to 2019.

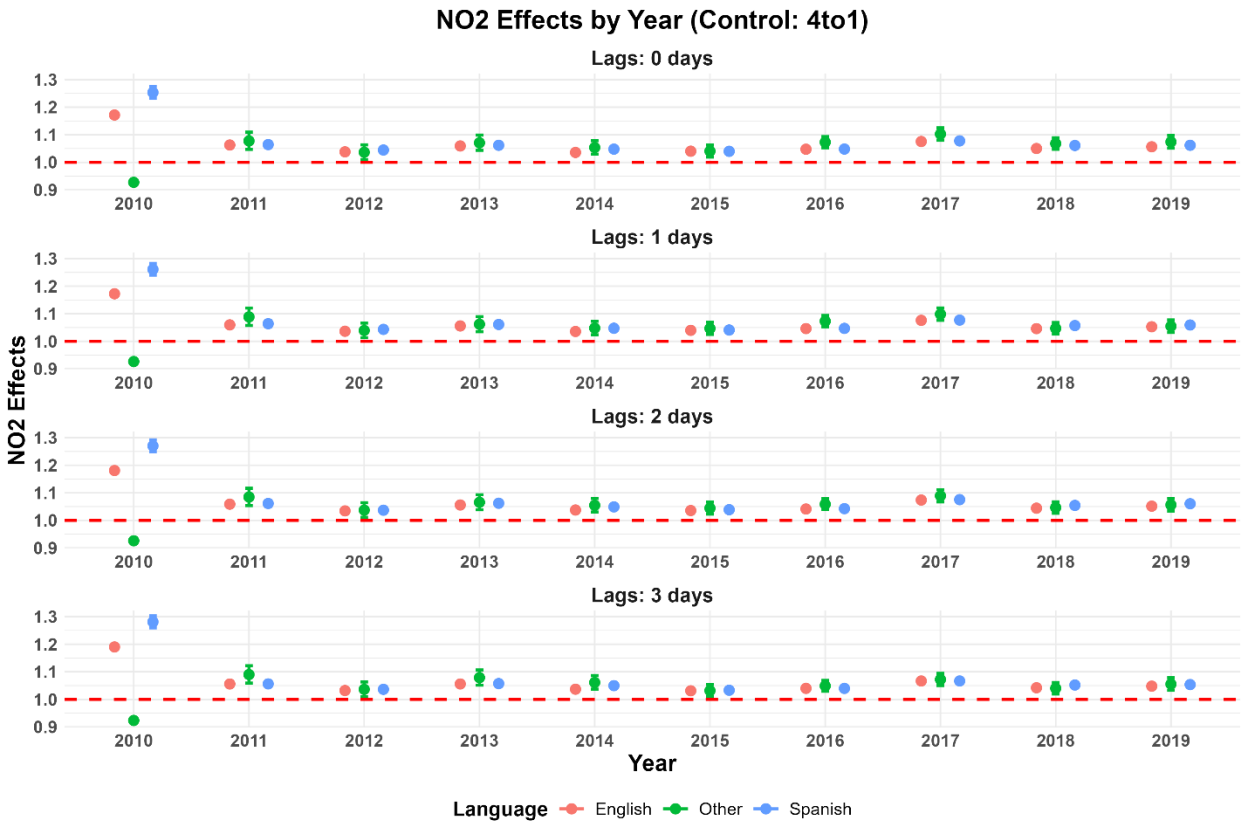

Figure 14. The associations between NO_2 exposure and ED visits for diabetic patients across language categories in California from 2010 to 2019.

In terms of $PM_{2.5}$ exposure (Figure 15), average levels across language groups steadily declined over the years, signaling overall improvements in air quality. For example, English speakers experienced a reduction in $PM_{2.5}$ mean levels from approximately 10.13 µg/m³ in 2010 to 8.54 µg/m³ in 2019, while Spanish speakers saw a similar decline from about 10.76 µg/m³ to 8.96 µg/m³ during the same period. Despite the overall decline in mean $PM_{2.5}$ concentrations, $PM_{2.5}$ concentrations rose significantly in 2018, accompanied by increases in both the SD and IQR. As previously discussed, this spike in $PM_{2.5}$ and its associated variability was likely driven by the surge in wildfire activity during 2018. The widespread and severe wildfires that year led to extreme air pollution events, causing sharp fluctuations in $PM_{2.5}$ levels across all three language speaker categories and contributing to the observed increase in SD and IQR.

On C-R functions, in 2010, only the English-speaking category exhibited a positive association between $PM_{2.5}$ exposure and health outcomes (Figure 16). However, starting in 2011, the impact on the Other language category became the highest, accompanied by a much wider confidence interval. This shift was largely driven by the reclassification of a substantial number of patients from the Other category into the English- and Spanish-speaking groups, leading to changes in the observed effects within each category. Beginning in 2011, the impact of $PM_{2.5}$ exposure also became positive for Spanish-speaking individuals, reflecting a more accurate categorization of patients. Over time, these effects gradually declined, reaching their lowest point in 2015, likely

due to the implementation of the ACA act. The ACA's expansion of healthcare access may have improved disease management and preventative care, reducing the overall sensitivity of different language-speaking populations to environmental exposures like $PM_{2.5}$. After 2015, the health impact of $PM_{2.5}$ exposure began to rise again, potentially driven by socioeconomic and environmental factors that heightened vulnerability within this group. The effect diminished in 2018, similar to the trends observed in other stratifications of $PM_{2.5}$ exposure impact.

Regarding lag times, the effects of $PM_{2.5}$ exposure were most pronounced within the 0–2 day lag period, with a slight reduction observed by day 3. For control periods, shorter control periods (e.g., one week prior) demonstrated smaller effects compared to more extended control periods (e.g., four weeks prior) (Figures S16, S17, S18). This pattern suggests that shorter control periods had exposure levels closer to those of the event day, while extended control periods introduced more variability, amplifying the estimated impact of $PM_{2.5}$.

Overall, the significant association between $PM_{2.5}$ exposure and ED visits across language groups underscores the persistent health risks posed by air pollution. These findings highlight the importance of targeted air quality interventions and the need to address disparities in $PM_{2.5}$ exposure, particularly in communities with higher proportions of non-English speakers who may face additional vulnerabilities.

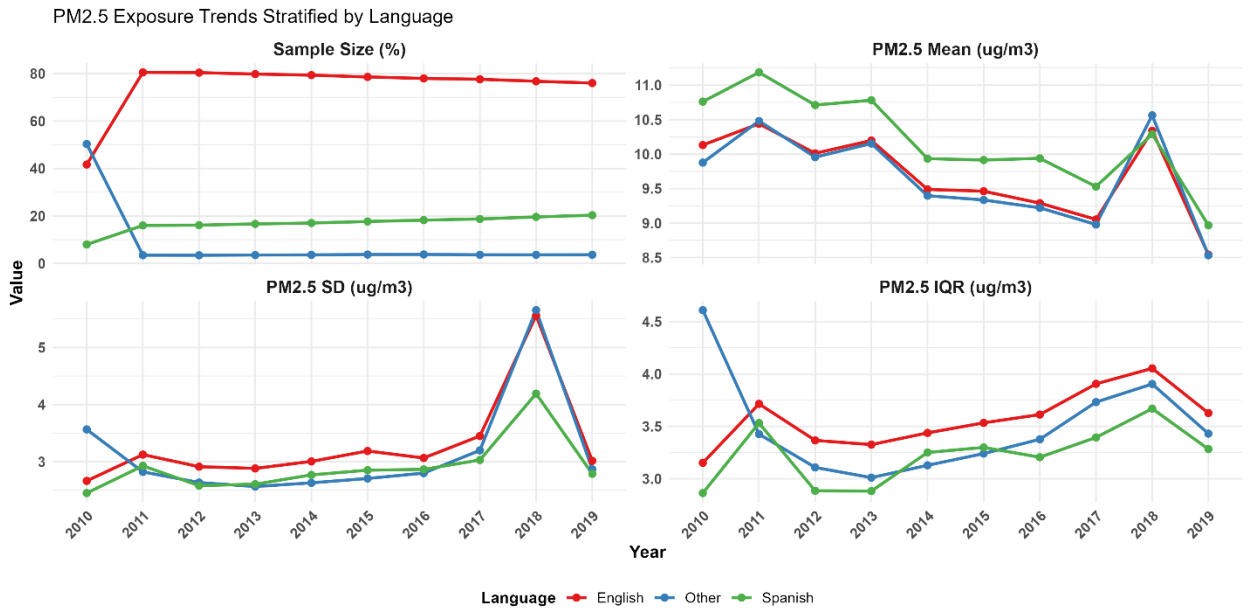

Figure 15. The temporal trend of the population, categorized by language, in California diagnosed with diabetes and $PM_{2.5}$ exposure from 2010 to 2019.

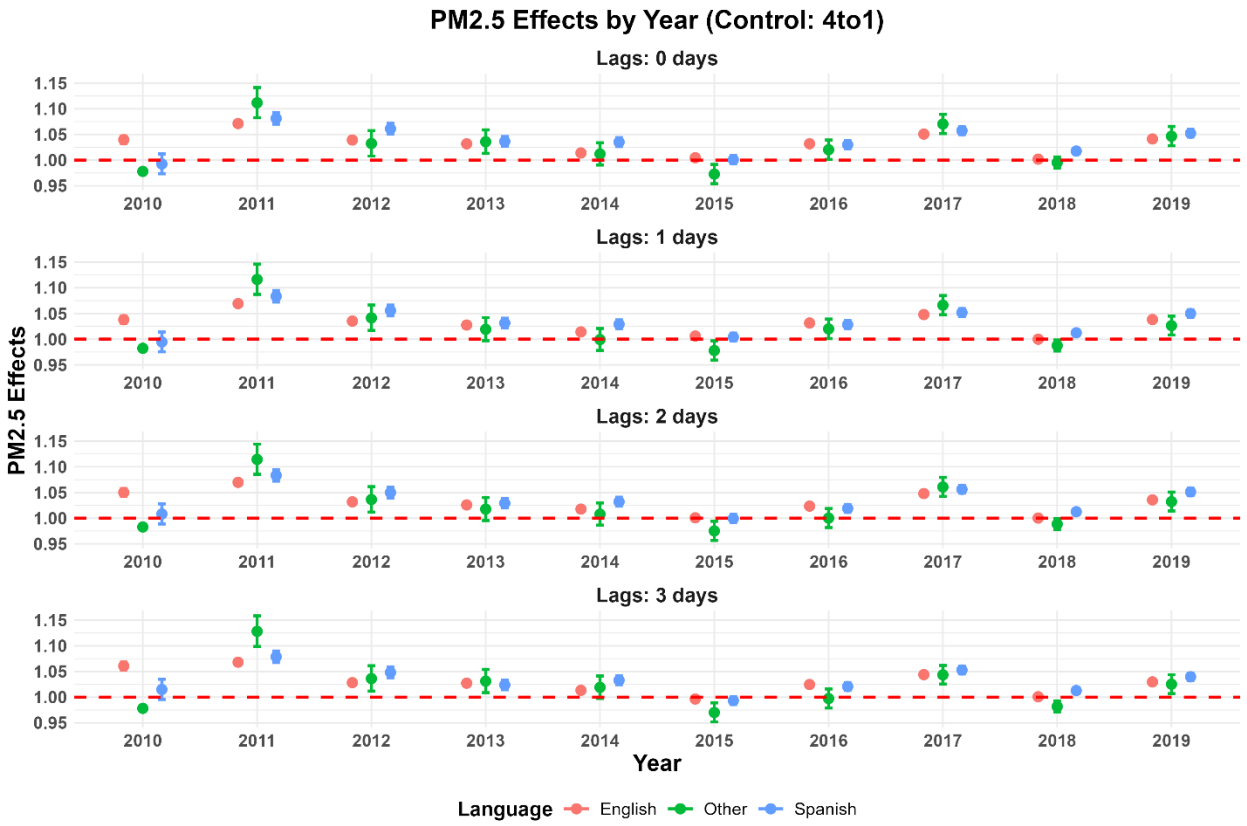

Figure 16. The associations between $PM_{2.5}$ exposure and ED visits for diabetic patients across language categories in California from 2010 to 2019.

Five Major Races Analysis

From 2010 to 2019, the racial distribution among Type 2 diabetes patients remained relatively stable (Figure 17). The largest group, White patients, saw a slight decrease from 56.24% to 53.91%, while the second-largest group, Hispanics, experienced a modest increase from 18.68% to 21.84%. Black patients, who made up 13.62% of the population in 2010, and Asian patients, comprising 6.98%, maintained relatively smaller proportions throughout the period. The "Other" category had the smallest composition, accounting for 4.46% in 2010.

In terms of NO_2 exposure, except for 2010, the mean levels across all racial groups displayed a clear downward trend from 2010 to 2019. For instance, the average NO_2 exposure for Black, Hispanic, and Other individuals dropped from 11.19 ppb, 11.64 ppb, and 10.18 ppb, in 2010 to 8.73 ppb, 8.75 ppb, and 8.13 ppb, in 2019. Similarly, Asian populations saw a reduction in mean NO_2 levels, from 10.76 ppb to 8.25 ppb over the same period, while the White population experienced a decrease from 10.08 ppb to 7.98 ppb. Overall, Hispanic patients had the greatest NO_2 exposure while White patients had the smallest exposure. Despite these improvements, the IQR of NO_2 exposure began to increase after 2016, signaling greater variability in exposure levels within the middle range. This trend suggests that while extreme pollution events became

less frequent, disparities in exposure across neighborhoods or regions may have grown, potentially driven by localized sources of pollution.

On C-R functions, the "Other" category largely exhibits the highest NO_2 effect and had the most significant changes, particularly in 2017, where its values exceed 1.10, marking the largest deviation from the baseline across all categories (Figure 18). The heightened impact observed in the "Other" category may be attributed to socioeconomic and environmental vulnerabilities, including limited access to preventive healthcare. In comparison, the other race-ethnicity groups remained relatively stable, though with some minor fluctuations. Starting in 2012, the effects of NO_2 exposure on ED visits began to decline across all racial groups, reaching their lowest levels around 2015. This trend likely reflects the benefits of expanded healthcare access and improved disease management facilitated by Medicaid expansion and broader reforms under the ACA. However, after 2015, the impact of NO_2 exposure on ED visits began to rise again, particularly among the "Other" category patients. This resurgence may be driven by increased susceptibility in these communities due to aging demographics and a rising prevalence of chronic conditions. Regarding lag effects, the influence of NO_2 exposure on ED visits remained consistent across 0–2 day lags, with a slight reduction in impact observed by day 3. This pattern suggests that the short-term health effects of NO_2 exposure diminish over time. For control periods, greater effect sizes were observed when the control period was farther removed from the event day, such as the four-week control period (Figures S19, S20, S21). This trend underscores the importance of temporal framing in analyses, as variations in seasonal and spatial exposure levels can significantly influence the observed relationships between pollution and health outcomes.

These findings demonstrate significant associations between NO_2 exposure and ED visits across all racial groups from 2010 to 2019, emphasizing the ongoing health burden of air pollution, particularly among vulnerable populations. Addressing these disparities through targeted interventions and sustained air quality improvements is essential for mitigating the health impacts of NO_2 exposure and promoting environmental justice for all racial groups.

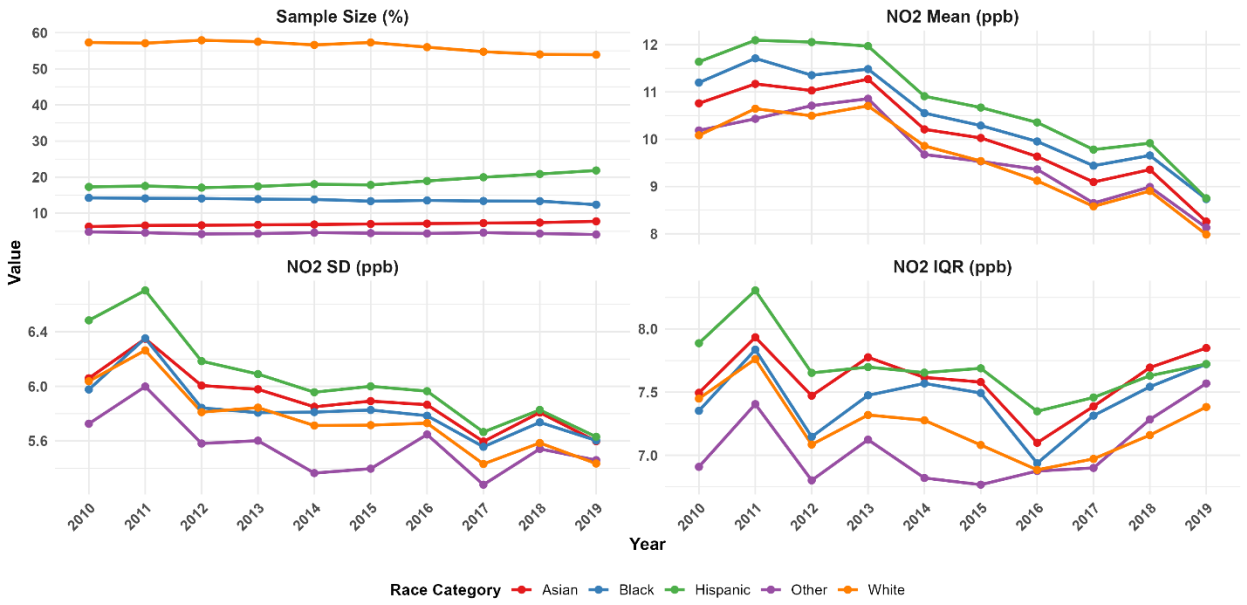

Figure 17. The temporal trend of the population, categorized by five major races, in California diagnosed with diabetes and NO_2 exposure from 2010 to 2019.

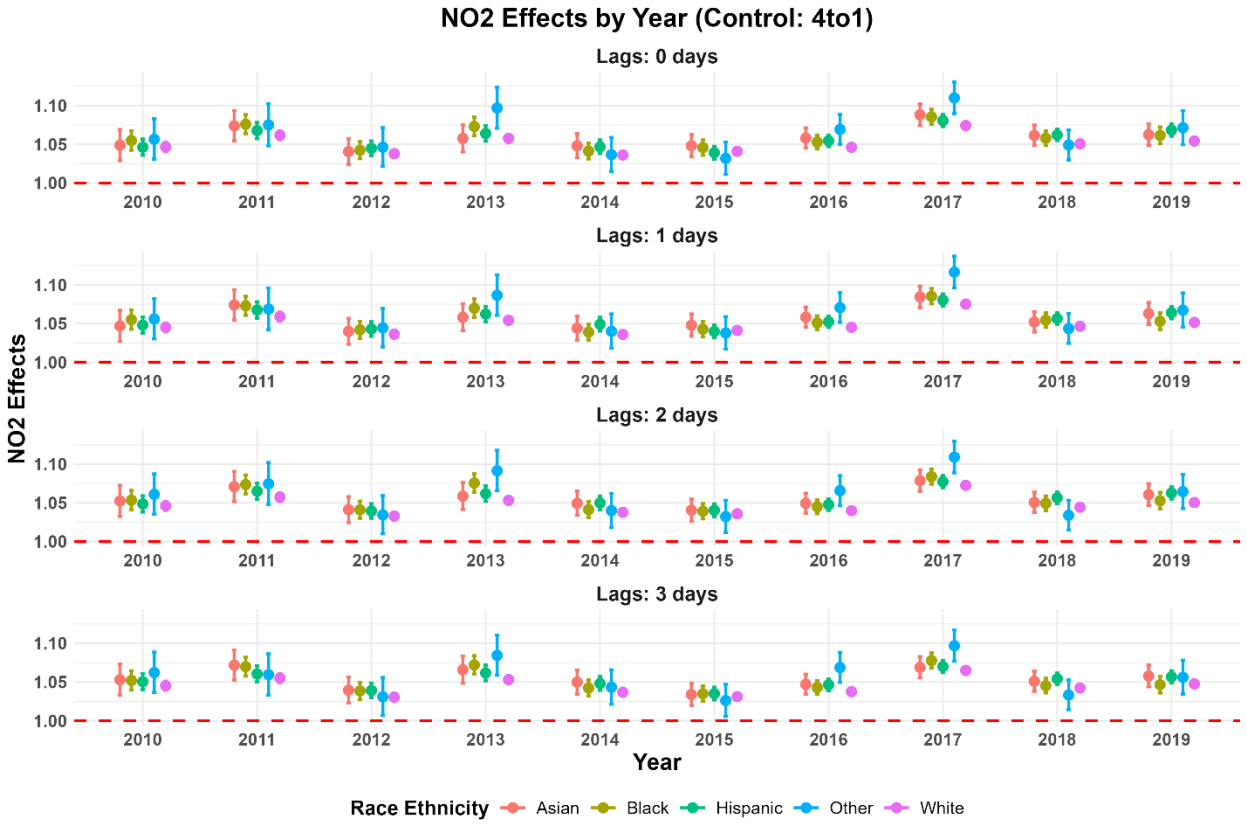

Figure 18.The associations between NO_2 exposure and ED visits for diabetic patients across five major race categories in California from 2010 to 2019.

On $PM_{2.5}$ exposure (Figure 19), the average exposure levels for Black, Hispanic, and Other individuals decreased from 10.09 μg/m³, 10.58 μg/m³, and 10.67 μg/m³ in 2010 to 8.69 μg/m³, 8.76 μg/m³, and 8.38 μg/m³ in 2019, respectively. Similarly, Asian individuals experienced a reduction in average $PM_{2.5}$ levels, dropping from 9.88 μg/m³ to 8.40 μg/m³ during the same timeframe. The White population also saw a decline in exposure, decreasing levels from 9.87 μg/m³ to 8.62 μg/m³. Overall, Hispanic and Other patients had the greatest exposure, and White patients had the smallest exposure. Despite the overall decline in mean $PM_{2.5}$ concentrations, levels rose significantly in 2018, accompanied by increases in both the SD and IQR. As previously discussed, this spike in $PM_{2.5}$ and its associated variability was likely driven by the surge in wildfire activity during 2018. The widespread and severe wildfires that year led to extreme air pollution events, causing sharp fluctuations in $PM_{2.5}$ levels across all race-ethnicity categories and contributing to the observed increase in SD and IQR.

On C-R functions, the Asian category exhibited the most significant changes, for example, from 2011 and 2015, where its values dropped from 1.08 to near 1.0 (Figure 20). Between 2012 and 2015, the effect of $PM_{2.5}$ exposure on ED visits declined across all race-ethnicity groups, reaching its lowest levels during this period. This reduction may be attributed to improvements in air quality and expanded access to preventive healthcare services facilitated by Medicaid expansion and other ACA initiatives.

However, after 2015, the impact of $PM_{2.5}$ exposure on ED visits began to rise again, particularly among Asian populations. This increase could point to heightened vulnerability in these groups due to a higher prevalence of chronic health conditions or other risk factors. Wider confidence intervals observed for Asian and "Other" groups suggest smaller sample sizes, contributing to greater variability and uncertainty in effect estimates.

On lagged effects, across all lag durations (0, 1, 2, and 3 days), the Asian category shows consistent fluctuations and variability, particularly in earlier years. The error bars for this category are relatively large, highlighting uncertainty in the estimates. Additionally, the choice of control periods significantly influenced the observed impacts, with longer control intervals (e.g., four weeks) showing greater estimated effects (Figures S22, S23, S24). This pattern likely reflects the dilution of exposure levels during distant reference periods, which amplifies the relative impact of event-day exposures.

Overall, these findings reveal a significant association between $PM_{2.5}$ exposure and ED visits across all racial groups, underscoring the critical role of air pollution in exacerbating health disparities. The results highlight the urgent need for targeted interventions to reduce $PM_{2.5}$ exposure and address health inequities, particularly within vulnerable racial and ethnic communities.

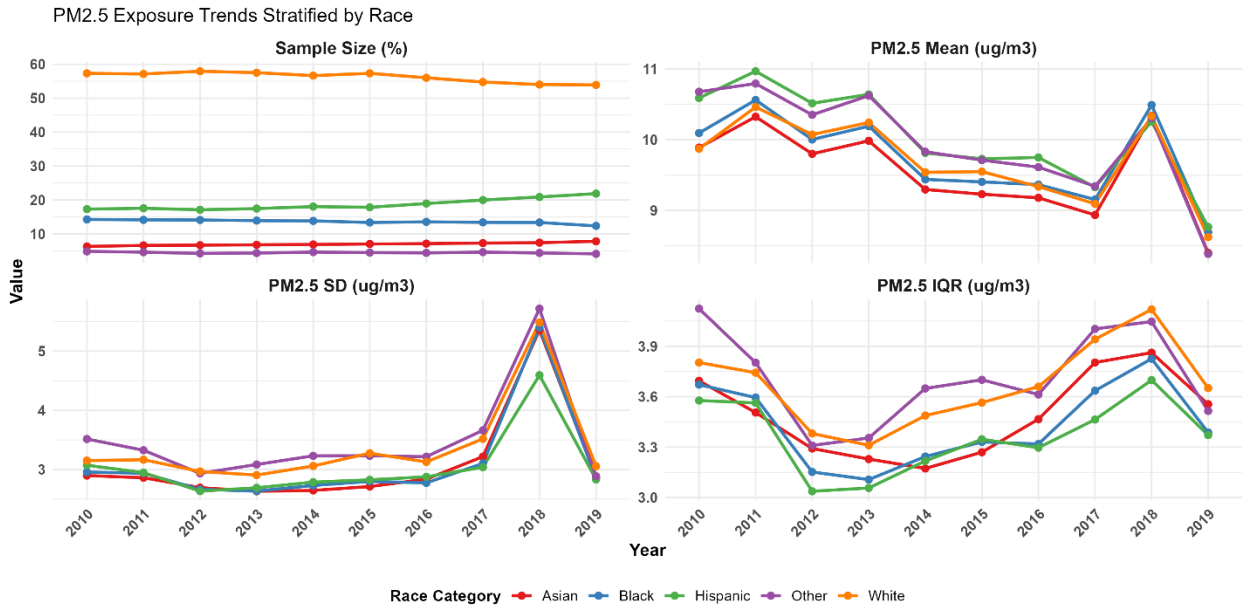

Figure 19. The temporal trend of the population, categorized by five major races, in California diagnosed with diabetes and $PM_{2.5}$ exposure from 2010 to 2019.

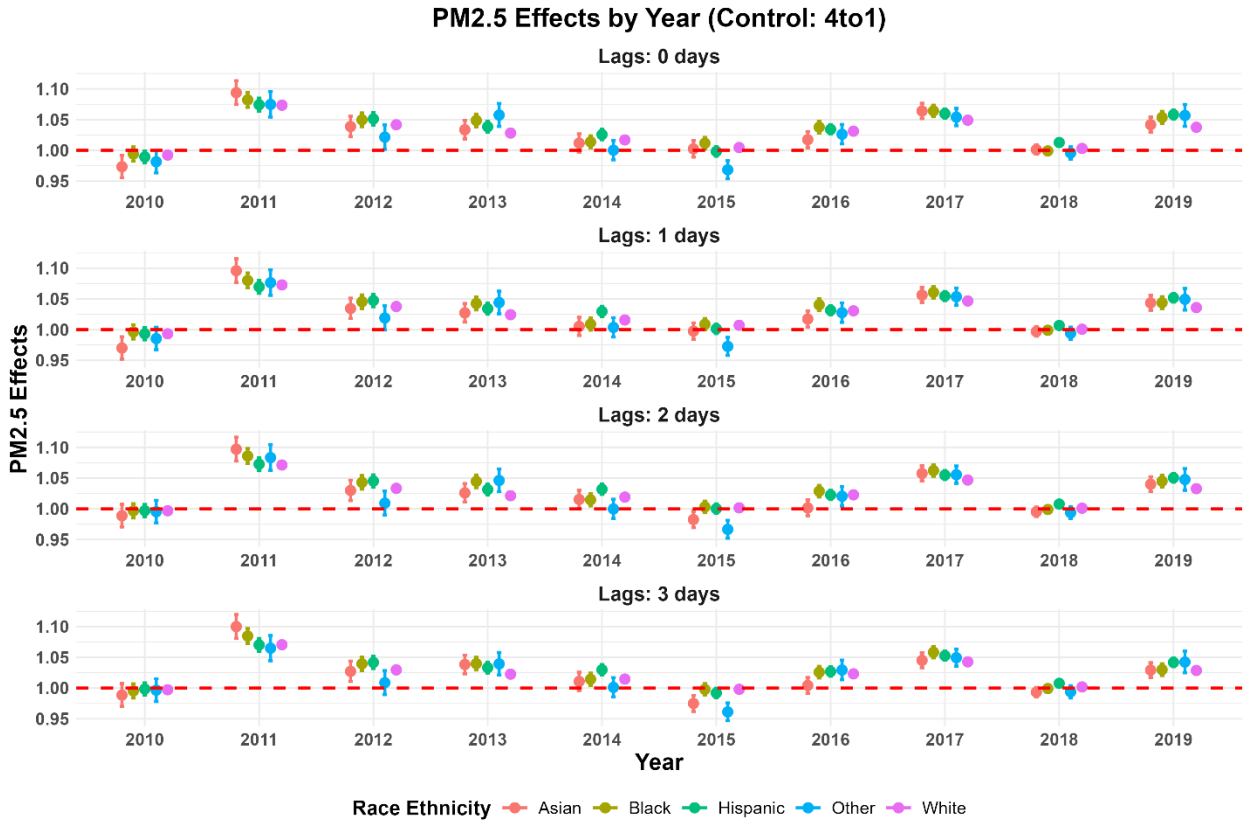

Figure 20.The associations between $PM_{2.5}$ exposure and ED visits for diabetic patients across five major race categories in California from 2010 to 2019.

Gender analysis

Between 2010 and 2012, the gender distribution of individuals remained relatively stable (Figure 21). Males consistently represented approximately 44.97% of the population, while females comprised 55.03%. However, beginning in 2013, there was a gradual increase in the proportion of male participants, reaching 46.16% by 2019.

Regarding NO_2 exposure, both genders experienced a consistent decline in mean levels after 2013. For instance, mean NO_2 exposure for males was relatively low at 10.52 ppb in 2010, increased slightly to 11.0 ppb in 2013, and then steadily decreased to 8.20 ppb by 2019. Similarly, for females, NO_2 exposure dropped from 10.56 ppb in 2010 to 8.31 ppb in 2019. Throughout the study period, females consistently had slightly higher NO2 exposure compared to males. Despite the overall reductions, the IQR of NO_2 exposure widened after 2016, suggesting increased variability within the middle distribution of exposure levels. This trend indicates that while extreme outliers became less frequent, fluctuations in moderate NO_2 exposure levels grew, possibly due to localized air quality changes.

On C-R functions, both genders exhibited nearly identical responses to NO_2 exposure, with their impact patterns rising and falling in close alignment over time. From 2014 to 2015, the effect of NO_2 exposure on ED visits declined for both genders, reaching its lowest point in 2015. This decline likely reflects improved healthcare access and preventive measures the ACA facilitated. However, after 2015, the impact of NO_2 exposure on ED visits began to rise again for both genders, potentially driven by demographic shifts such as an aging population or increased vulnerability in specific subgroups.

Regarding lag times, the effects of NO_2 exposure on ED visits remained consistent across both genders, with a slight decrease observed as the lag period extended from zero to three days. In the control period, smaller effect estimates were noted when the control period was closer to the event day, while greater impacts were observed with longer control intervals, such as four weeks prior (Figures S25, S26, S27). This trend underscores the importance of carefully selecting temporal frameworks to ensure accurate exposure assessments and their health impacts.

Overall, the statistically significant association between NO_2 exposure and ED visits across genders highlights the pervasive health risks posed by air pollution.

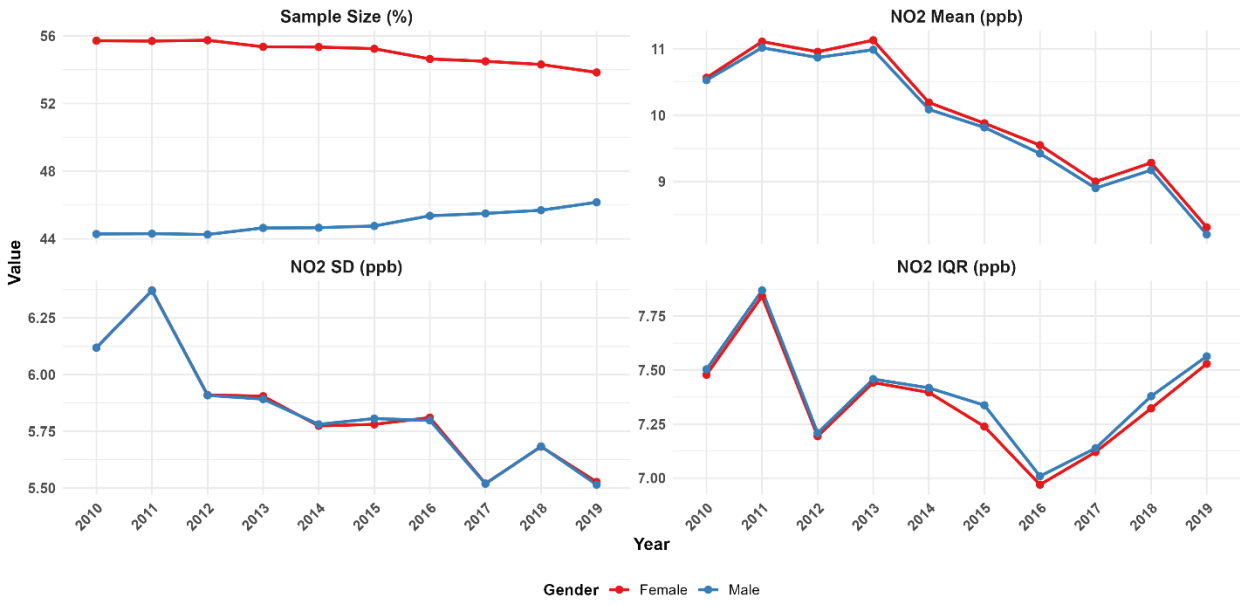

Figure 21. The temporal trend of the population, categorized by gender, in California diagnosed with diabetes and NO_2 exposure from 2010 to 2019.

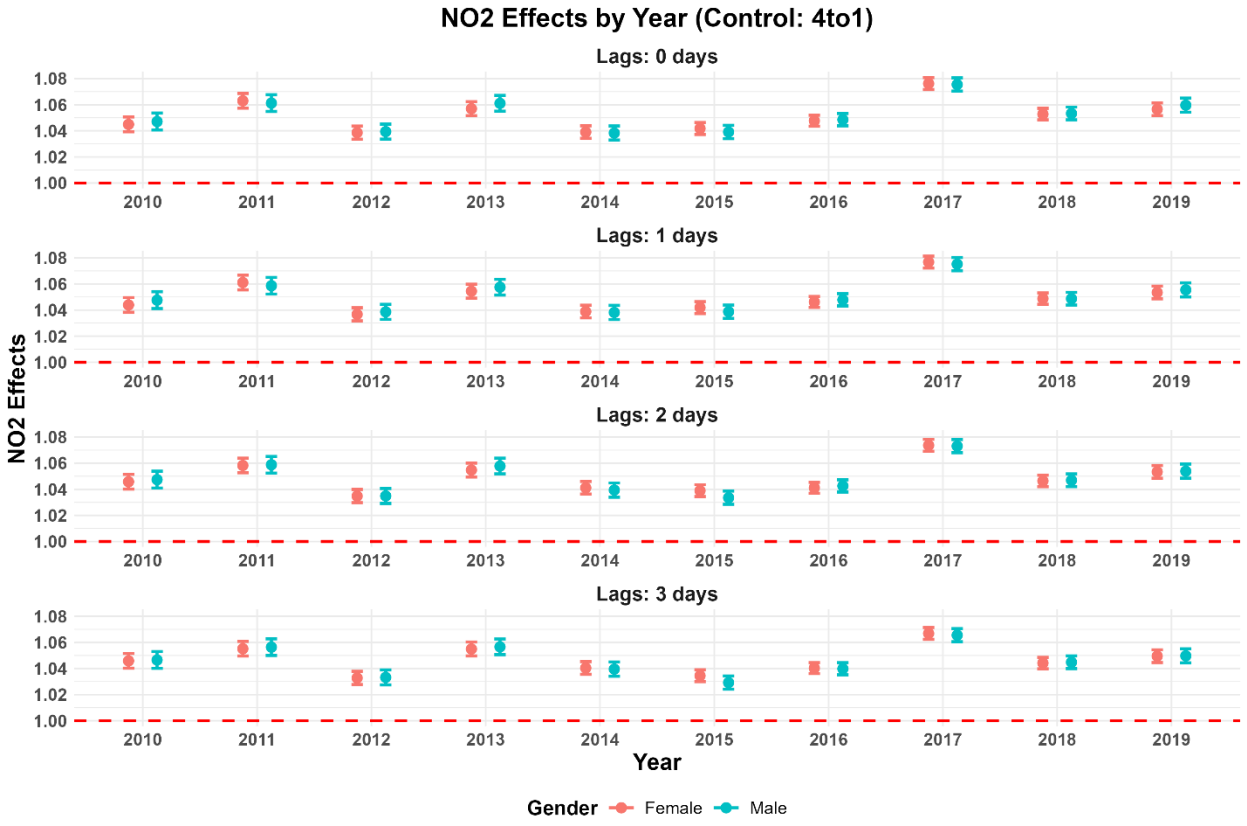

Figure 22. The associations between NO_2 exposure and ED visits for diabetic patients across gender categories in California from 2010 to 2019.

Regarding $PM_{2.5}$ exposures (Figure 23), though a small increase was seen from 2010 to 2011, overall exposure levels for both genders declined over the study period. For example, mean $PM_{2.5}$ exposure for males decreased from 10.02 μg/m³ in 2010 to 8.58 μg/m³ in 2019. Similarly, mean exposure for females dropped from 10.08 μg/m³ in 2010 to 8.61 μg/m³ in 2019. Despite these improvements, the IQR of $PM_{2.5}$ exposure widened after 2014, indicating greater variability within the middle 50% of exposure levels. This suggests that while extreme pollution levels diminished, variability in exposure among individuals within the central range increased, potentially due to localized sources of pollution. Again, as observed in the unstratified analysis, $PM_{2.5}$ exposure increased significantly in 2018 due to the substantial impact of wildfire events.

On C-R functions, similar to NO_2 exposure effect, both genders have almost identical impact from $PM_{2.5}$ exposure, with their impact patterns rising and falling in close alignment over time. (Figure 24). Also similar to NO_2 exposure effect, from 2014 to 2015, the effect of $PM_{2.5}$ exposure on ED visits declined for both genders, reaching its lowest point in 2015. After 2015, the health impacts of $PM_{2.5}$ exposure on ED visits began to rise slightly for both genders, similar to what happened to NO_2 exposure. Furthermore, the effect diminished significantly in 2018, similar to the trends observed in other stratifications of $PM_{2.5}$ exposure impact.

Regarding lag times, the acute effects of $PM_{2.5}$ exposure were relatively consistent across 0–3 day lags, with a slight reduction in impact over longer lag periods. This pattern indicates that the immediate effects of $PM_{2.5}$ exposure on ED visits diminish within three days. Control periods also influenced effect estimates, with smaller impacts observed for control periods closest to the event. As the control period extended from one to four weeks before the event, the impact estimates increased, likely due to more pronounced contrasts in exposure levels between the event and control periods (Figures S28, S29, S30).

Overall, the significant association between $PM_{2.5}$ exposure and ED visits for both genders underscores the pervasive health risks of air pollution.

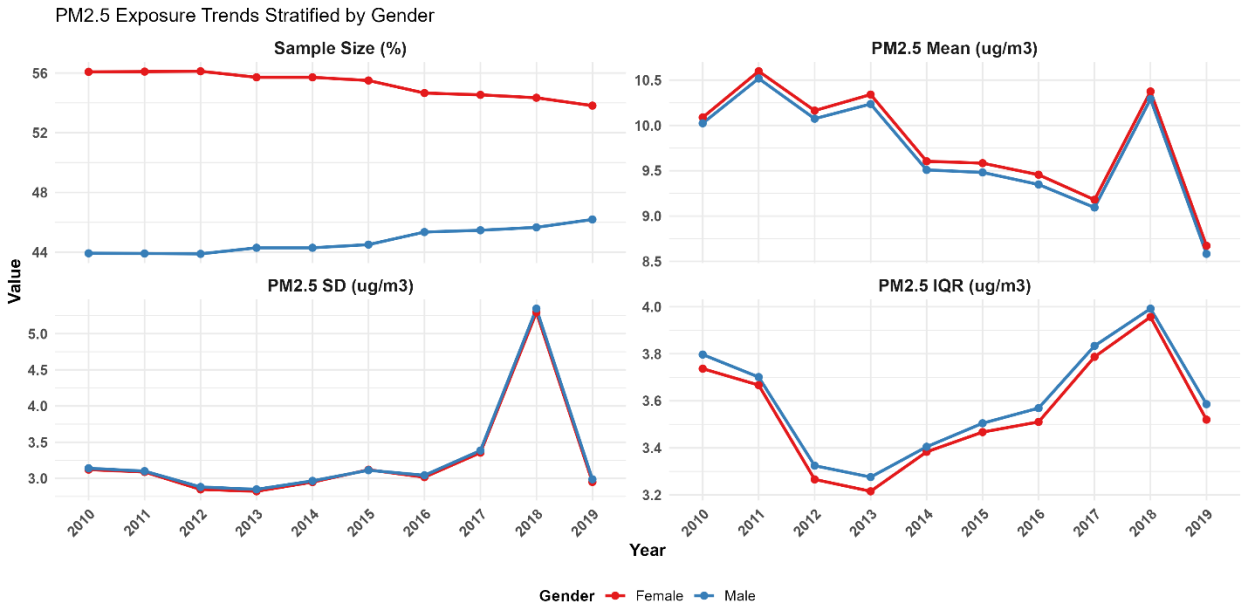

Figure 23. The temporal trend of the population, categorized by gender, in California diagnosed with diabetes and $PM_{2.5}$ exposure from 2010 to 2019.

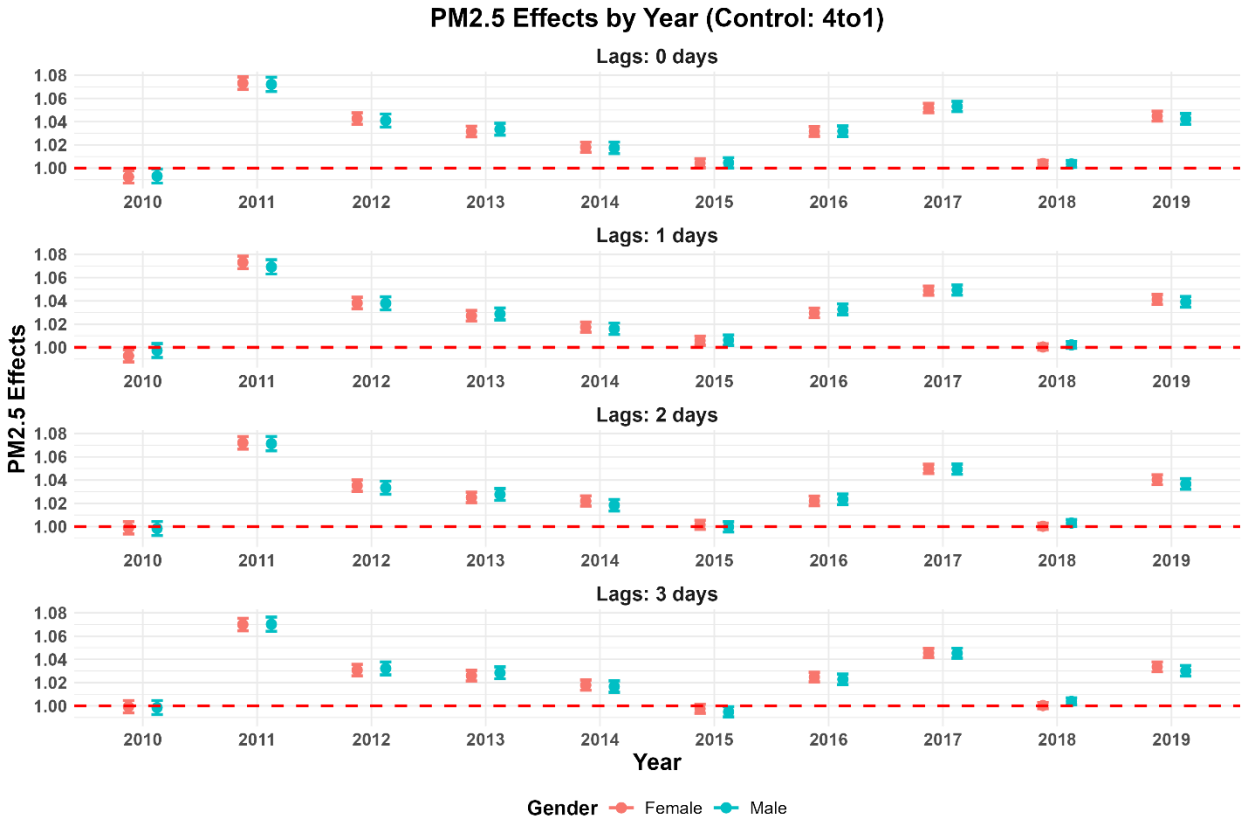

Figure 24.The associations between $PM_{2.5}$ exposure and ED visits for diabetic patients across gender categories in California from 2010 to 2019.

Age analysis

Between 2010 and 2019, the distribution of type 2 diabetic patients by age group remained relatively stable, with only minor variations across categories (Figure 25). Ages 45-64 had the most composition, while ages 0-17, 16-24, and 85+ had the smallest composition, In 2010, they were 43.24%, 0.4%, 1.24% and 6.36%, respectively. Though relatively stable, we can still observe the gradual aging of the patient population after 2016, particularly as the "baby boomer" generation entered their senior years. By 2019, the percentage of individuals aged 65–74 increased to 21.08 %, and those aged 75–84 rose to 14.64%. This aging trend underscores the growing presence of older adults in the patient population, likely contributing to increased susceptibility to air pollution exposure.

Regarding NO_2 exposure, the mean levels across all age groups consistently declined over the study period. For example, mean NO_2 exposure for individuals aged 0–17 decreased from 10.95 ppb in 2010 to 8.66 ppb in 2019, 18-24 decreased from 10.55 ppb in 2010 to 8.37 ppb in 2019, 25-44 decreased from 10.76 ppb in 2010 to 8.36 ppb in 2019. Similarly, the 45–64 age group saw a reduction in mean NO_2 levels from 10.62 ppb in 2010 to 8.34 ppb in 2019. Individuals aged 65–74 decreased from 10.45 ppb in 2010 to 8.15 ppb in 2019, 75-84 decreased from 10.26 ppb in 2010 to 8.14 ppb in 2019, and finally, 85+ decreased from 10.103 ppb in 2010 to 8.09 ppb in 2019. Across all the years, the 0-17 age group experienced the highest exposure to NO_2, while the 85+ age group had the lowest exposure. Despite overall air quality improvements, the IQR of NO_2 exposure widened after 2016, indicating increased variability within the middle 50% of exposure levels. This suggests that while average concentrations declined, certain areas experienced inconsistent air quality improvements, possibly due to localized pollution sources.

The 0–17 age group exhibits the most significant changes, particularly in 2013 and 2017, where values rise above 1.2, marking substantial deviations from the baseline (Figure 26). This heightened impact is likely influenced by the increased severity of influenza in California during those years, which may have led to a surge in ED visits. During the 2014-2015 period, the impact for the 0-17 age group reached its lowest levels. This decline may be attributed to enhanced preventive care and improved access to healthcare services introduced under the ACA. The significant change in NO_2's impact on ED visits for the 0–17 age group reflects children's heightened vulnerability to air pollution, driven by their developing respiratory systems and higher exposure rates during outdoor activities. Additionally, the relatively small sample size for this age group, which results in wider confidence intervals, may contribute to the observed variability in NO_2's effect on ED visits, making year-to-year fluctuations more pronounced. For the other age groups, the effects of NO_2 on ED visits remain relatively stable, consistently showing a significant impact over the years.

Regarding lag times, the effects of NO_2 exposure remained relatively stable across all age groups within 0–2 day periods, with a slight reduction observed by day 3. For control periods, smaller

impacts were noted when the control period was closest to the event, whereas larger effects were observed with extended control periods of up to four weeks (Figures S31, S32, S33). This pattern highlights the importance of accounting for temporal variability when selecting control periods to analyze the health impacts of NO_2 exposure accurately.

Overall, significant effects of NO_2 exposure on ED visits were observed across all age groups, underscoring the pervasive health risks posed by air pollution. These findings emphasize the need for targeted air quality policies and interventions to protect vulnerable populations, such as children and older adults, who are disproportionately affected by the health impacts of NO_2 exposure.

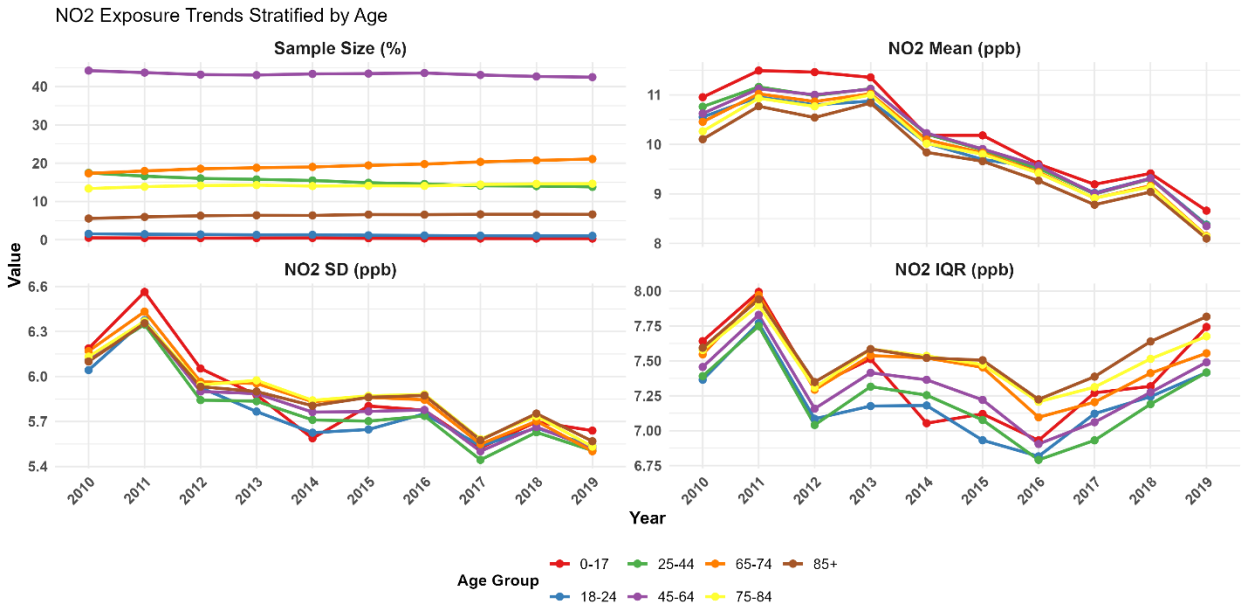

Figure 25. The temporal trend of the population, categorized by age, in California diagnosed with diabetes and NO_2 exposure from 2010 to 2019.

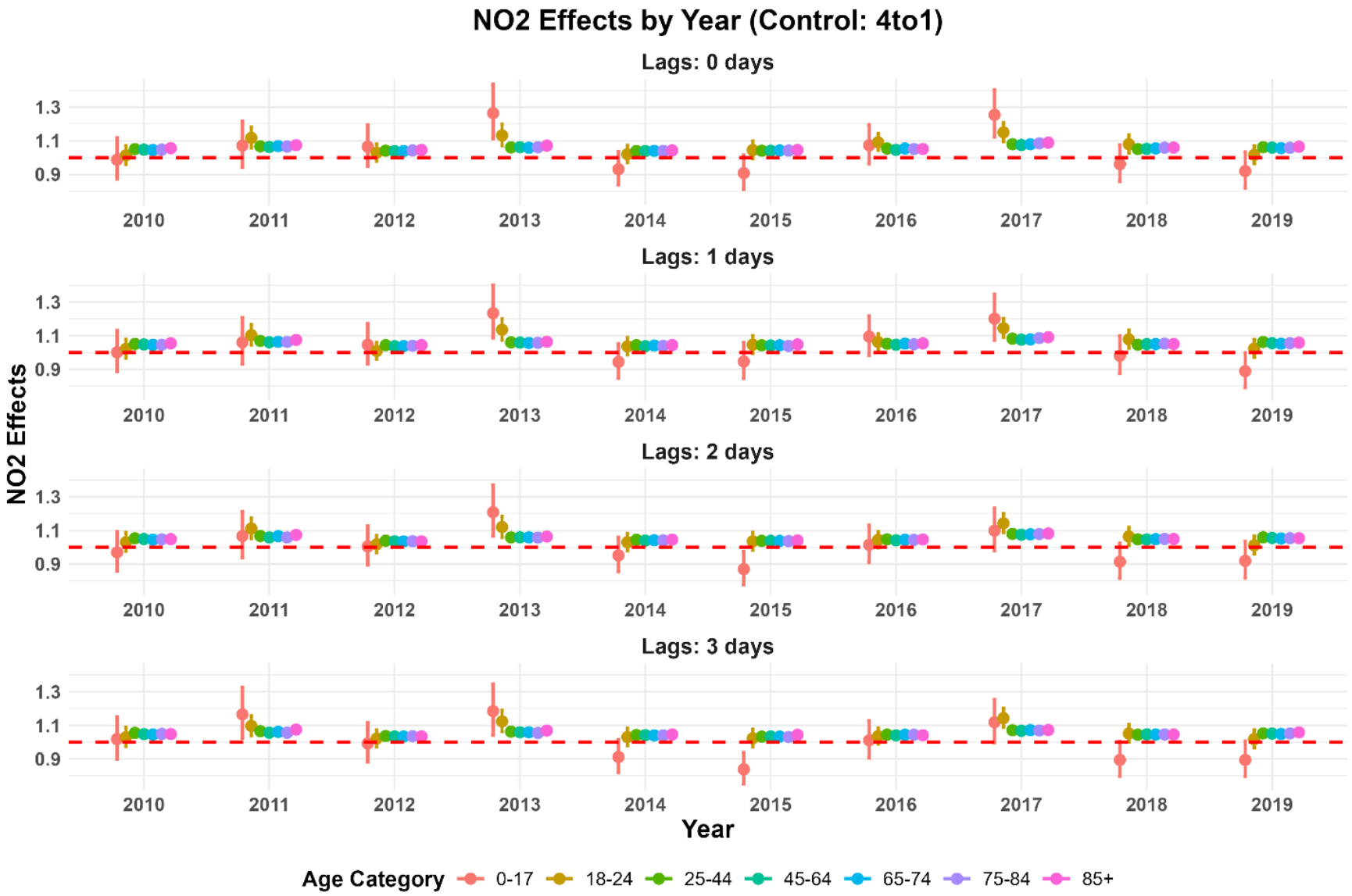

Figure 26.The associations between NO_2 exposure and ED visits for diabetic patients across age categories in California from 2010 to 2019.

Regarding $PM_{2.5}$ exposure, the mean levels across all age groups consistently declined over the study period (Figure 27). For example, mean $PM_{2.5}$ exposure for individuals aged 0–17 decreased from 10.19 μg/m³ in 2010 to 8.81 μg/m³ in 2019, 18-24 decreased from 10.22 μg/m³ in 2010 to 8.82 μg/m³ in 2019, 25-44 decreased from 10.26 μg/m³ in 2010 to 8.79 μg/m³ in 2019. Similarly, the 45–64 age group saw a reduction in mean $PM_{2.5}$ levels from 10.10 μg/m³ in 2010 to 8.71 μg/m³ in 2019. Individuals aged 65–74 decreased from 9.98 μg/m³ in 2010 to 8.56 μg/m³ in 2019, 75-84 decreased from 9.87 μg/m³ in 2010 to 8.47 μg/m³ in 2019, and finally, 85+ decreased from 9.69 μg/m³ in 2010 to 8.30 μg/m³ in 2019. Similar to NO_2 exposure, across all the years, the 0-17 age group experienced the highest exposure to $PM_{2.5}$, while the 85+ age group had the lowest exposure. Despite the overall decline in mean $PM_{2.5}$ concentrations, levels rose significantly in 2018, accompanied by increases in both the SD and IQR for each age group. As previously discussed, this spike in $PM_{2.5}$ and its associated variability was likely driven by the surge in wildfire activity during 2018. The widespread and severe wildfires that year led to extreme air pollution events, causing sharp fluctuations in $PM_{2.5}$ levels across all three language speaker categories and contributing to the observed increase in SD and IQR.

On C-R functions, the 0–17 age group exhibits the most significant changes, with high reaching over 1.1 and lows below 0.9 (Figure 28). This heightened impact is likely due to the likelihood of children engaging in outdoor activities, increasing their exposure and vulnerability to air pollution. Similar to what we have seen for other stratifications, the effect of $PM_{2.5}$ exposure on ED visits for individuals aged 0–17 began to decline after 2011, reaching its lowest point in 2015. This decline likely reflects improved air quality and the improved health care from the ACA act to protect this demographic. After 2015, individuals aged 65 and older experienced a slight increase in the impact of $PM_{2.5}$ exposure on ED visits. This rise is likely attributable to the heightened vulnerability of older adults, driven by aging, chronic health conditions, and increased sensitivity to air pollution. Furthermore, the effect diminished significantly in 2018, similar to the trends observed in other stratifications of $PM_{2.5}$ exposure impact.

Regarding lag times, the effects of $PM_{2.5}$ exposure across all age groups remained relatively consistent over 0–2 day periods, with a slight decrease observed by day 3. For control period, the smallest effects were observed for control periods when the control period was closest to the event day. As the control period extended from one to four weeks prior, the estimated impact of $PM_{2.5}$ exposure increased, underscoring the importance of careful temporal framing in exposure analyses (Figures S34, S35, S36).

Overall, $PM_{2.5}$ exposure significantly influenced ED visits across all age groups throughout the study period, emphasizing the widespread health risks associated with air pollution. These findings highlight the critical need for targeted interventions to reduce $PM_{2.5}$ exposure, particularly for vulnerable populations such as children and older adults, who are disproportionately affected by its health impacts.

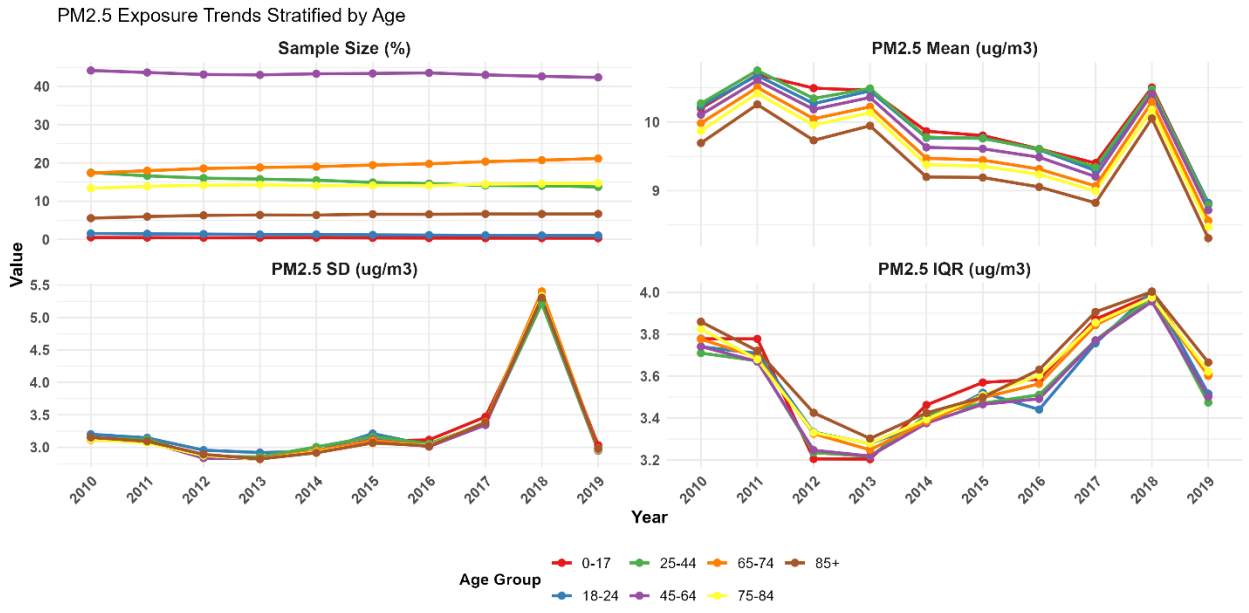

Figure 27. The temporal trend of the population, categorized by age, in California diagnosed with diabetes and $PM_{2.5}$ exposure from 2010 to 2019.

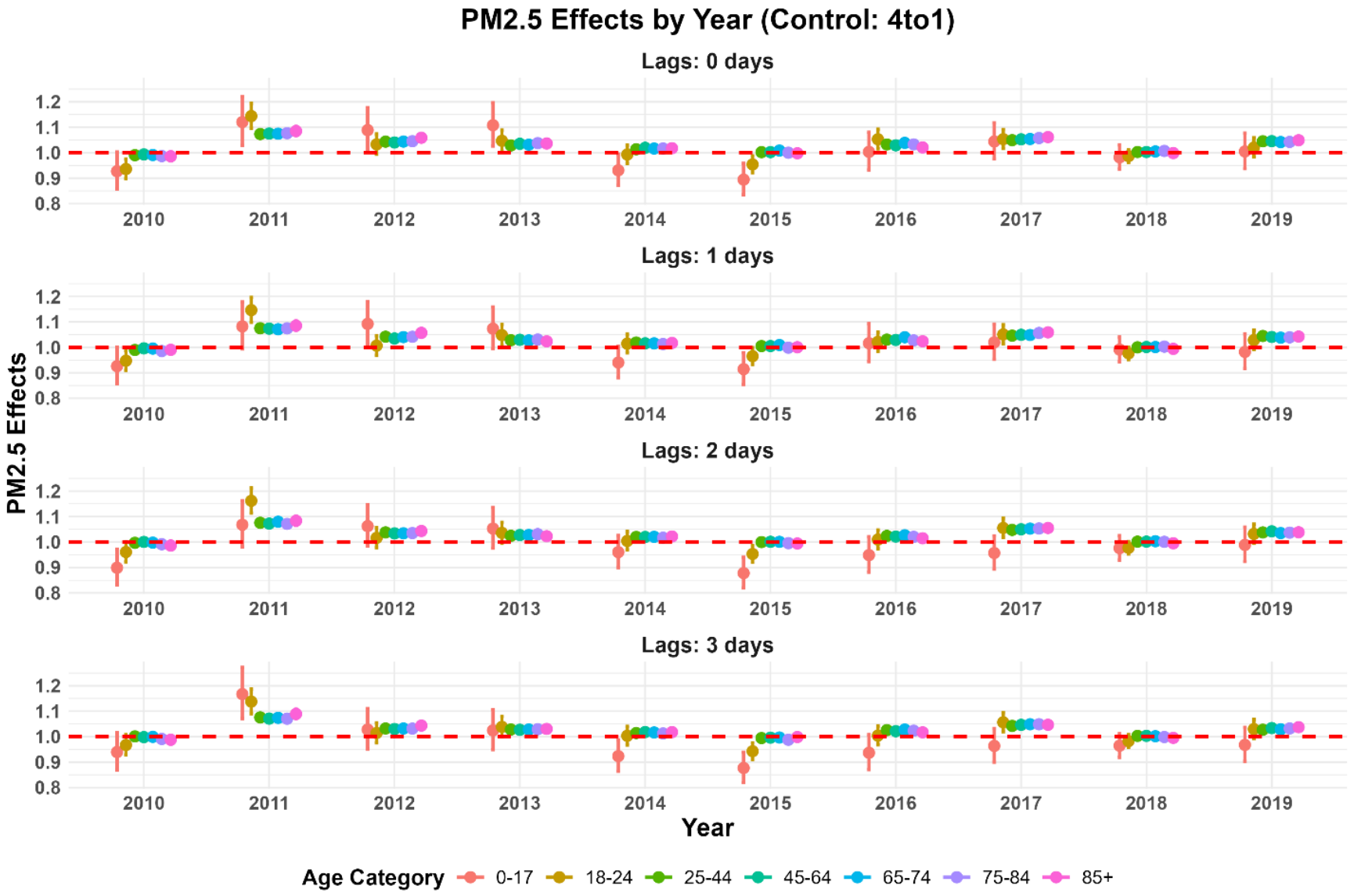

Figure 28.The associations between $PM_{2.5}$ exposure and ED visits for diabetic patients across age categories in California from 2010 to 2019.

Supplementary Figures

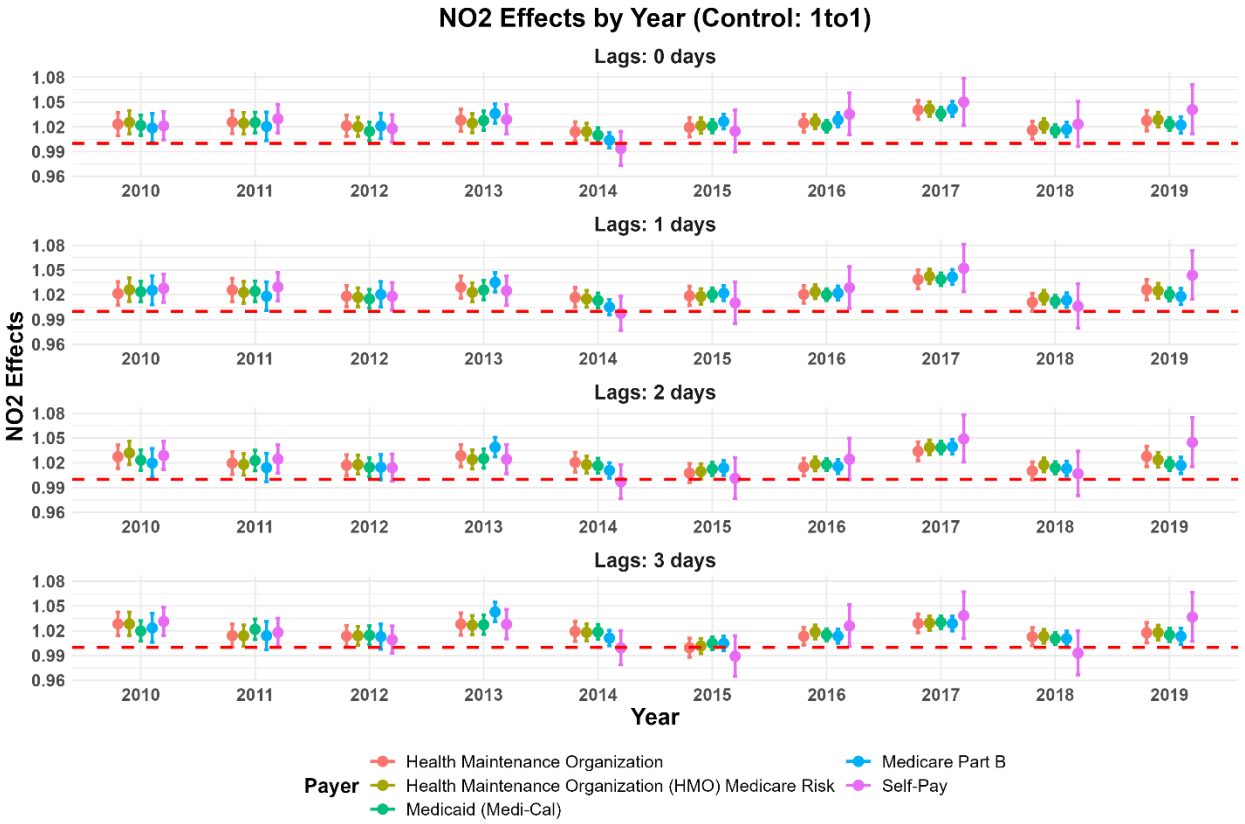

Figure S1. The associations between NO_2 exposure and ED visits for diabetic patients across different health insurance payer categories in California from 2010 to 2019.

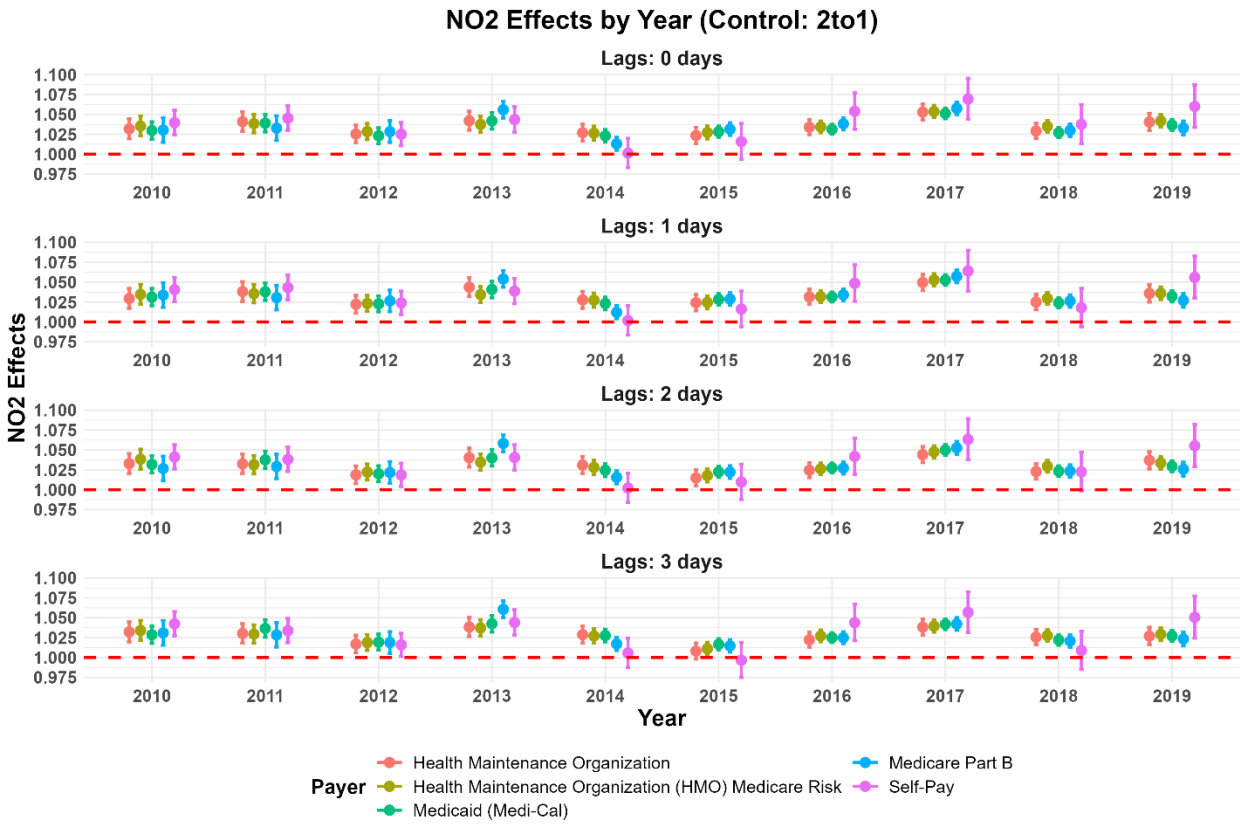

Figure S2. The associations between NO_2 exposure and ED visits for diabetic patients across different health insurance payer categories in California from 2010 to 2019.

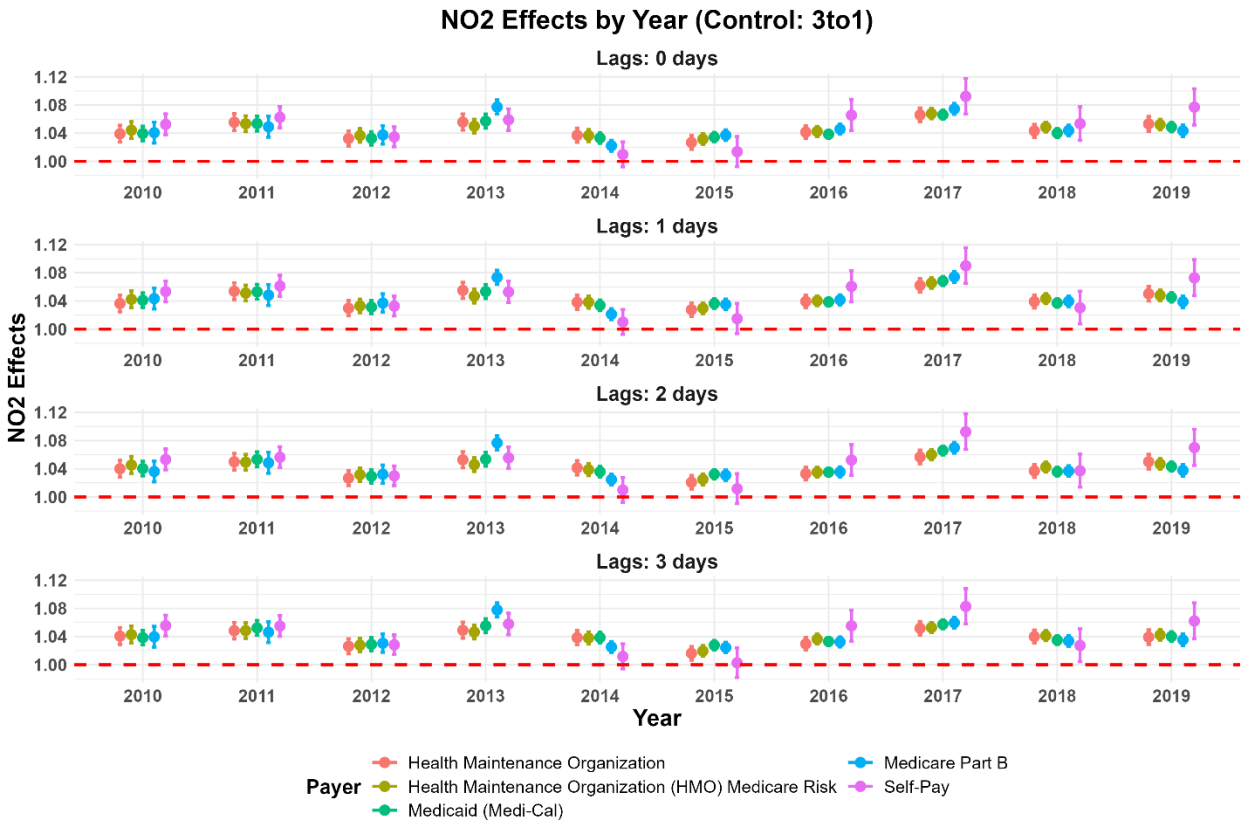

Figure S3.The associations between NO_2 exposure and ED visits for diabetic patients across different health insurance payer categories in California from 2010 to 2019.

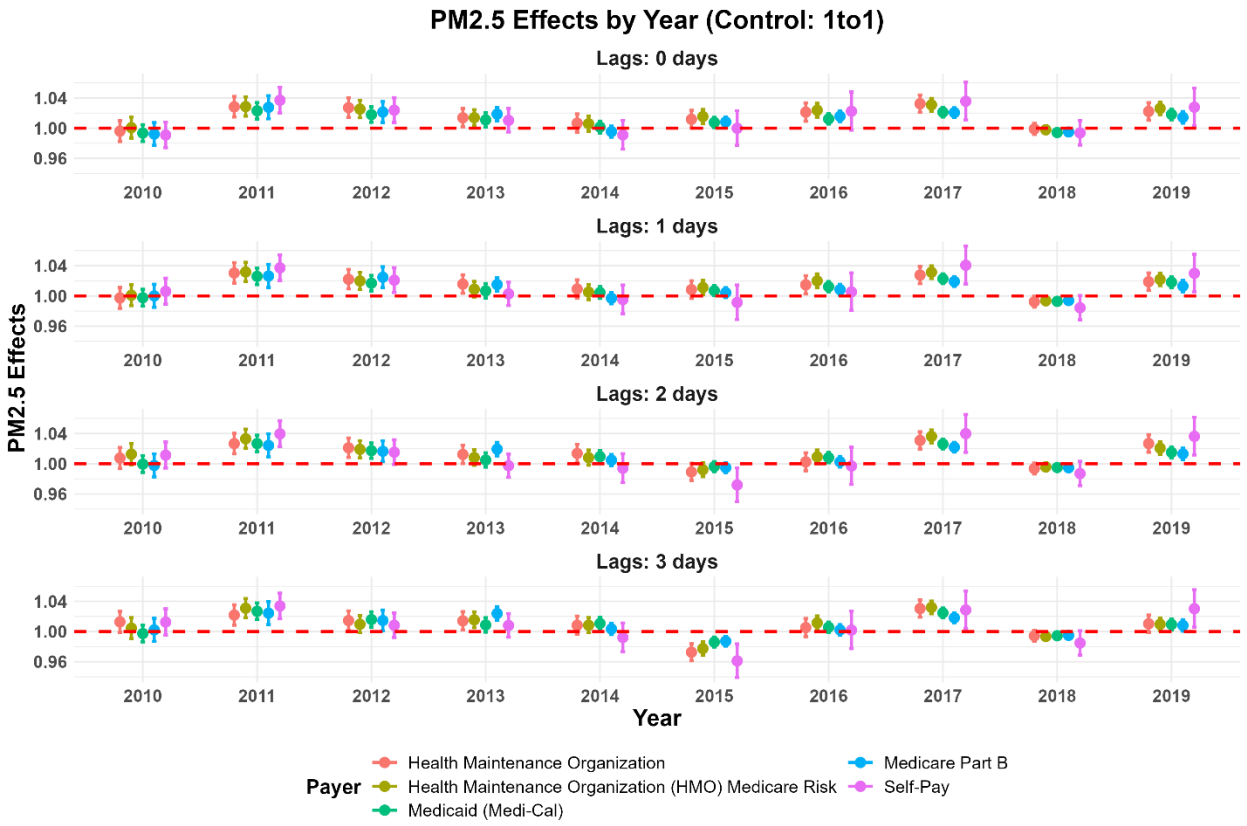

Figure S4. The associations between $PM_{2.5}$ exposure and ED visits for diabetic patients across different health insurance payer categories in California from 2010 to 2019.

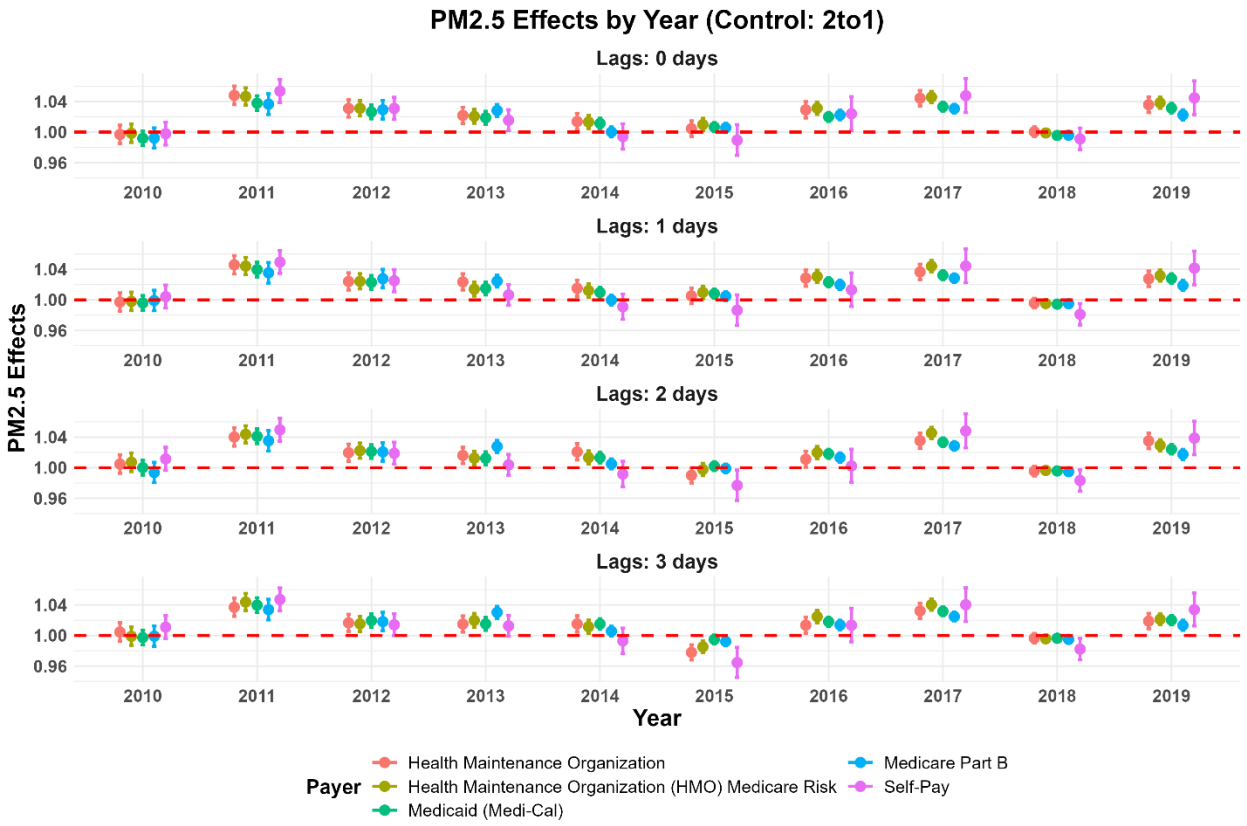

Figure S5. The associations between $PM_{2.5}$ exposure and ED visits for diabetic patients across different health insurance payer categories in California from 2010 to 2019.

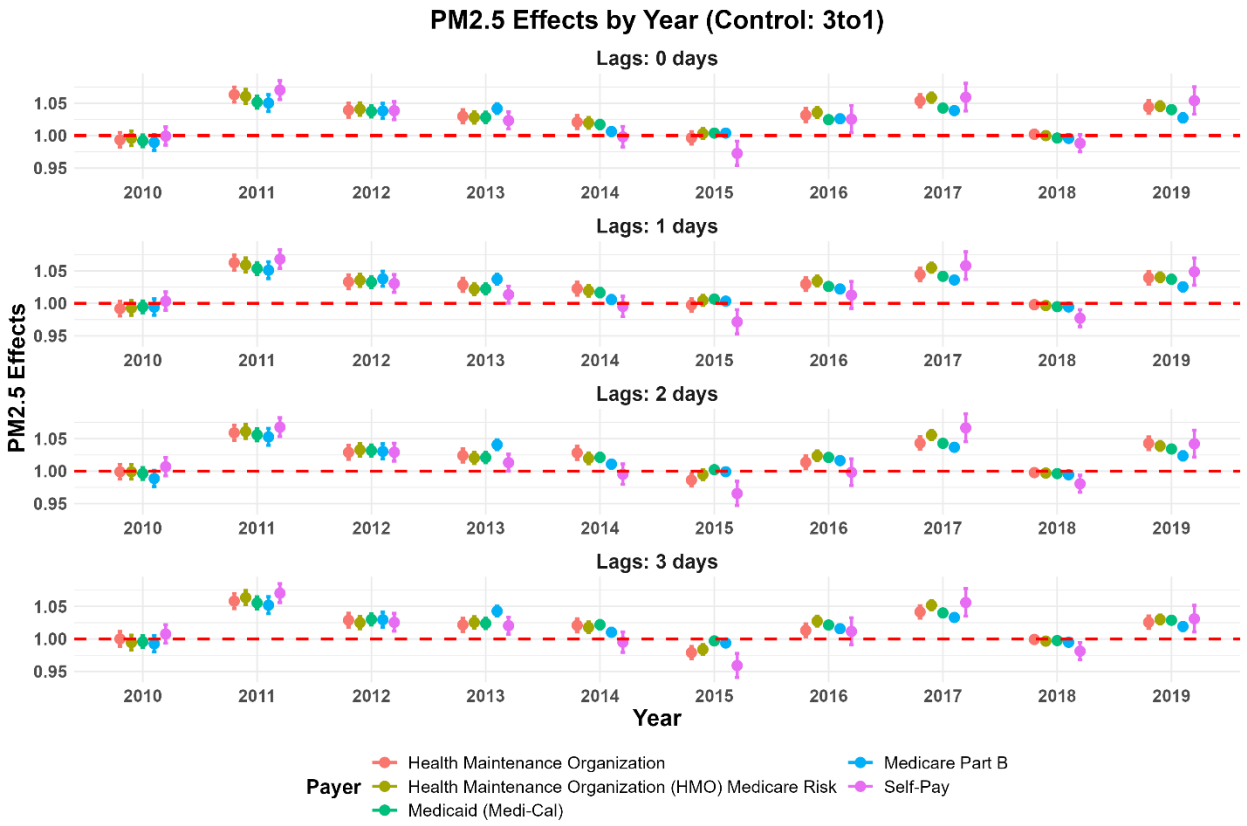

Figure S6. The associations between $PM_{2.5}$ exposure and ED visits for diabetic patients across different health insurance payer categories in California from 2010 to 2019.

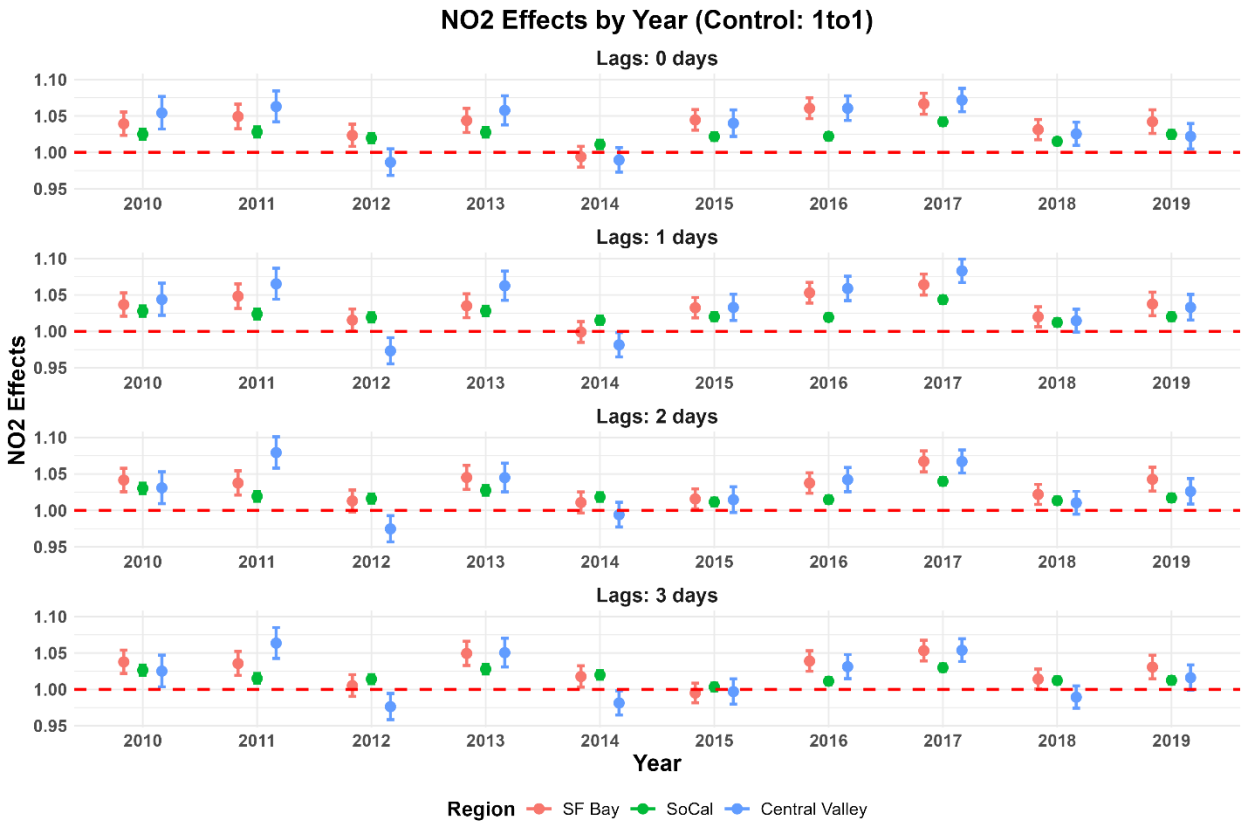

Figure S7. The associations between NO_2 exposure and ED visits for diabetic patients across region categories in California from 2010 to 2019.

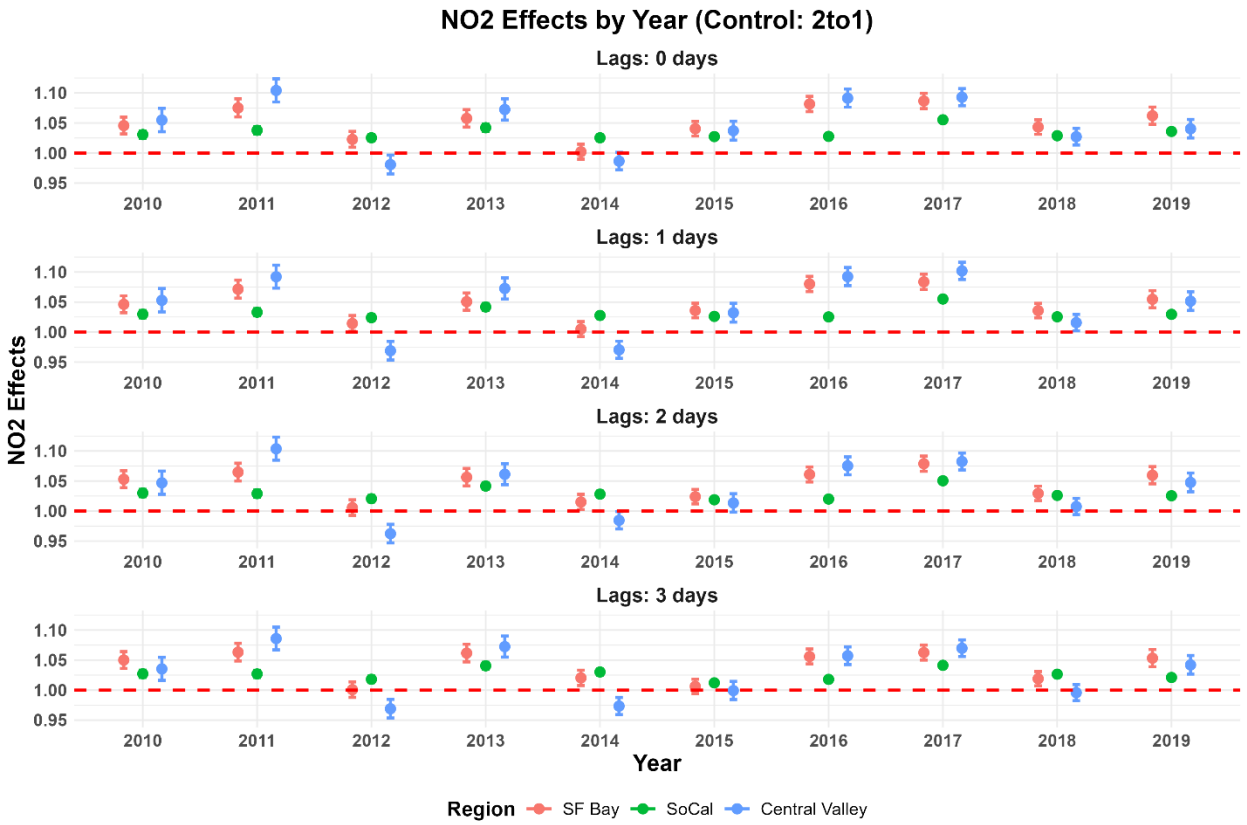

Figure S8. The associations between NO_2 exposure and ED visits for diabetic patients across region categories in California from 2010 to 2019.

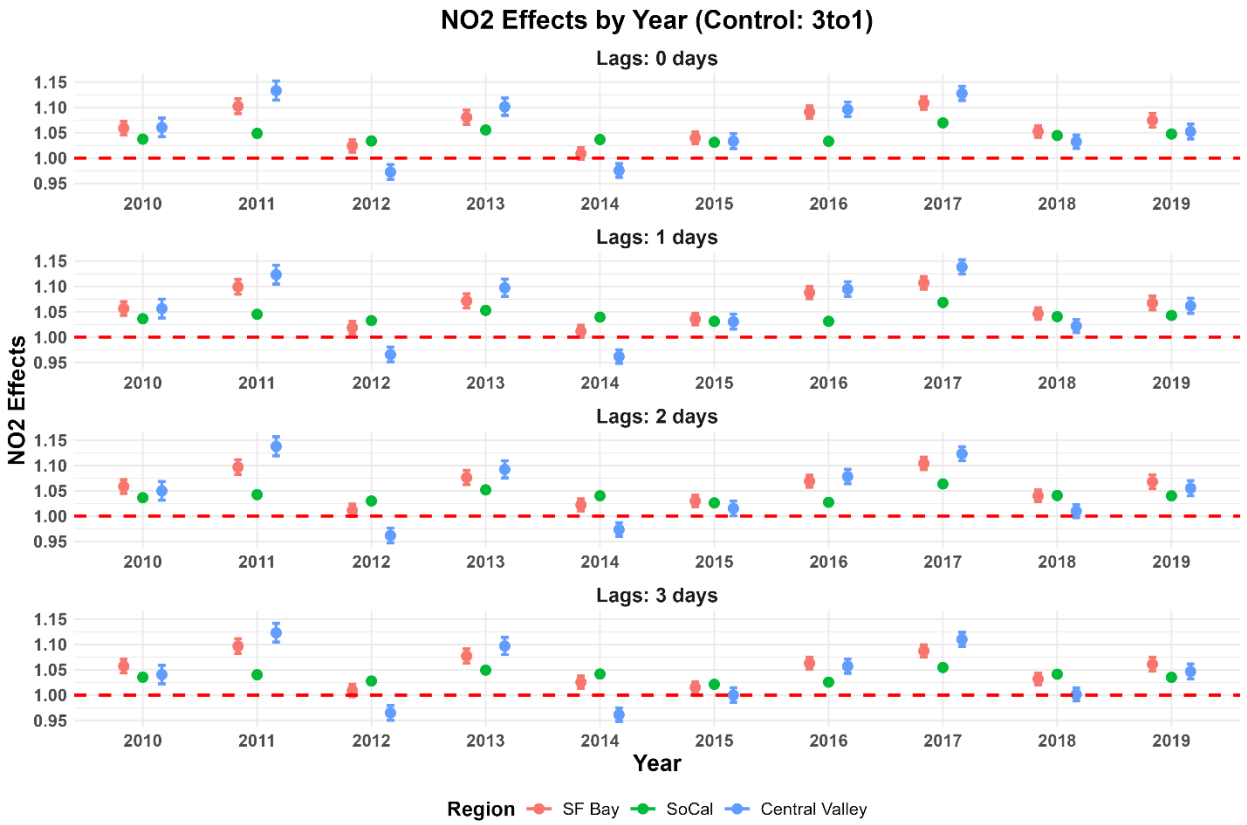

Figure S9. The associations between NO_2 exposure and ED visits for diabetic patients across region categories in California from 2010 to 2019.

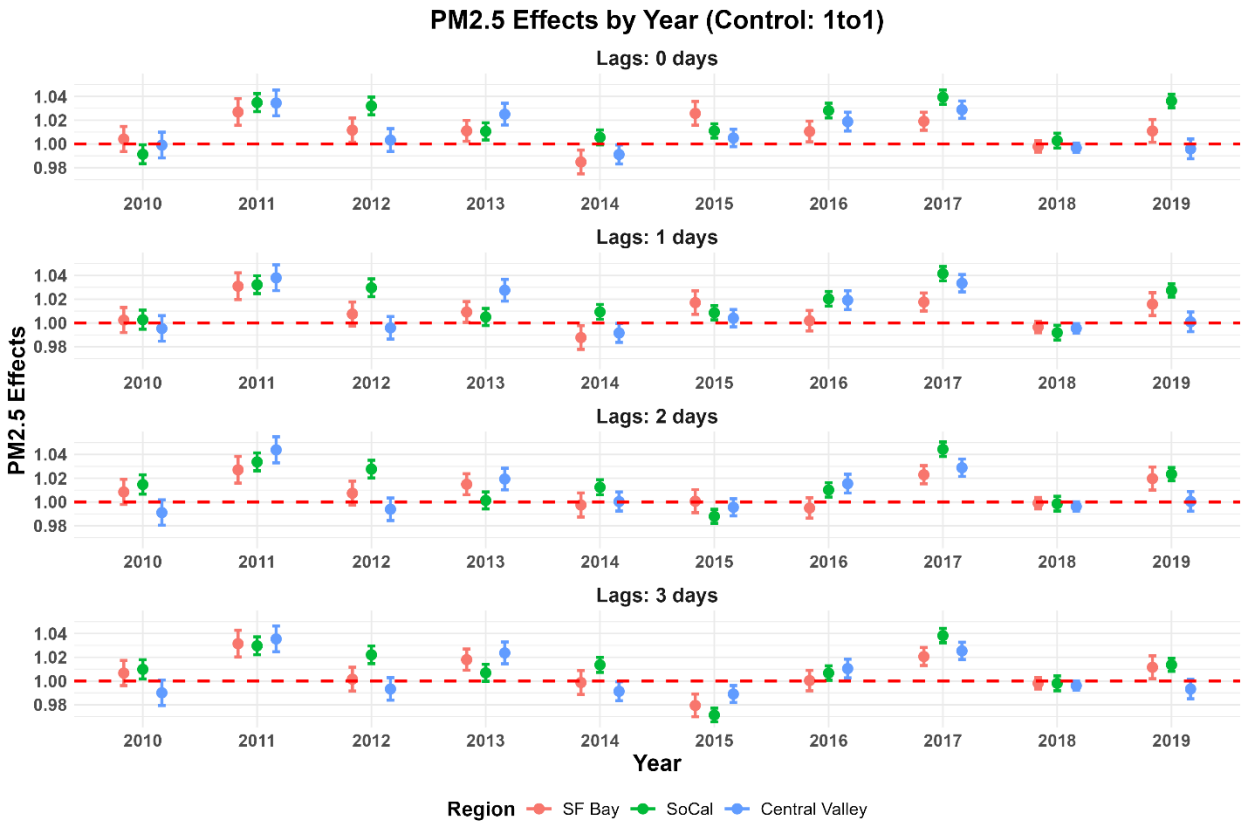

Figure S10. The associations between $PM_{2.5}$ exposure and ED visits for diabetic patients across region categories in California from 2010 to 2019.

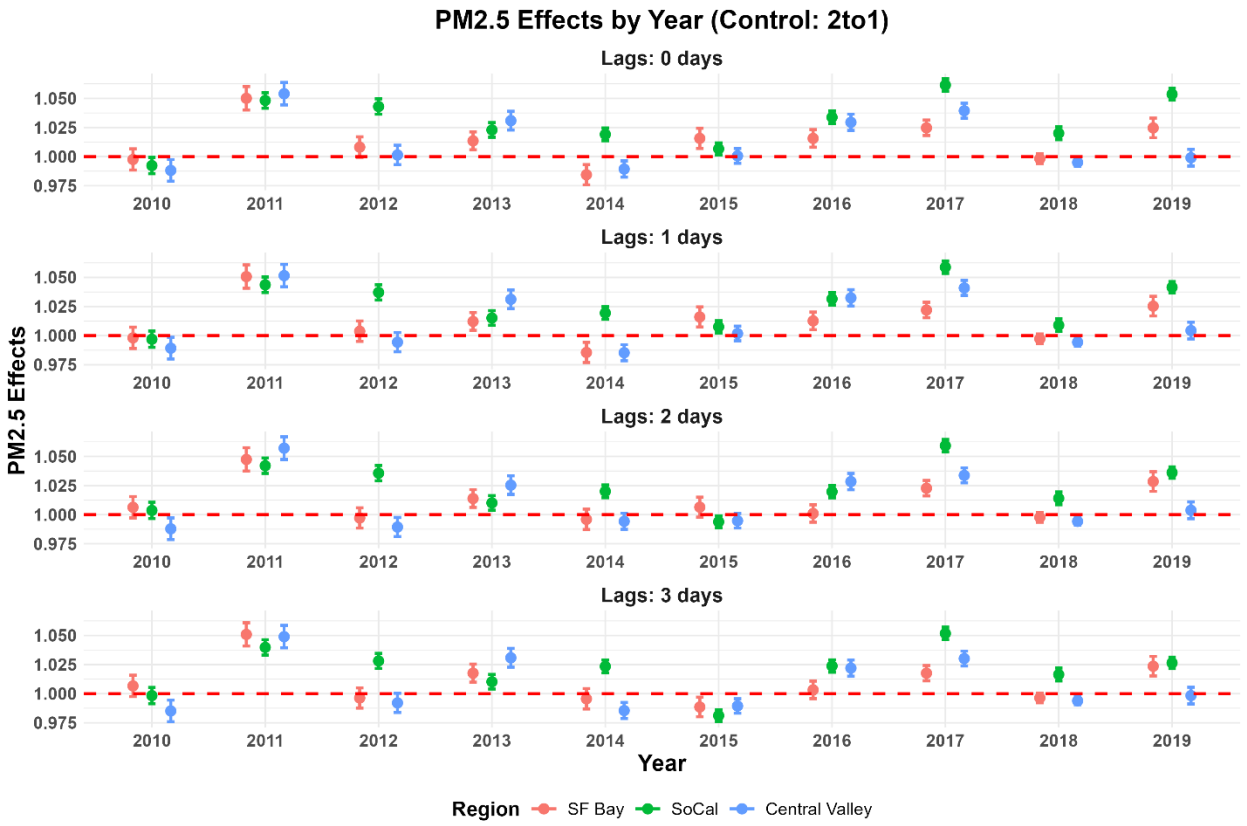

Figure S11. The associations between $PM_{2.5}$ exposure and ED visits for diabetic patients across region categories in California from 2010 to 2019.

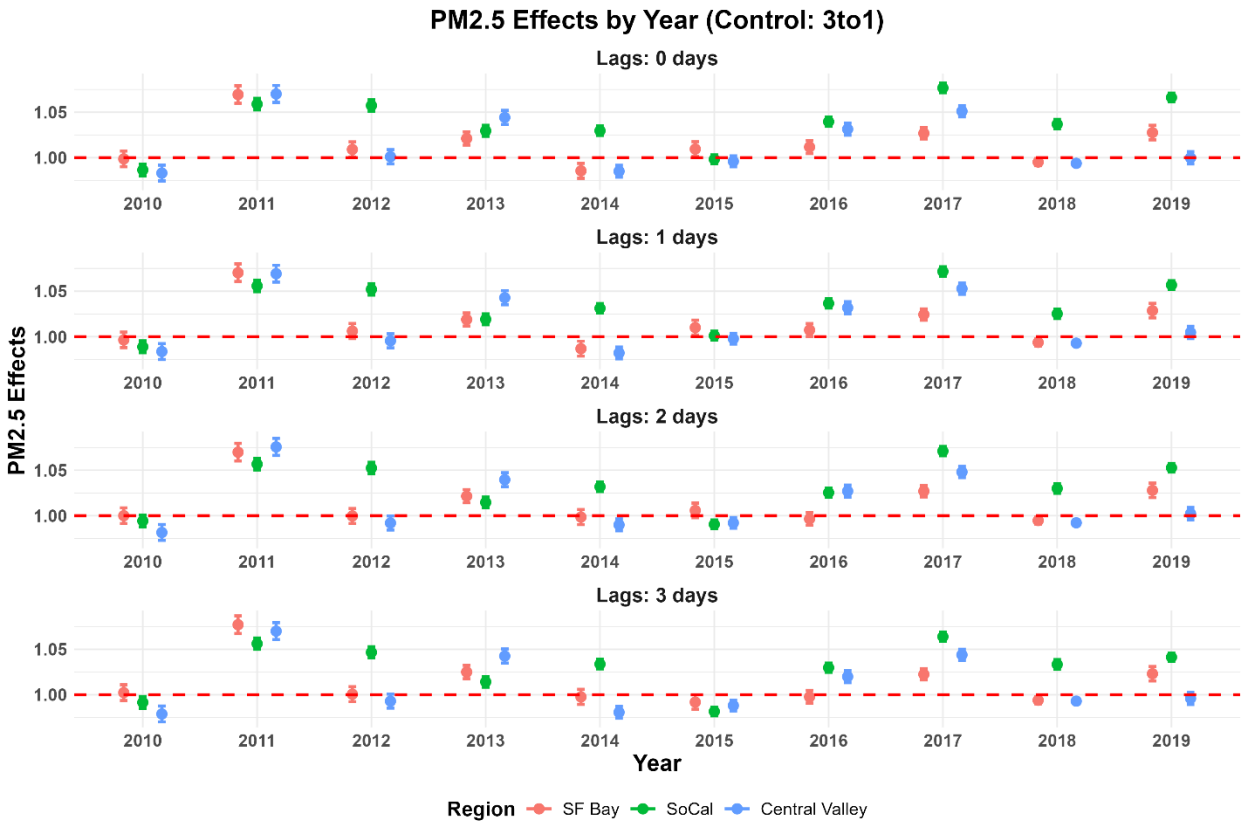

Figure S12. The associations between $PM_{2.5}$ exposure and ED visits for diabetic patients across region categories in California from 2010 to 2019.

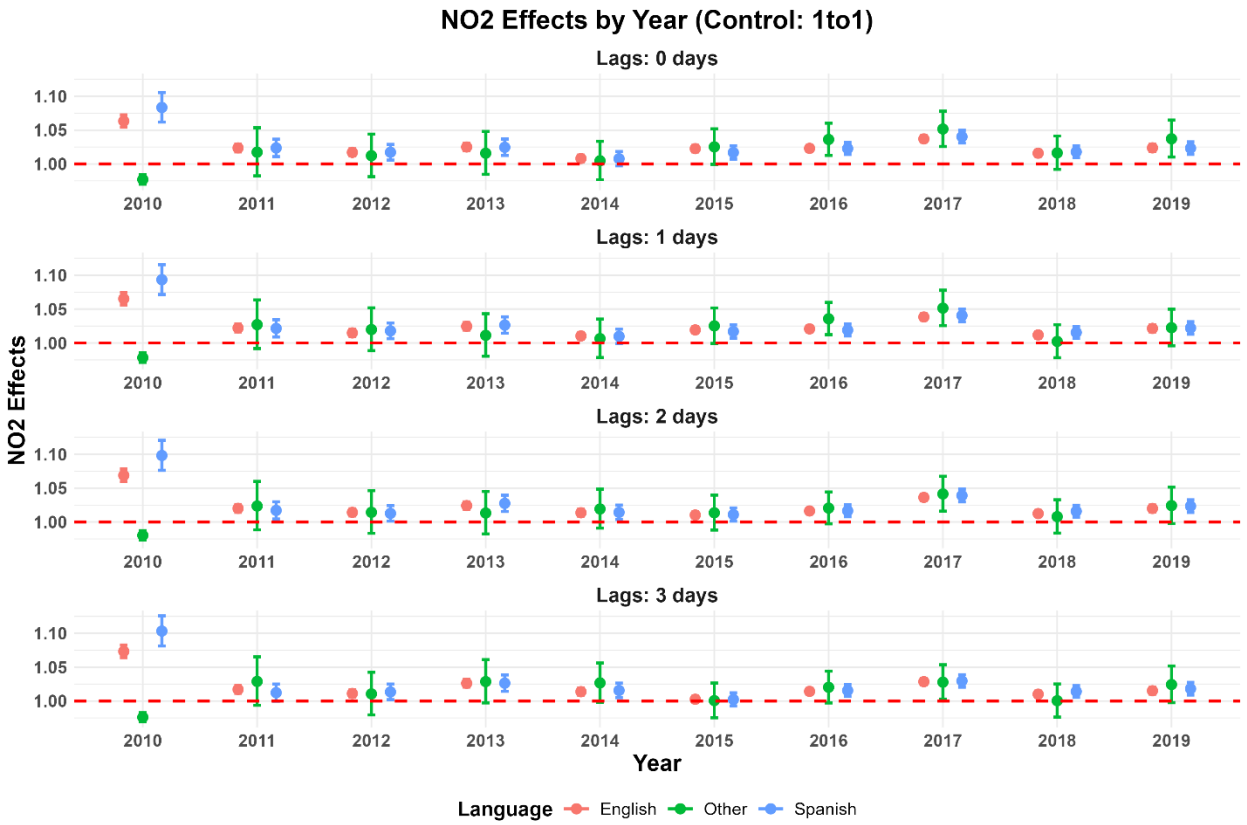

Figure S13. The associations between NO_2 exposure and ED visits for diabetic patients across language categories in California from 2010 to 2019.

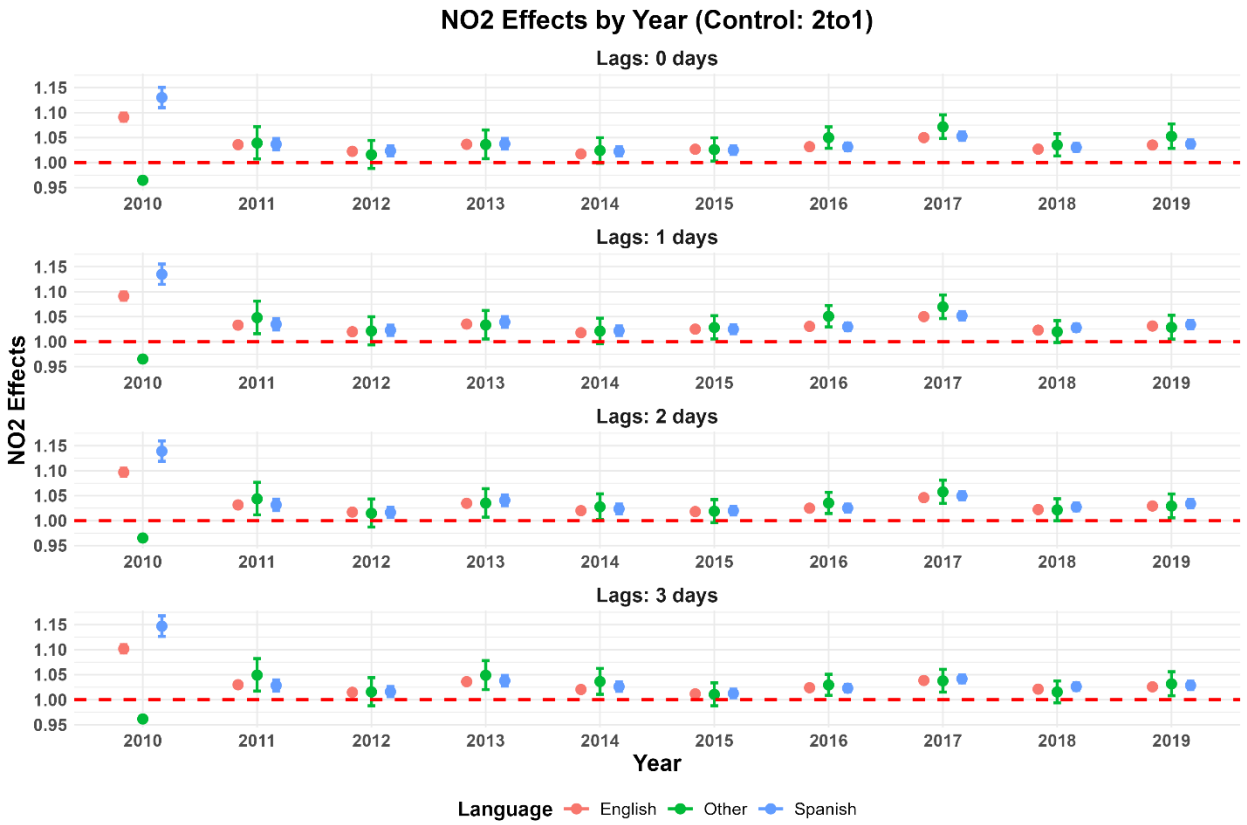

Figure S14. The associations between NO_2 exposure and ED visits for diabetic patients across language categories in California from 2010 to 2019.

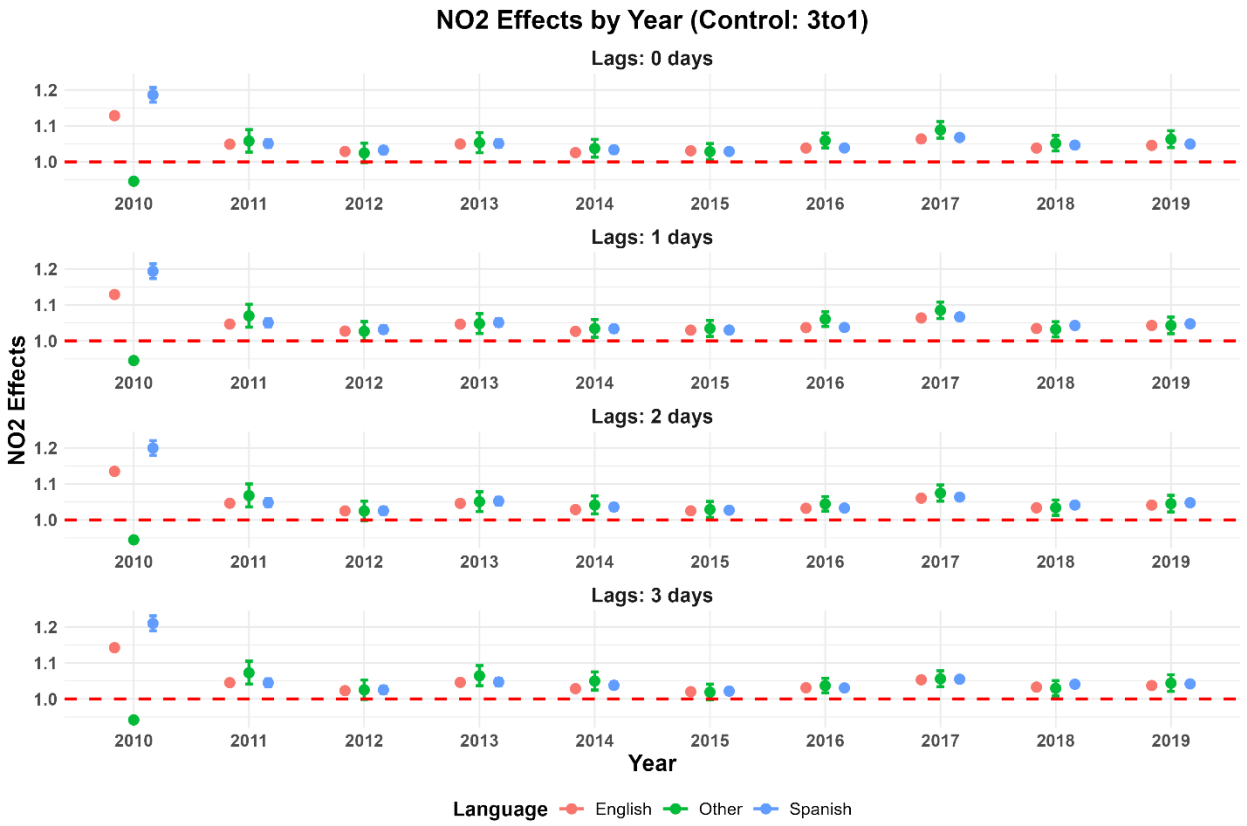

Figure S15. The associations between NO_2 exposure and ED visits for diabetic patients across language categories in California from 2010 to 2019.

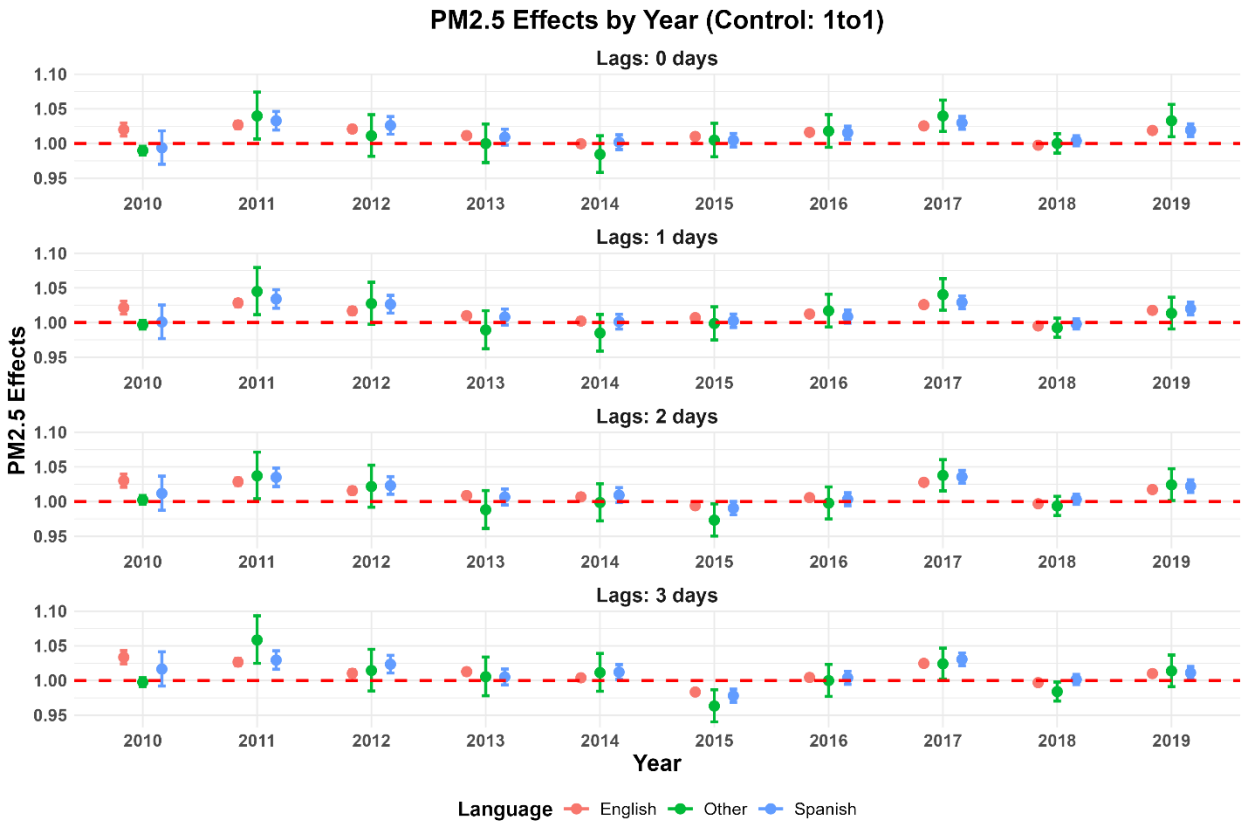

Figure S16. The associations between $PM_{2.5}$ exposure and ED visits for diabetic patients across language categories in California from 2010 to 2019.

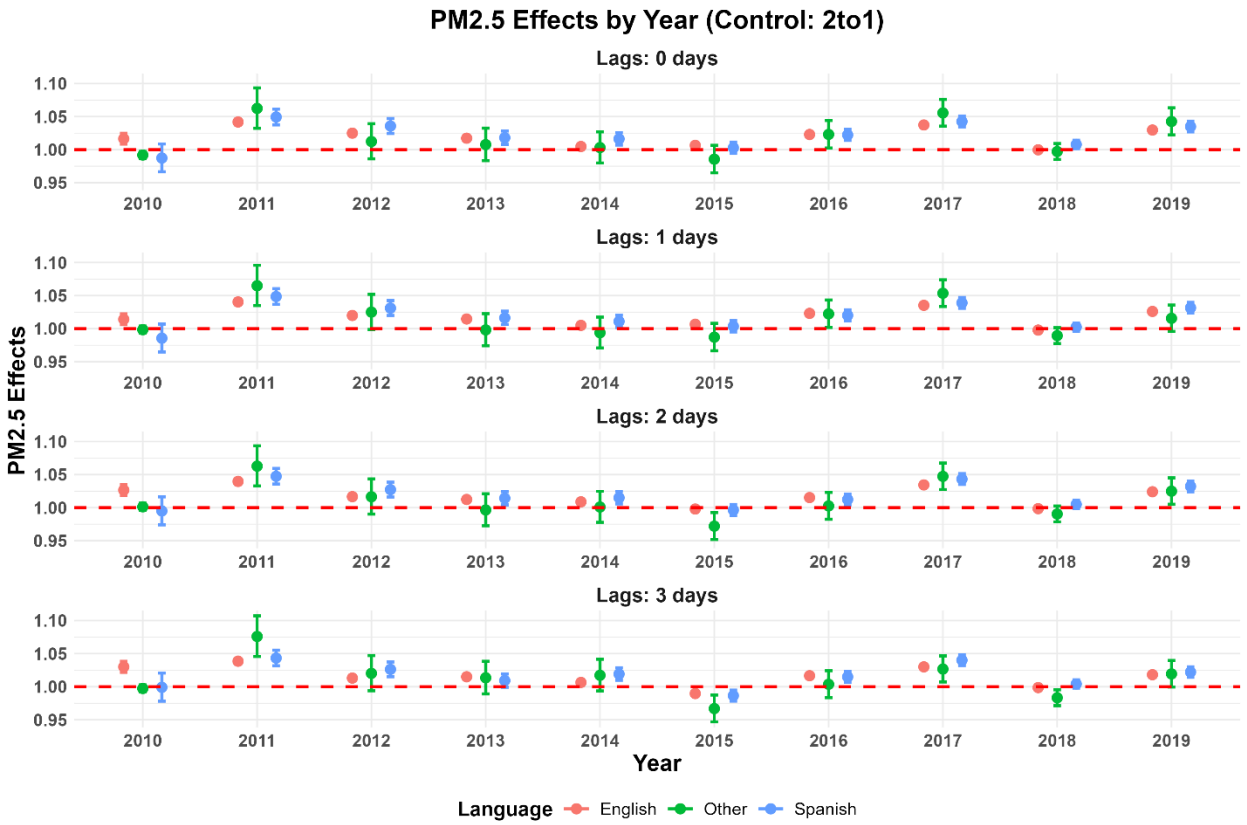

Figure S17. The associations between $PM_{2.5}$ exposure and ED visits for diabetic patients across language categories in California from 2010 to 2019.

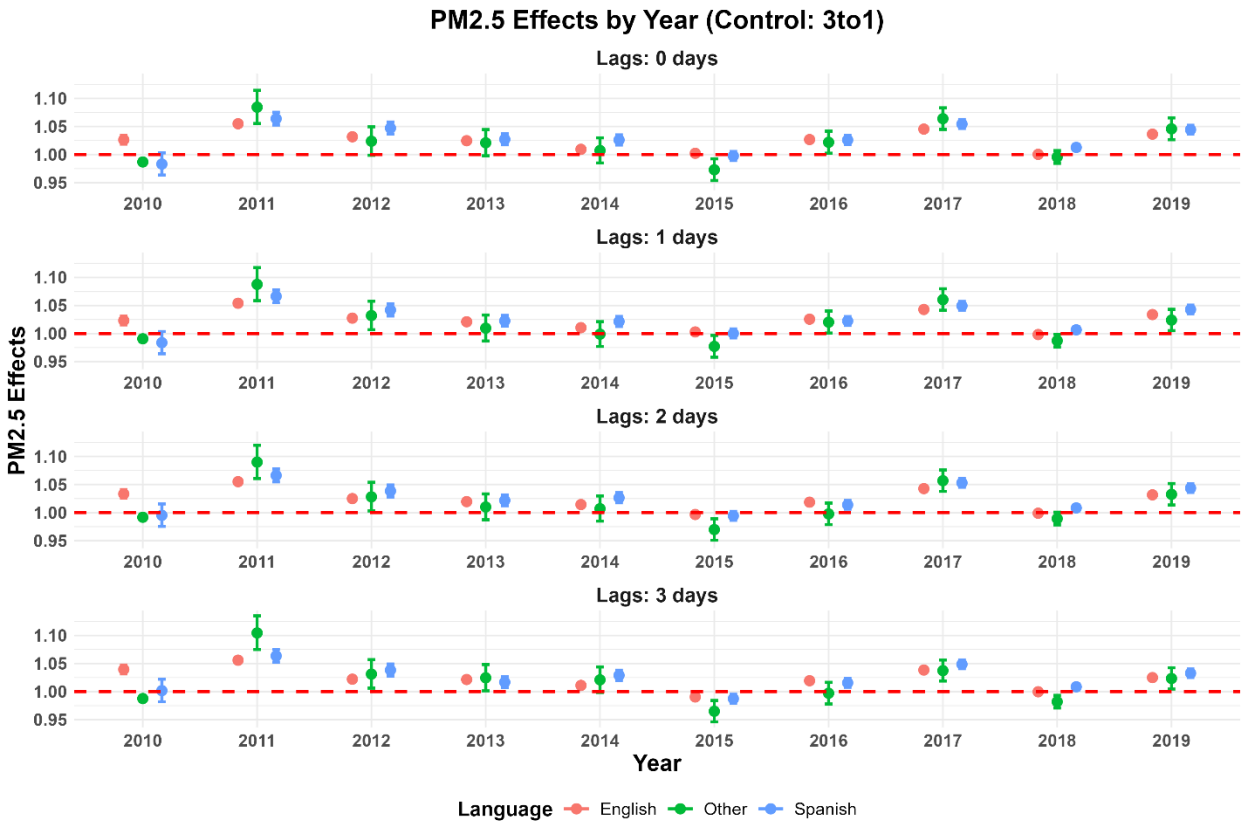

Figure S18. The associations between $PM_{2.5}$ exposure and ED visits for diabetic patients across language categories in California from 2010 to 2019.

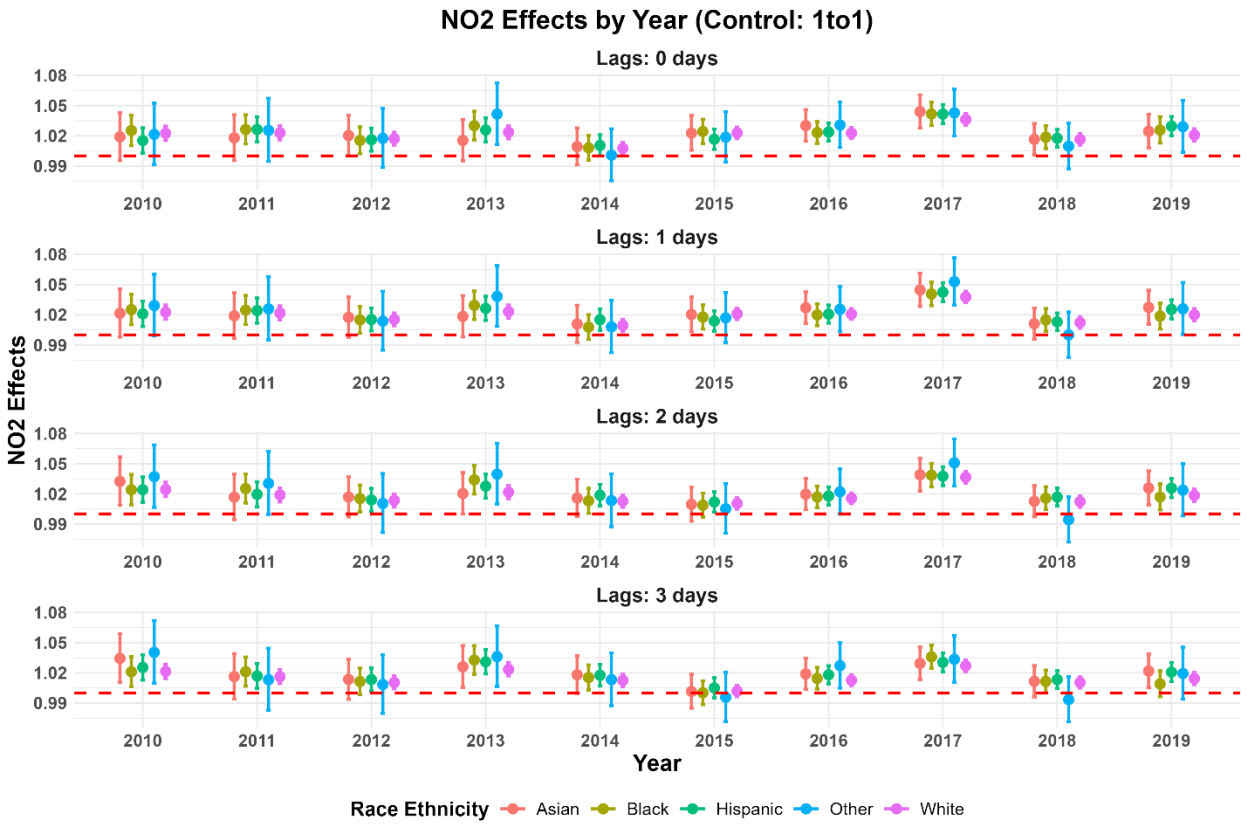

Figure S19. The associations between NO_2 exposure and ED visits for diabetic patients across five major race categories in California from 2010 to 2019.

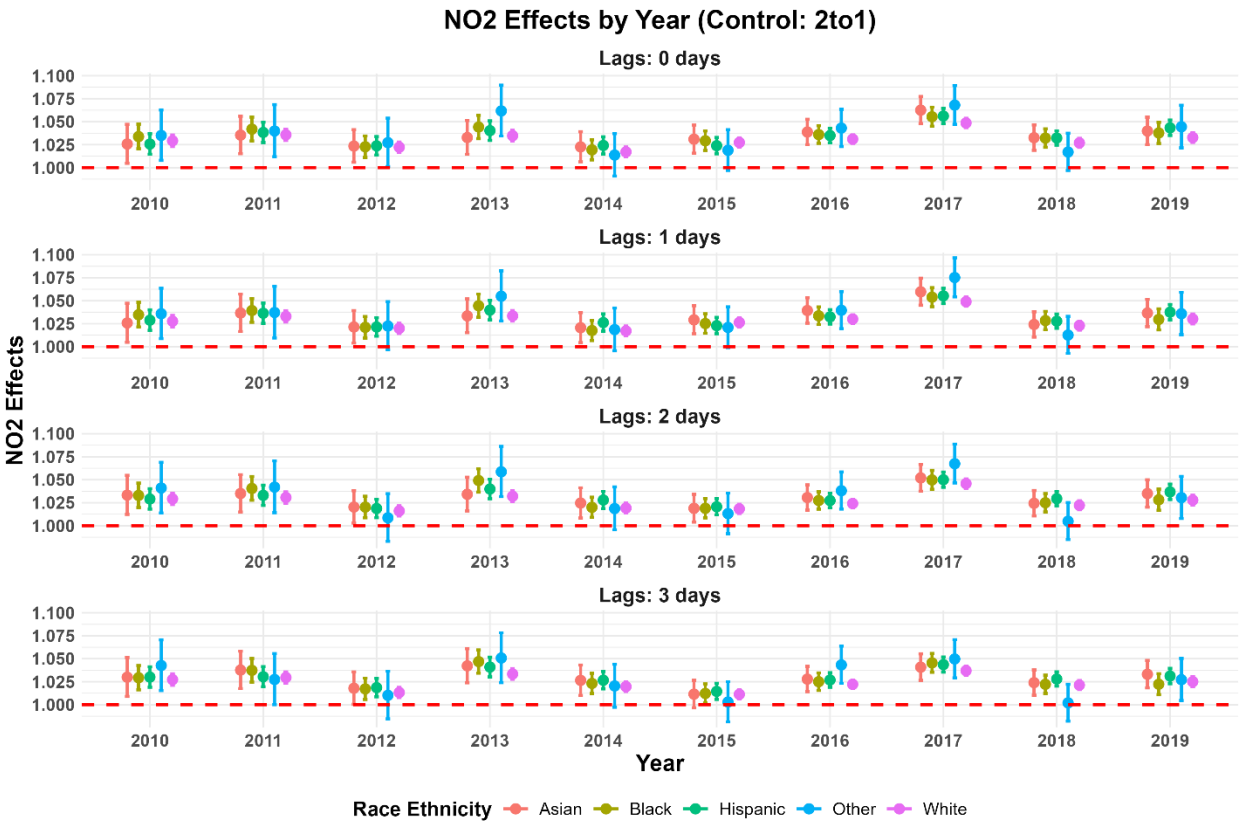

Figure S20. The associations between NO_2 exposure and ED visits for diabetic patients across five major race categories in California from 2010 to 2019.

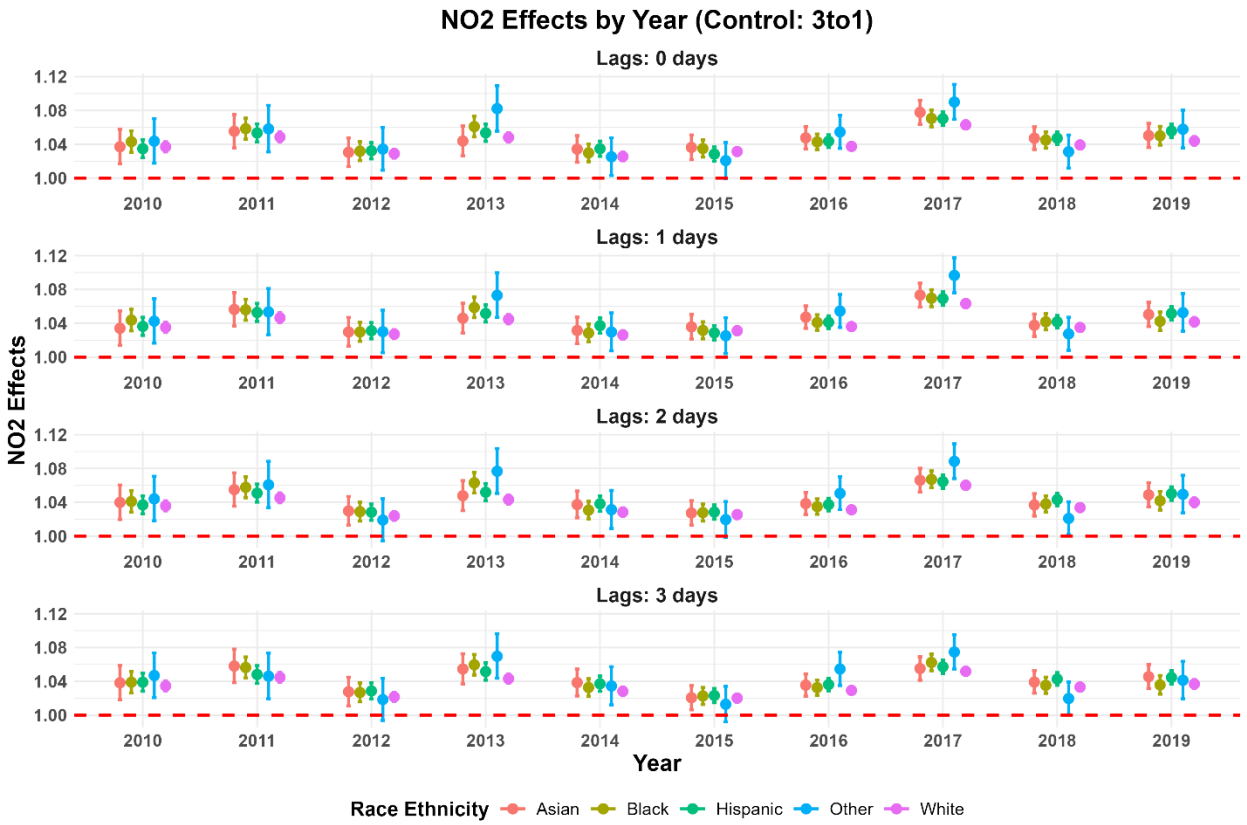

Figure S21. The associations between NO_2 exposure and ED visits for diabetic patients across five major race categories in California from 2010 to 2019.

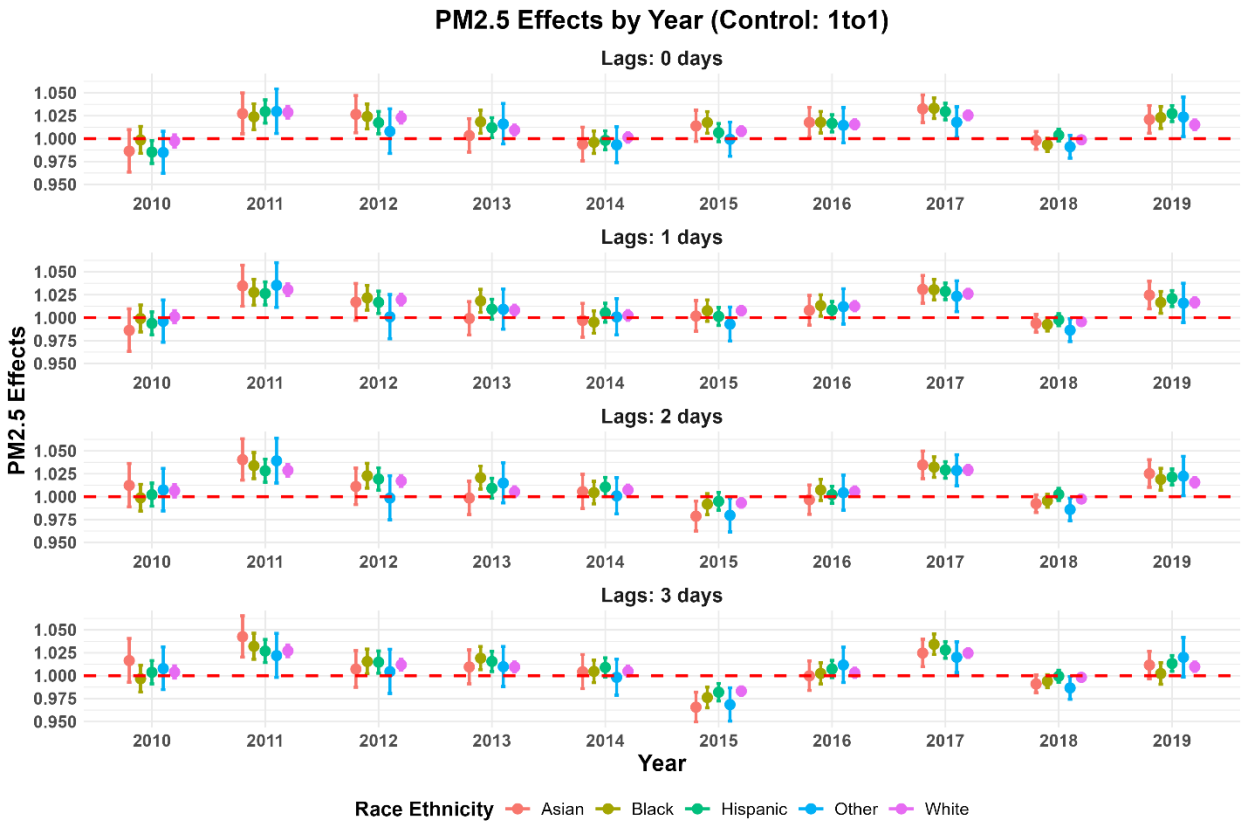

Figure S22. The associations between $PM_{2.5}$ exposure and ED visits for diabetic patients across five major race categories in California from 2010 to 2019.

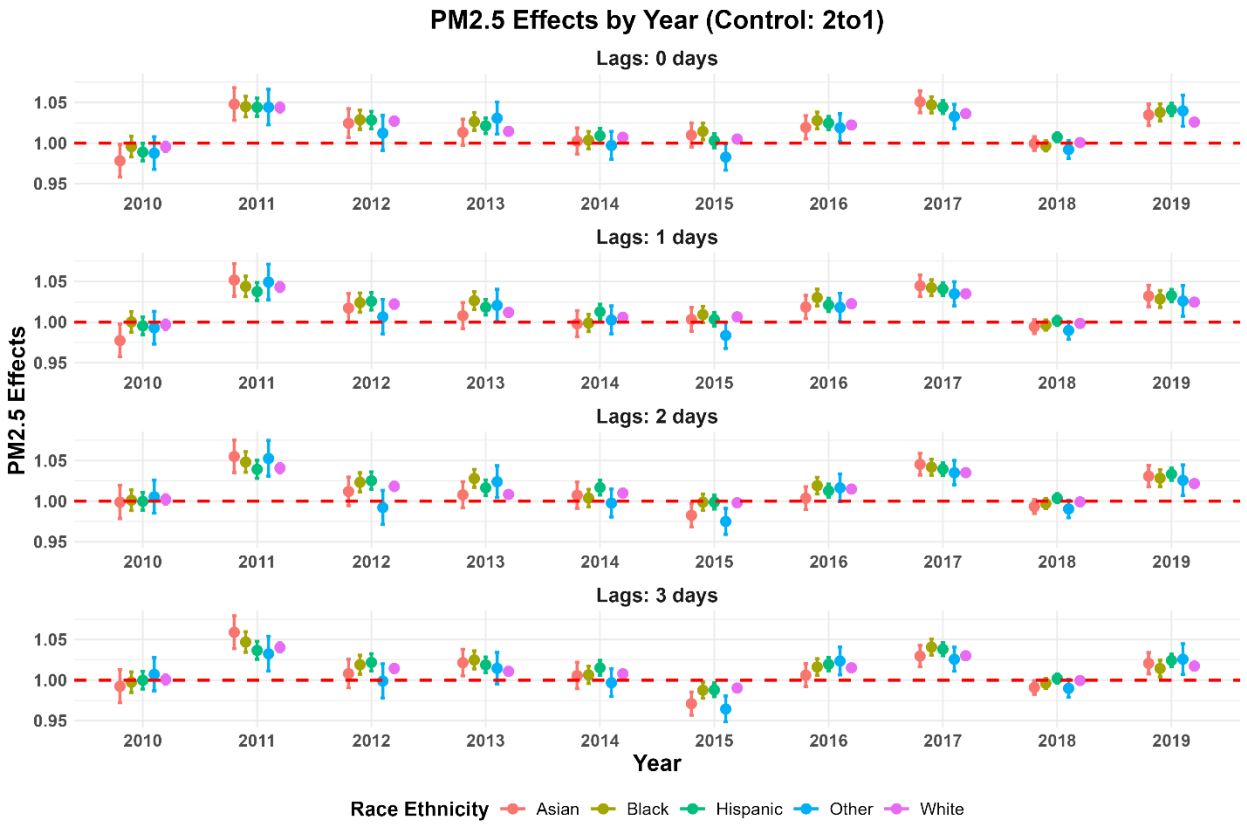

Figure S23. The associations between $PM_{2.5}$ exposure and ED visits for diabetic patients across five major race categories in California from 2010 to 2019.

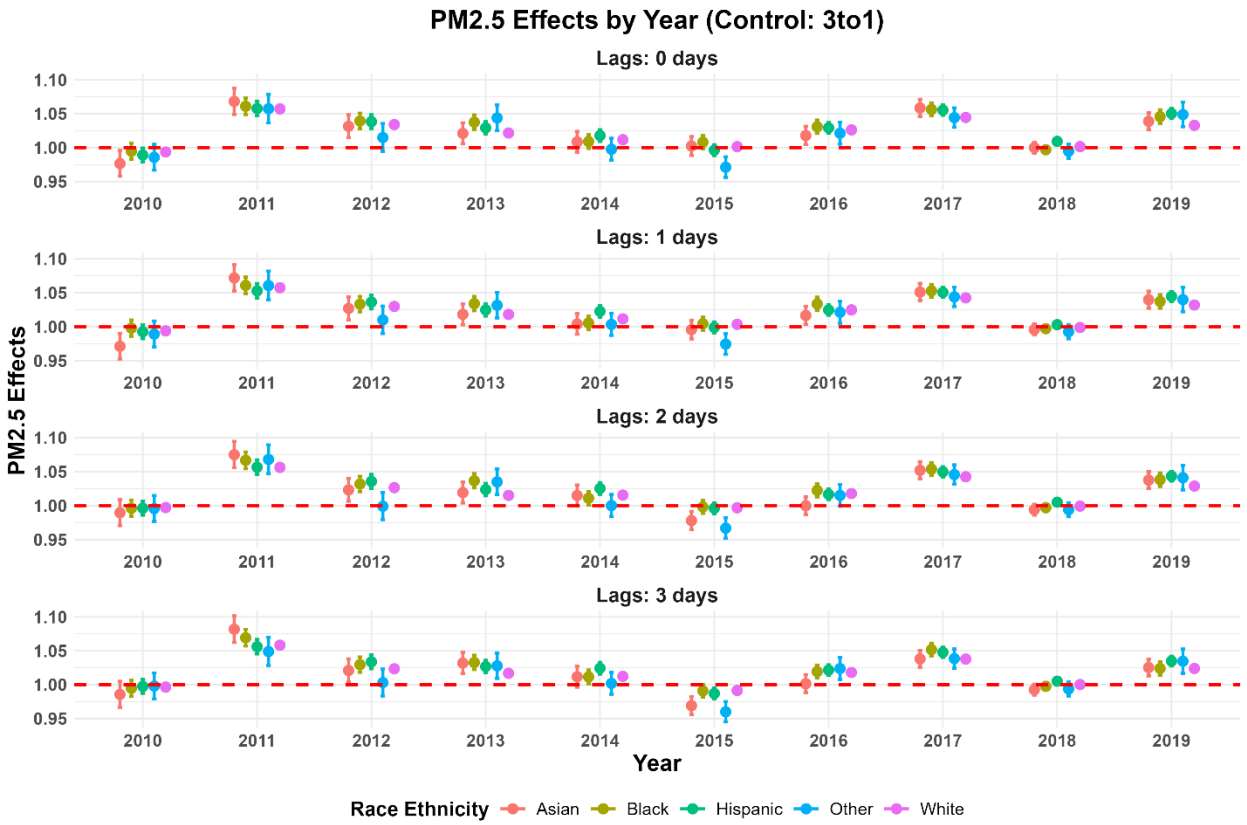

Figure S24. The associations between $PM_{2.5}$ exposure and ED visits for diabetic patients across five major race categories in California from 2010 to 2019.

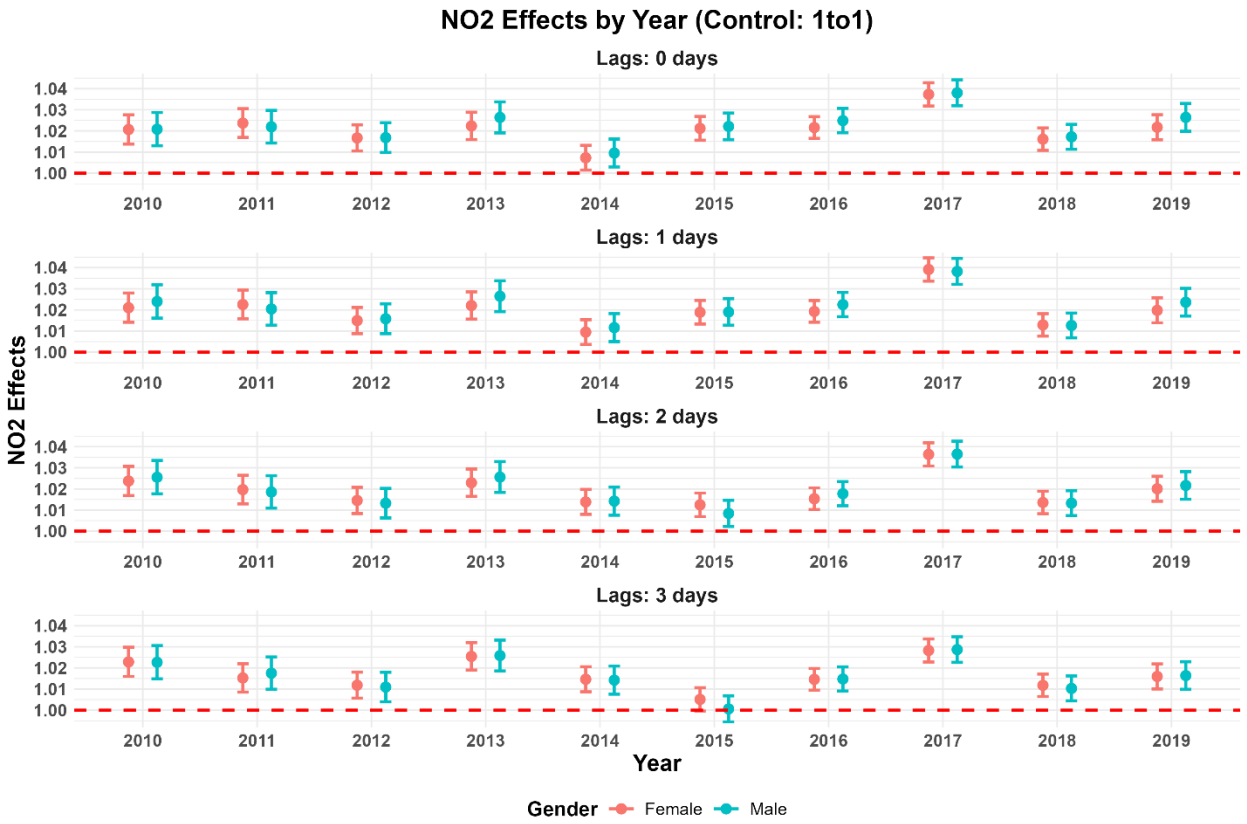

Figure S25. The associations between NO_2 exposure and ED visits for diabetic patients across gender categories in California from 2010 to 2019.

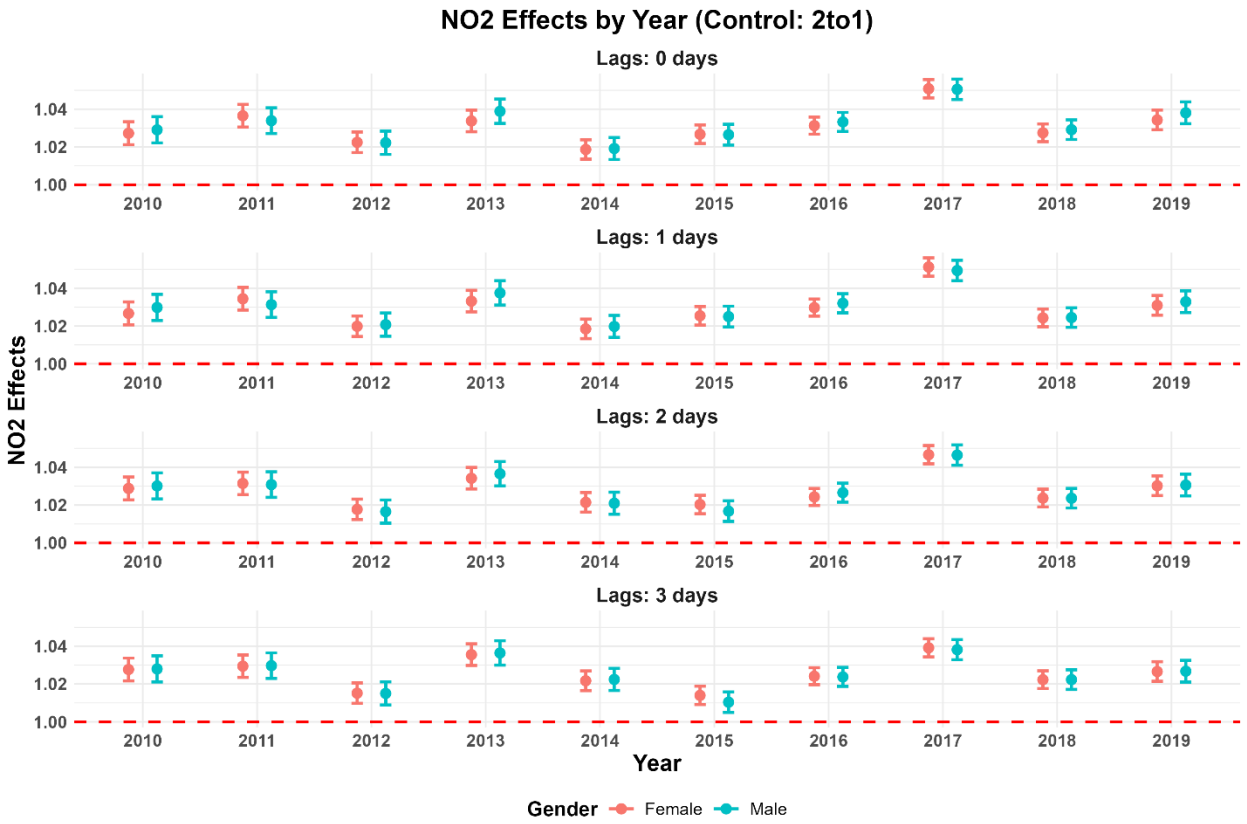

Figure S26. The associations between NO_2 exposure and ED visits for diabetic patients across gender categories in California from 2010 to 2019.

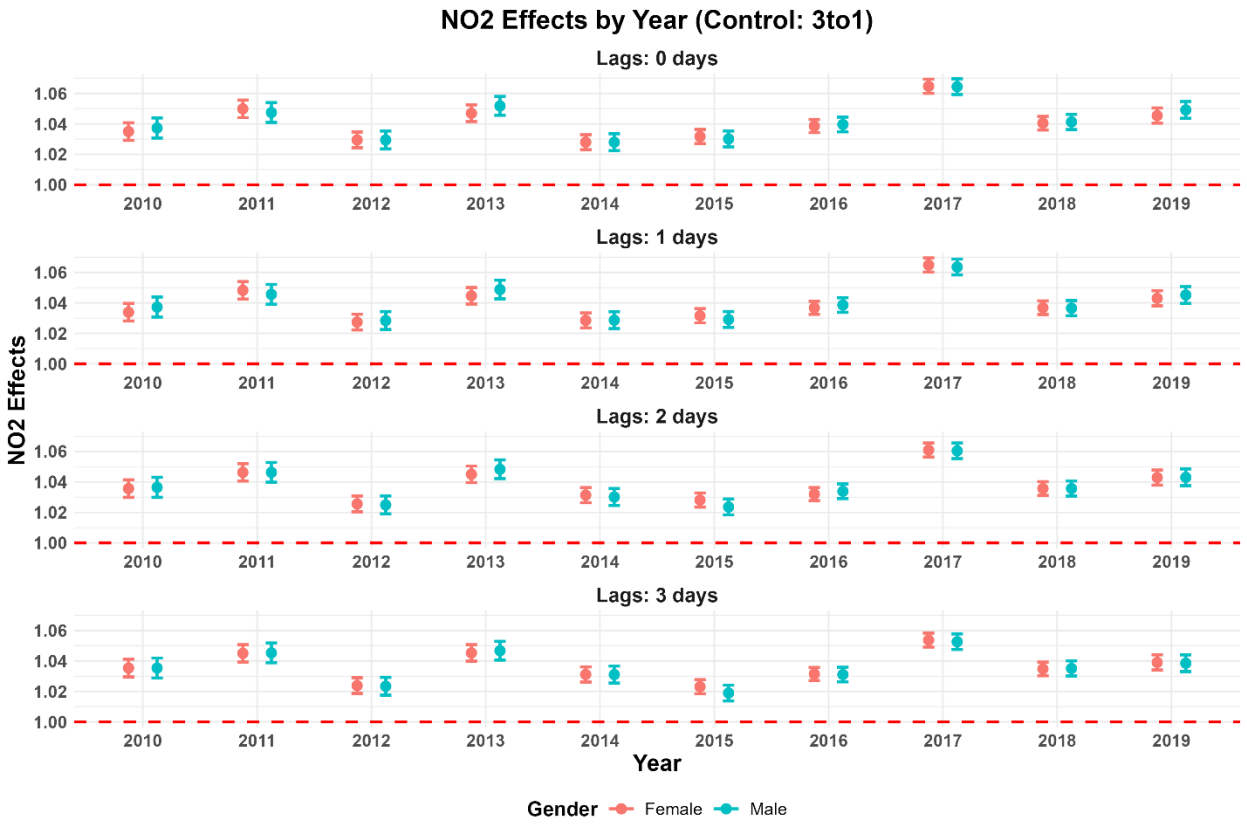

Figure S27. The associations between NO_2 exposure and ED visits for diabetic patients across gender categories in California from 2010 to 2019.

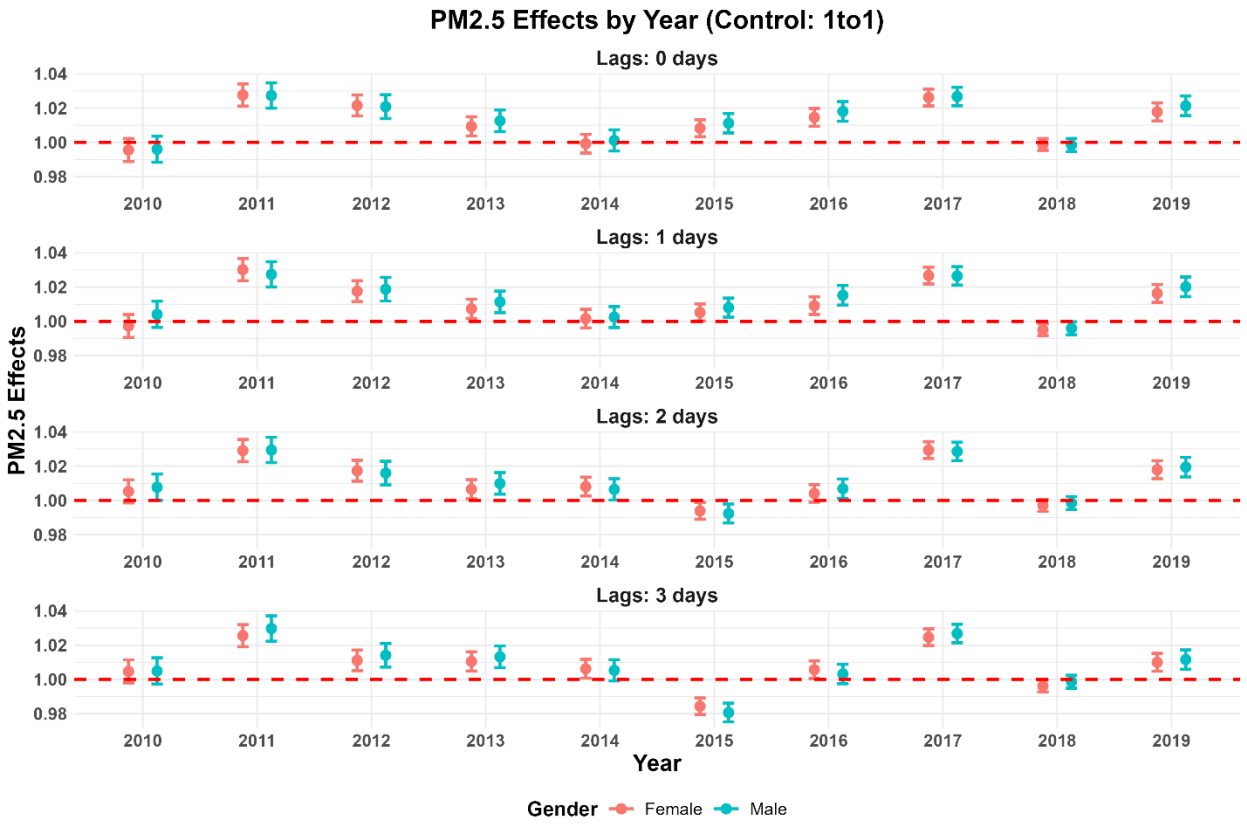

Figure S28. The associations between $PM_{2.5}$ exposure and ED visits for diabetic patients across gender categories in California from 2010 to 2019.

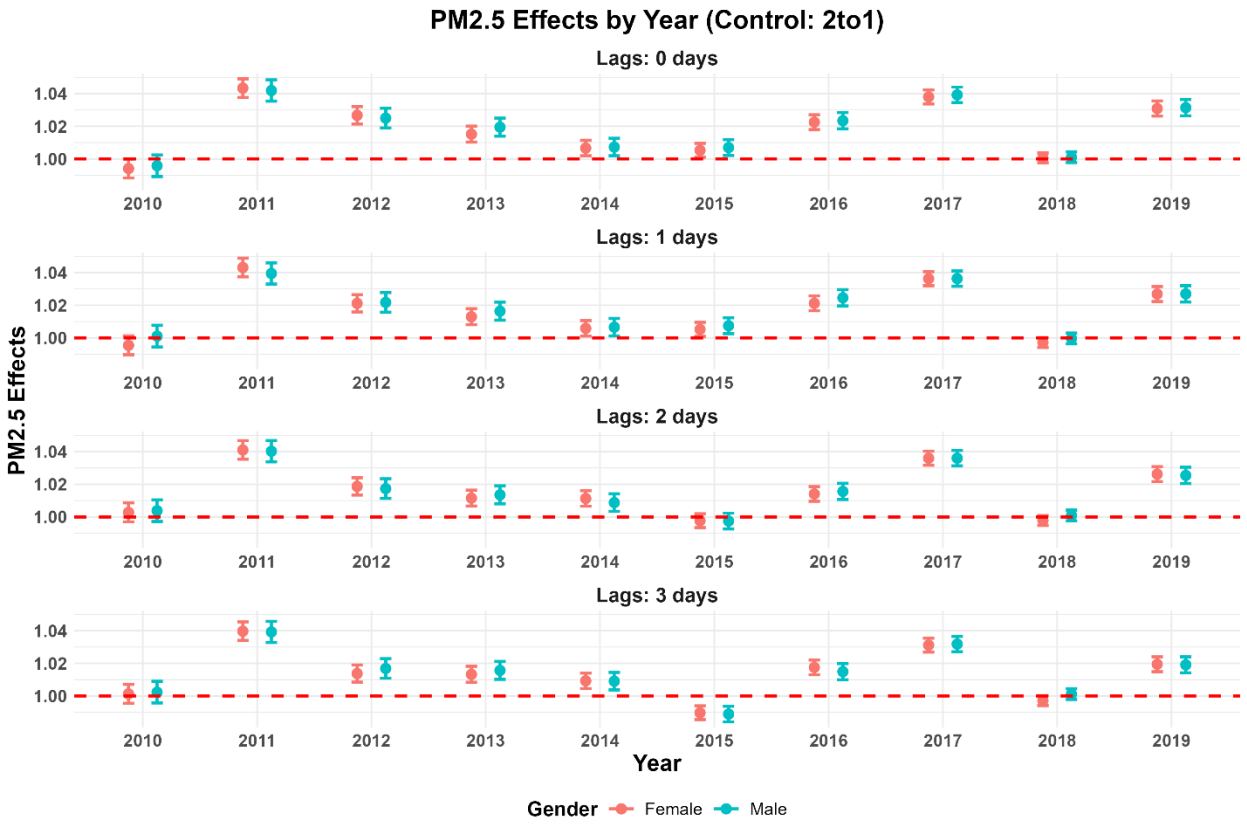

Figure S29. The associations between $PM_{2.5}$ exposure and ED visits for diabetic patients across gender categories in California from 2010 to 2019.

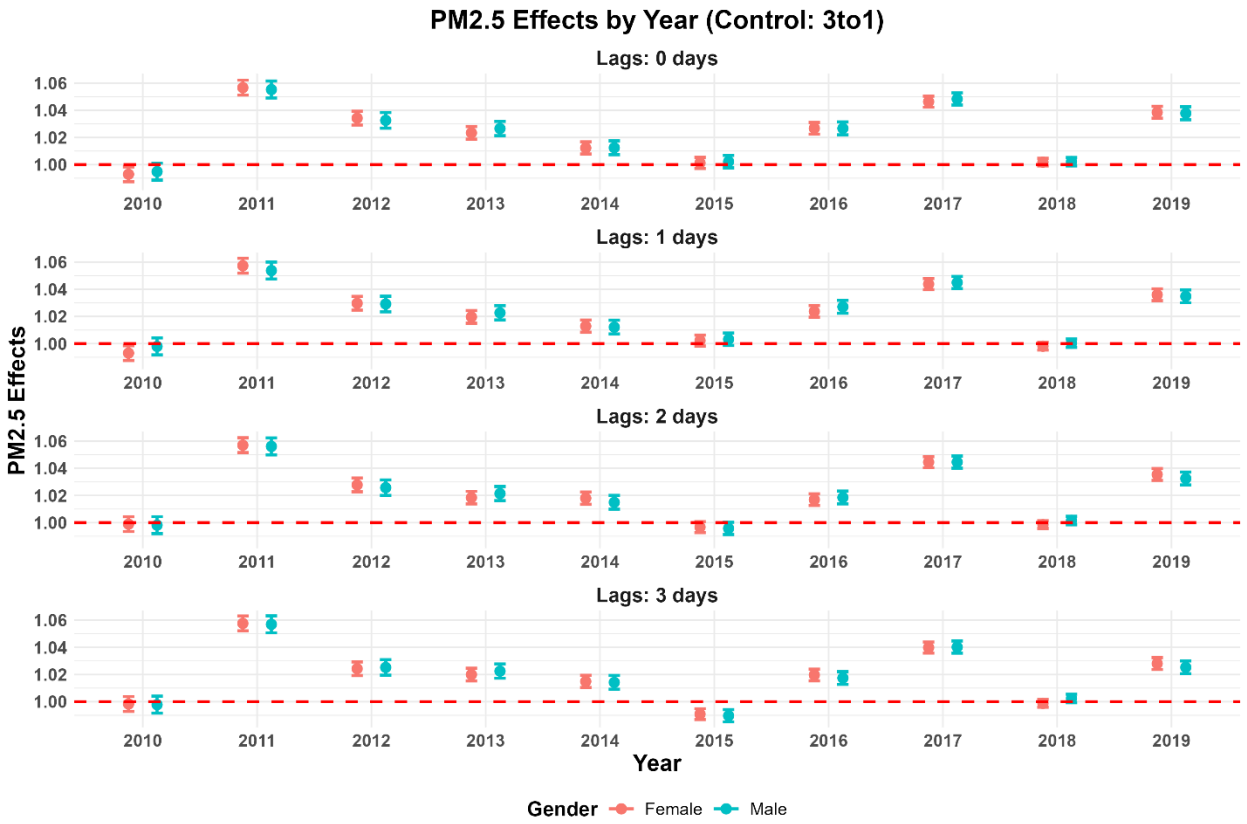

Figure S30. The associations between $PM_{2.5}$ exposure and ED visits for diabetic patients across gender categories in California from 2010 to 2019.

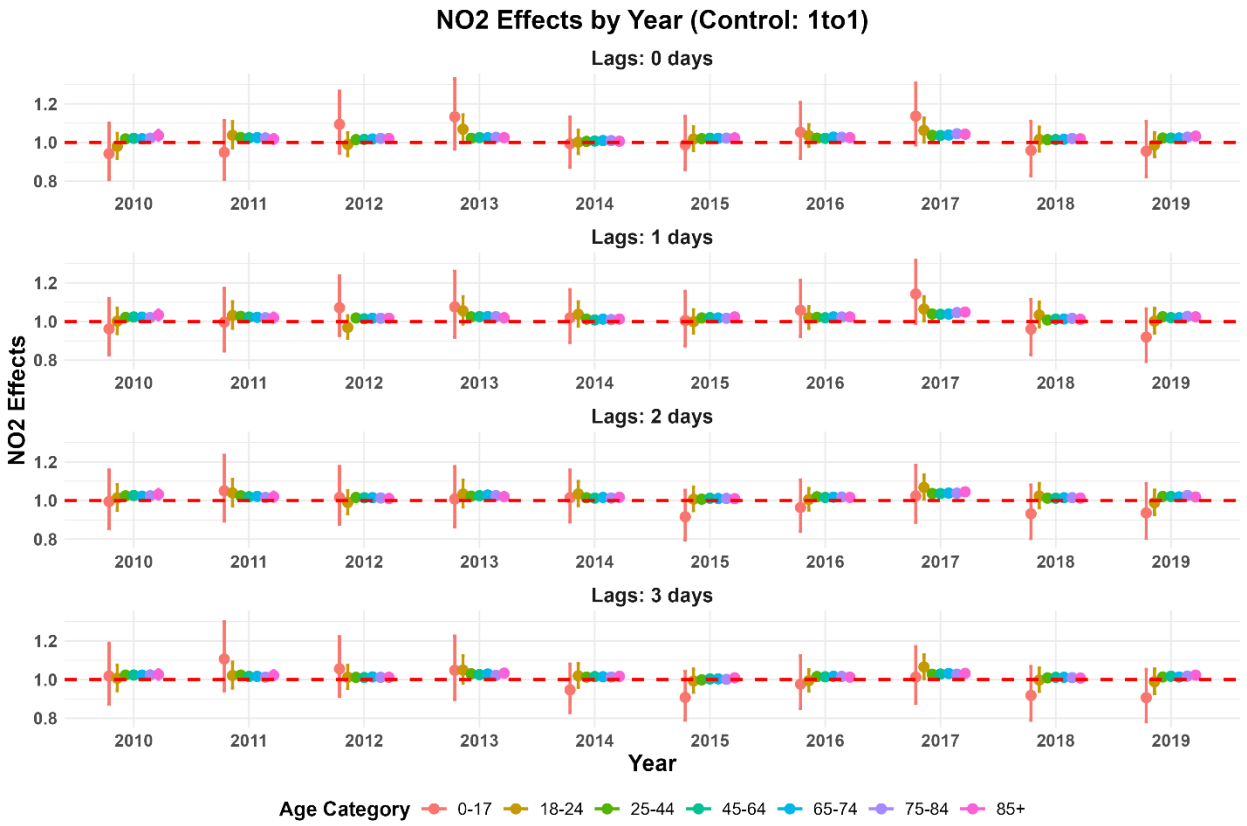

Figure S31. The associations between NO_2 exposure and ED visits for diabetic patients across age categories in California from 2010 to 2019.

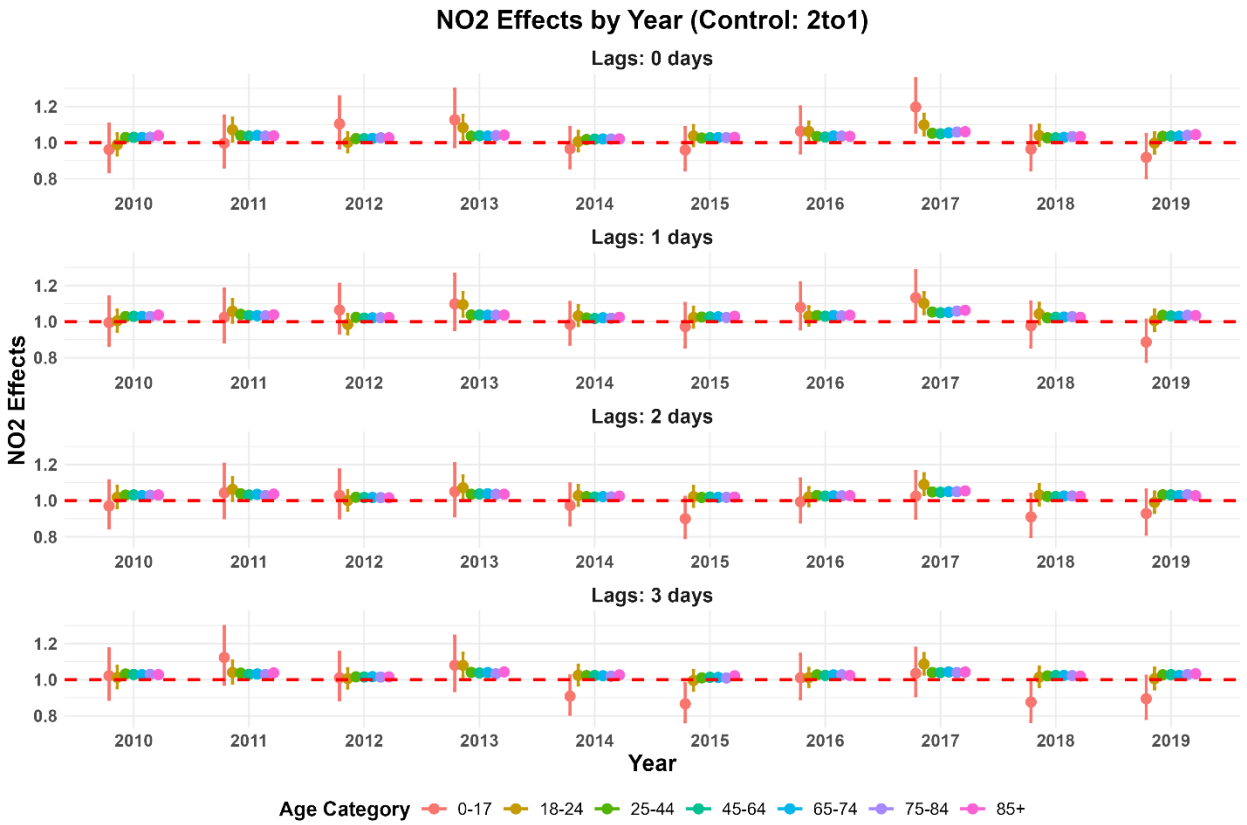

Figure S32. The associations between NO_2 exposure and ED visits for diabetic patients across age categories in California from 2010 to 2019.

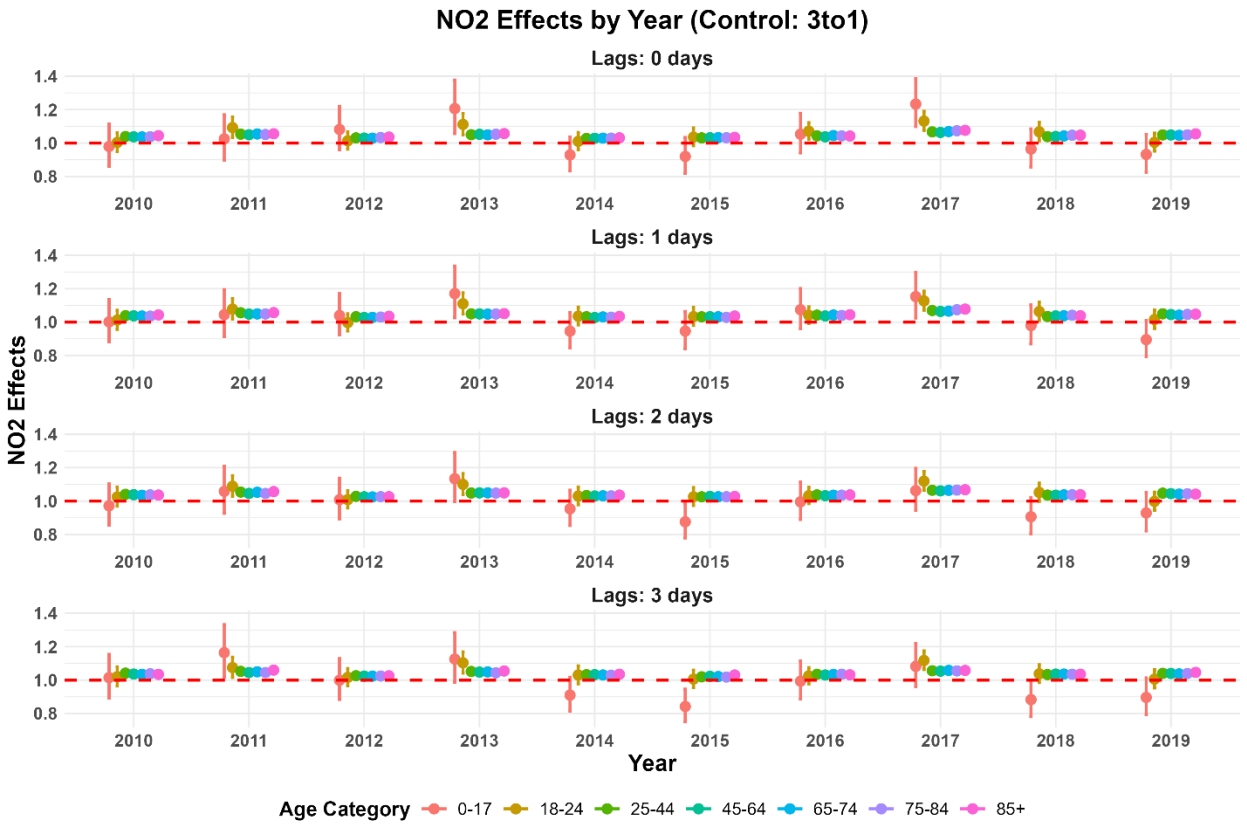

Figure S33. The associations between NO_2 exposure and ED visits for diabetic patients across age categories in California from 2010 to 2019.

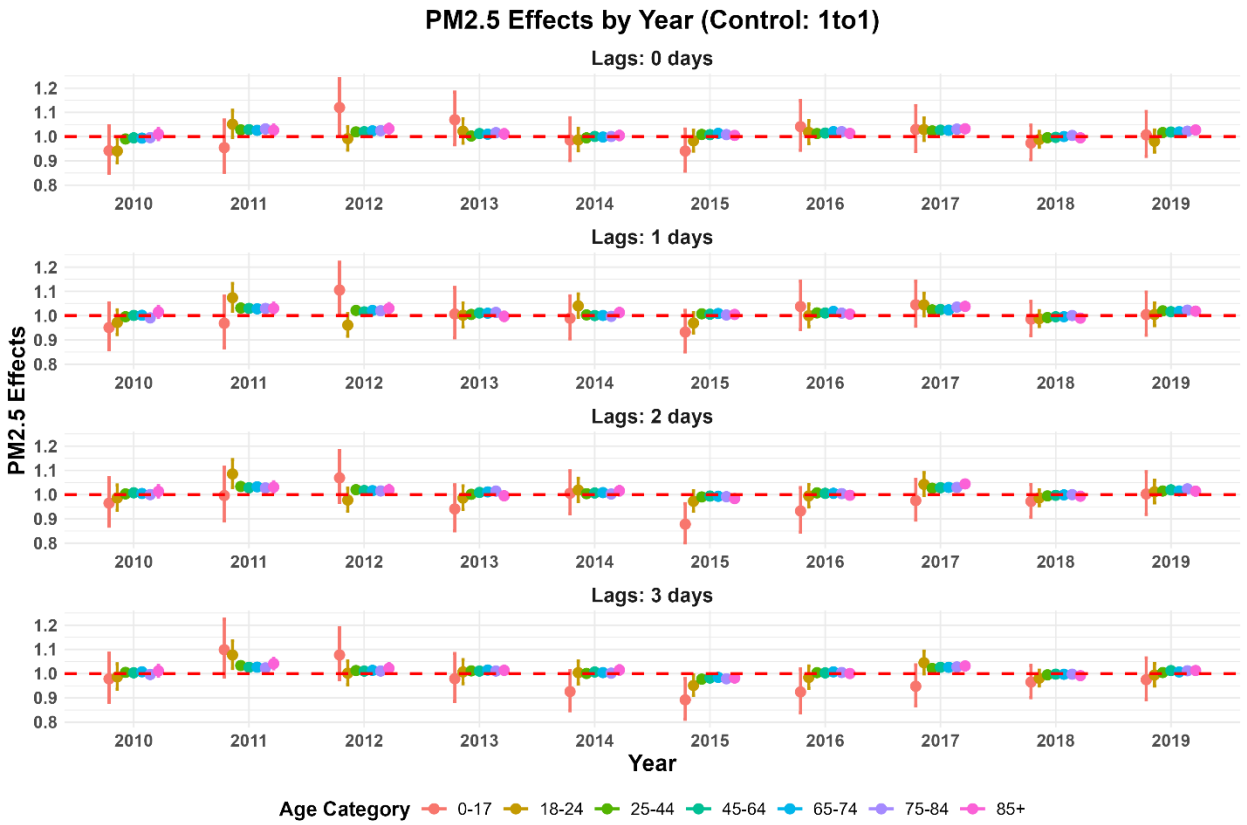

Figure S34. The associations between $PM_{2.5}$ exposure and ED visits for diabetic patients across age categories in California from 2010 to 2019.

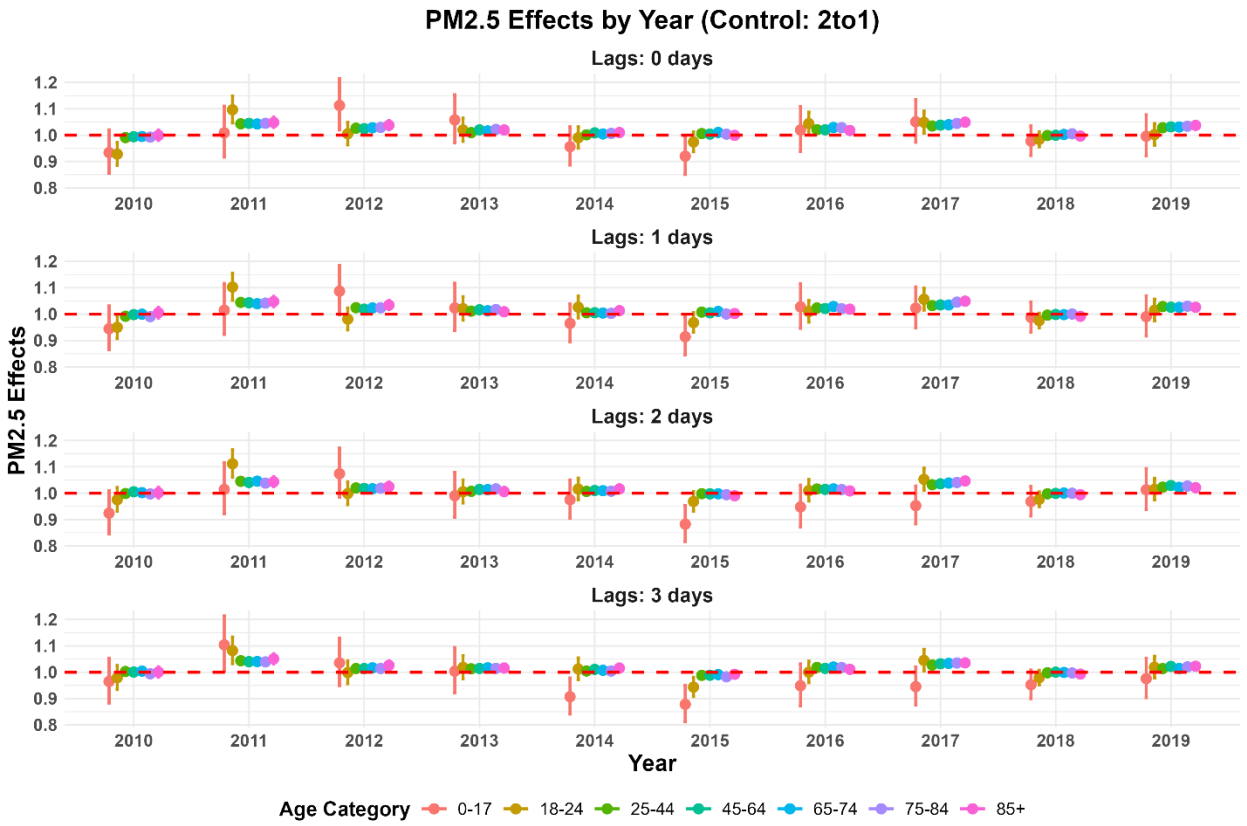

Figure S35. The associations between $PM_{2.5}$ exposure and ED visits for diabetic patients across age categories in California from 2010 to 2019.

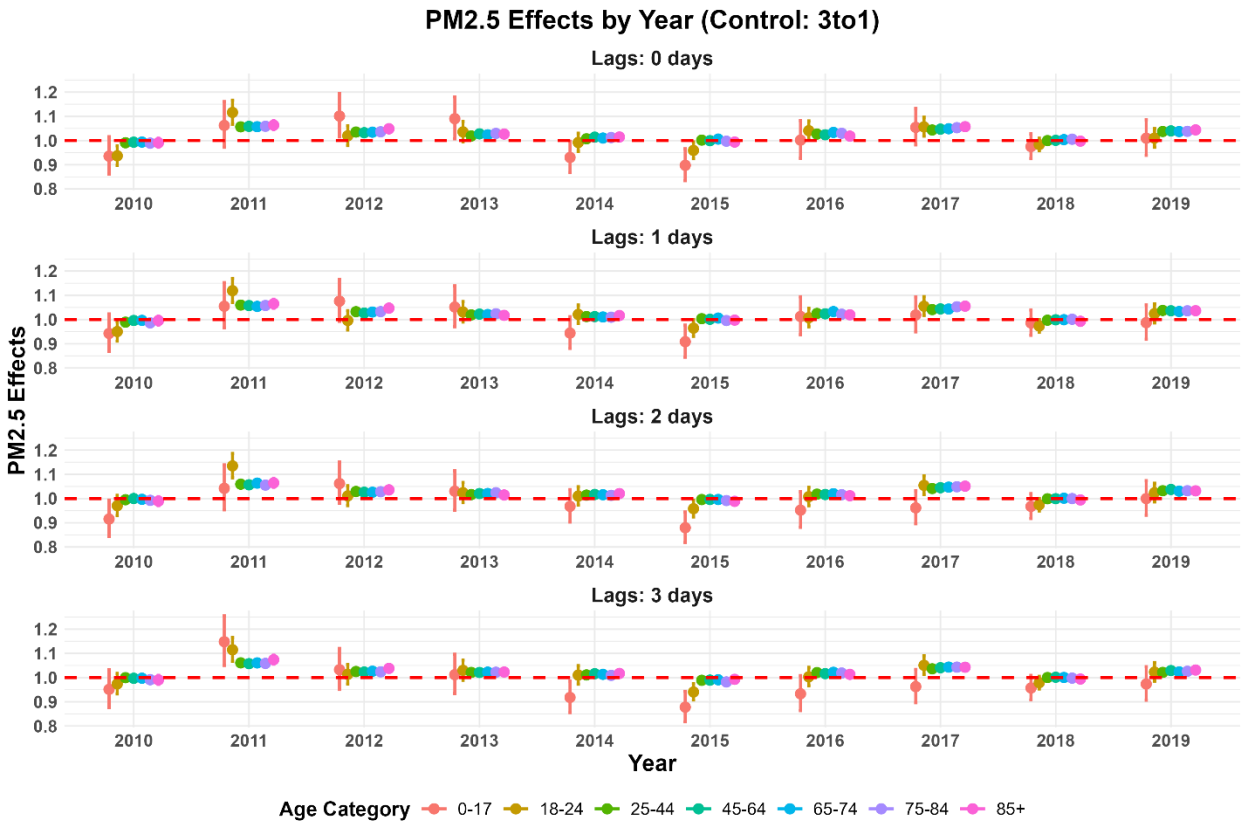

Figure S36. The associations between $PM_{2.5}$ exposure and ED visits for diabetic patients across age categories in California from 2010 to 2019.

Supplementary File 2

Year-by-Year Analyses of Diabetes-Related Hospital Inpatient Admissions (Binary) and Length of Stay (Continuous)

Contents

1. Introduction

Type 2 diabetes (T2D) continues to be one of the most prevalent chronic conditions globally, characterized by insulin resistance and persistent hyperglycemia. Its rising incidence poses a significant challenge to healthcare systems, not only due to its long-term complications such as cardiovascular disease, nephropathy, and neuropathy, but also because of the acute burden it places on hospitals through emergency visits and prolonged inpatient stays. In the United States, California is home to a particularly high burden of T2D, with substantial racial and socioeconomic disparities shaping both disease outcomes and access to care.

While lifestyle and genetic predispositions are established contributors to T2D development and progression, environmental exposures, especially air pollution are increasingly recognized as important, modifiable risk factors. Ambient air pollution, notably fine particulate matter ($PM_{2.5}$) and nitrogen dioxide (NO_2), has been implicated in the onset of insulin resistance, systemic inflammation, and impaired glucose regulation, all of which can accelerate the development and complications of T2D ((Brook et al., 2010; Guo et al., 2025; Hong et al., 2025; Liu et al., 2019; Rajagopalan & Brook, 2012; Zhang et al., 2025). Experimental and epidemiologic studies suggest that even short-term exposure to these pollutants can exacerbate underlying metabolic dysfunction, particularly among individuals with chronic diseases (Hu et al., 2025; Liang et al., 2025).

Although the connection between air pollution and T2D incidence has been well documented, far fewer studies have examined how acute fluctuations in pollution influence hospitalization-related outcomes among individuals already living with T2D. Hospital admissions and length of stay (LOS) offer valuable insights into the severity and destabilization of disease, often reflecting acute responses to environmental stressors. These outcomes are particularly relevant in settings like California, where overall pollution levels have declined due to regulatory efforts, yet local disparities in exposure remain pronounced, especially in low-income and racially diverse communities near traffic corridors or industrial zones.

Wildfires' growing frequency and severity add complexity to the air pollution landscape, contributing episodic yet intense increases in $PM_{2.5}$. The interaction between wildfire smoke exposure and chronic disease burden remains an underexplored but increasingly relevant public health issue in the western U.S., particularly for vulnerable populations such as those with T2D (Saeed, 2025; Wettstein et al., 2018). Moreover, the implementation of healthcare policy reforms, such as the Affordable Care Act (ACA), has altered healthcare access and utilization patterns over the last decade, offering a unique opportunity to evaluate how systemic changes may buffer or exacerbate environmental health risks.

Although California has experienced substantial environmental and policy shifts over the past decade, few U.S.-based studies have evaluated how short-term air pollution exposure influences hospitalization and length of stay (LOS) among individuals with Type 2 Diabetes (T2D). Most

existing research has focused on long-term exposures or has been conducted in international settings with higher baseline pollution levels. There is a pressing need for high-resolution, individual-level analyses in regions like California, where moderate but variable pollution coincides with significant healthcare reforms and demographic diversity.

To address this gap, we assessed the short-term associations between daily $PM_{2.5}$ and NO_2 exposures and hospitalization outcomes among T2D patients in California from 2010 to 2019. Leveraging a large statewide hospitalization dataset linked to fine-scale air pollution and meteorological data, we examined temporal patterns, racial and ethnic disparities, and the influence of contextual factors such as major wildfire events and changes in healthcare access under the Affordable Care Act (ACA). By disaggregating results year-by-year, this study builds on our prior pooled analysis to capture shifts in pollution–health relationships that may be masked in multi-year averages. Our aim is to generate evidence that supports equitable, targeted environmental health strategies and enhances healthcare system resilience in the face of emerging environmental challenges.

2. Materials and methods

2.1. Study population and Health data

This study investigates hospitalizations related to type 2 diabetes (T2D) in California from 2010 to 2019. Patient-level hospitalization data were sourced from the California Department of Health Care Access and Information (HCAI). The dataset includes individuals with either a primary or secondary diagnosis of T2D, identified using ICD-9 code 250 or ICD-10 code E11. Key variables encompass ZIP code of residence, admission and discharge dates, length of stay (LOS), age, sex, race/ethnicity, insurance type, type of care received, and primary language spoken.

Diagnostic and procedural fields were cleaned and standardized, and LOS was calculated as a derived metric. Residential ZIP codes were geocoded and spatially linked to air pollution exposure data.

2.2. Exposure data

Daily exposure estimates for $PM_{2.5}$ and NO_2 were developed using high-resolution land-use regression (LUR) models, as described in (Su et al., 2024). These models integrated various data sources, including satellite-based observations (e.g., Ozone Monitoring Instrument – OMI), weather variables, traffic density, land use characteristics, and vegetation indices such as the Normalized Difference Vegetation Index (NDVI). The models were trained using Decision/Support/Analysis (D/S/A) algorithms and validated through V-fold cross-validation to minimize overfitting and control for spatial autocorrelation. Pollution estimates were initially produced at a 30-meter spatial resolution and then aggregated into 100-meter grids to enhance computational efficiency. Individual exposure levels were calculated by deriving ZIP code-level

and population-weighted pollutant concentration averages, based on block group-level data weighted by population. Meteorological variables such as daily maximum temperature, maximum relative humidity, and precipitation were also assigned at the ZIP code level using the same methodology applied to air pollution estimates.

2.3. Study Design

To evaluate the short-term relationship between air pollution exposure and hospitalizations for type 2 diabetes (T2D), we employed a time-stratified case-crossover design. In this approach, each case day defined as the patient's admission date was matched with up to four control days on the same weekday in prior weeks. Control days were assigned by subtracting 7, 14, 21, and 28 days from the admission date, corresponding to one, two, three, and four weeks earlier. This matching strategy controls for weekly temporal trends and minimizes confounding from short-term patterns such as day-of-week effects.

We created separate datasets for different case-control matching ratios (1:1, 2:1, 3:1, and 4:1), reflecting the number of control days paired with each case. This self-matched design inherently adjusts for fixed individual-level characteristics including age, sex, race/ethnicity, and underlying health conditions while reducing bias from time-varying confounders. The exposure windows were selected based on established evidence from prior studies, and additional lag structures were explored through sensitivity analyses to ensure robustness of the findings.

2.4. Statistical analysis

Analyses were stratified by individual years from 2010 to 2019 were performed using R version 4.3.1(R Core Team, 2023). Data management and visualization were conducted using several R packages, including dplyr (Wickham, 2015), tidyr(Wickham & Wickham, 2017), lubridate(Spinu et al., 2016), survival (Therneau & Lumley, 2015), and ggplot2 (Wickham et al., 2016). We used conditional logistic regression to estimate the association between short-term exposure to ambient air pollutants and the odds of T2D-related hospitalization. Models adjusted for time-varying meteorological variables, including daily temperature, relative humidity, precipitation, and wildfire events.

The relationship between the effects of daily and lagged air pollution and hospital length of stay (LOS) was examined using generalized linear models (GLMs) with a Poisson link function. These models accounted for demographic and clinical covariates such as age at admission, insurance payer, race/ethnicity, type of care, and primary language along with daily meteorological conditions (maximum temperature, relative humidity, and precipitation). We evaluated pollutant effects using lag periods from 0 to 3 days before admission, reporting results as percent change in outcomes per interquartile range (IQR) increase in pollutant concentration, accompanied by 95% confidence intervals (CIs). Stratified analyses by calendar year and race/ethnicity were performed to capture temporal patterns and identify disproportionately affected populations. Because sample sizes varied by year, we conducted sensitivity analyses to

evaluate the robustness of annual estimates. Statistical significance was determined using a two-sided p-value threshold of < 0.05.

3. Results

3.1. Effect on hospital admission

Between 2010 and 2019, the number of Californians diagnosed with T2D nearly doubled, rising from 569,653 to 690,672. This increase **Error! Reference source not found.**can be largely attributed to an aging and increasingly obese population, improvements in data collection, and expanded healthcare access through the Affordable Care Act (ACA) (Fig. 1). The ACA facilitated broader screening and diagnosis efforts via Medi-Cal and subsidized insurance programs, identifying many previously undiagnosed cases. In 2010, NO_2 exposure levels among individuals with T2D were relatively low. The economic downturn following the Great Recession (2007–2009) contributed to this reduction in air pollution, particularly in urban areas where transportation emissions are a primary source of NO_2 and particulate matter. Additionally, wildfire activity in 2010 was lower than in subsequent years, which helped prevent significant spikes in particulate pollution from that source. NO_2 exposure increased between 2011 and 2013 but began to decline steadily afterward. This downward trend in both average NO_2 concentrations and their standard deviation (SD) reflects improvements in air quality driven by regulatory policies and advancements in cleaner technologies. Measures such as stricter vehicle emissions standards, tighter industrial regulations, and the adoption of cleaner fuels helped reduce emissions. They led to a uniform decrease in NO_2 levels, minimizing extreme pollution events that previously contributed to greater variability. Although the mean NO_2 concentrations and SD continued to decline, the interquartile range (IQR) of NO_2 exposure began to rise after 2016. This pattern suggests that while extreme pollution events became less common, variability within the middle range of NO_2 concentrations increased. A declining SD alongside a rising IQR indicates that data points are clustered more closely around the mean. Still, the spread within the central portion of the distribution became wider, reflecting a more stretched distribution of typical NO_2 exposure levels, even as extreme outliers diminished.

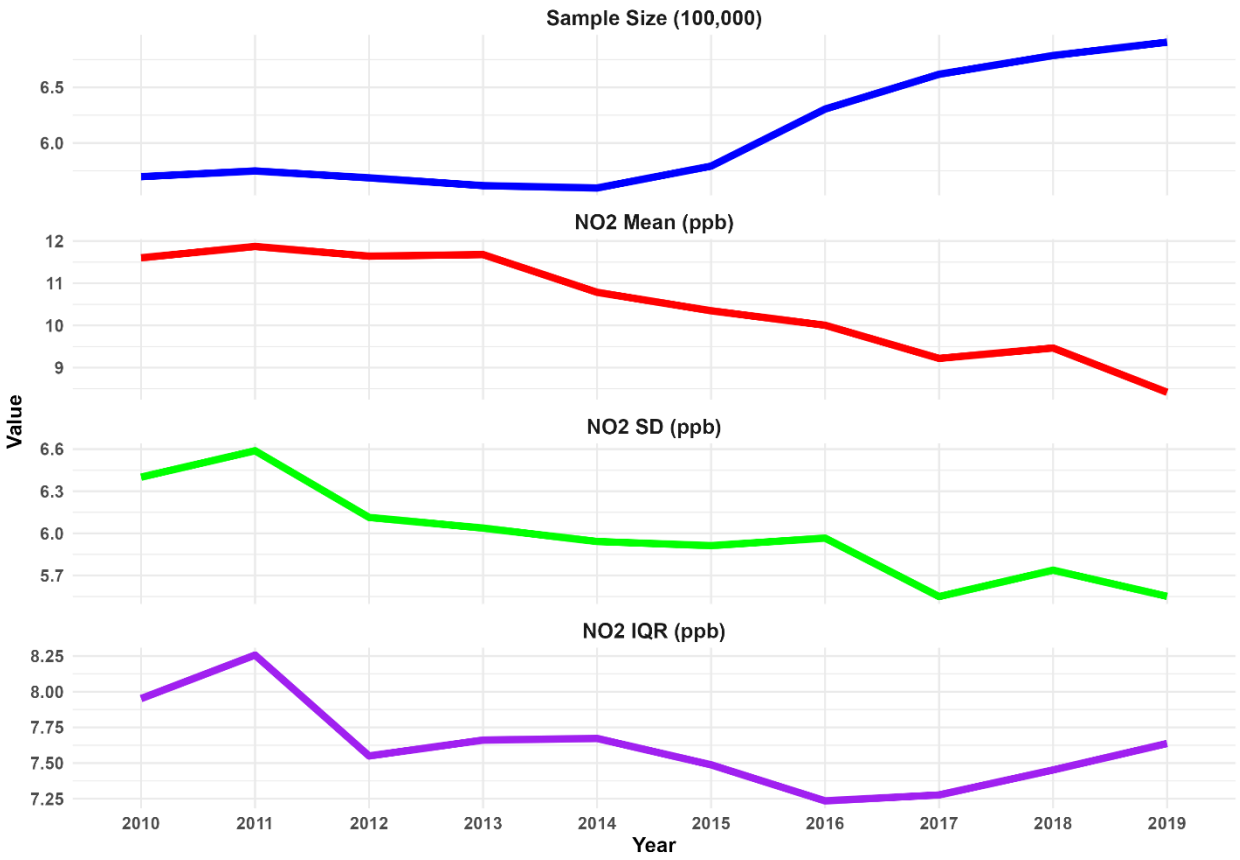

Fig. 1. The temporal trend of the population in California diagnosed with diabetes and NO_2 exposure from 2010 to 2019.

The concentration-response (CR) functions show the relationship between NO_2 exposure and hospitalization, revealing a declining trend in effect estimates from 2010 to 2015, followed by an upward trend from 2015 to 2019 (Fig. 2). Several key factors contribute to this pattern. Expanding healthcare access through Medicaid has likely enhanced disease management and preventive care for low-income populations during the earlier period, reducing dependence on emergency departments for acute health issues. Consequently, the influence of environmental exposures like NO_2 on hospitalization decreased between 2010 and 2015. However, after 2015, a broader distribution of NO_2 exposure levels may have contributed to the observed resurgence in its health impact, even though average concentrations continued to decline. Additionally, shifts in population vulnerability likely played a role. As the "baby boomer" generation (born between 1946 and 1964) aged and increasingly utilized healthcare services, their heightened susceptibility to air pollution may have amplified the health effects of NO_2 during this later period.

Regarding lagged effects, the impact of NO_2 exposure remained relatively stable over the first two days (lags 0–2), with only a slight decline observed by day 3. This suggests that the health effects of NO_2 are primarily acute and tend to diminish within a few days following exposure.

Concerning control period comparisons, using a 1-to-1 control (one week before the event) resulted in lower effect estimates, whereas applying a 4-to-1 control (four weeks before the event) produced higher estimates. This pattern may be explained by the dilution of exposure levels further from the event day, making the exposure on the event day appear comparatively higher and resulting in a stronger estimated effect. The association between NO_2 exposure and hospitalization remained statistically significant across the entire study period (2010–2019), regardless of the lag structure (0–3 days) or control strategy (one to four weeks prior). This consistency demonstrates the robustness of the relationship between short-term NO_2 exposure and adverse health outcomes, particularly among individuals with diabetes.

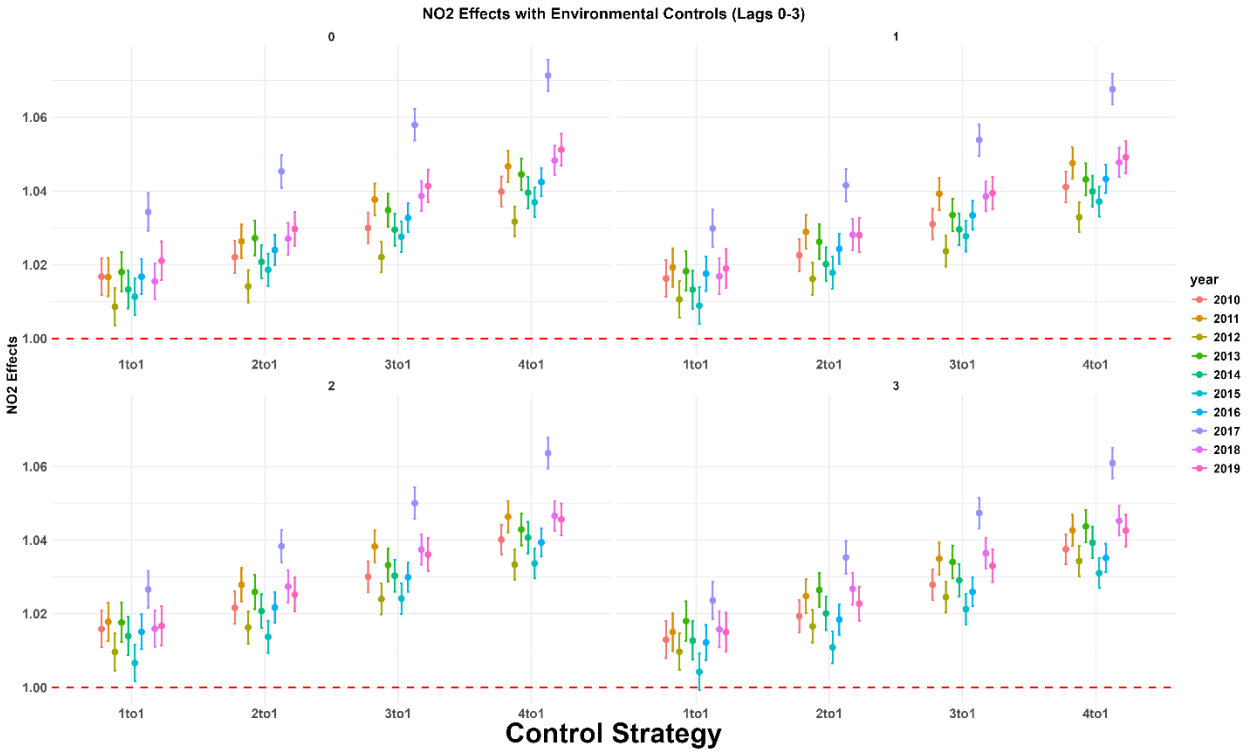

Fig. 2. The association between NO_2 exposure and hospitalization over 0–3 lag days across four control categories, modeled annually from 2010 to 2019.

In parallel with trends in NO_2 exposure, $PM_{2.5}$ levels among individuals with T2D were relatively low in 2010, likely due to the economic slowdown following the Great Recession and reduced wildfire activity that year (Fig. 3). Starting in 2011, average $PM_{2.5}$ concentrations steadily declined, reflecting significant progress in air quality driven by stricter environmental regulations and advancements in cleaner technologies. Enhanced vehicle emission standards, tighter industrial pollution controls, and the transition to cleaner fuels were key contributors to this improvement. The standard deviation (SD) of $PM_{2.5}$ levels also decreased, indicating reduced extreme pollution events and more consistent air quality improvements across regions. However, after 2016, the interquartile range (IQR) of $PM_{2.5}$ exposure began to rise, suggesting increased

variability in mid-range pollution levels. While extreme pollution events became less frequent, disparities in regional pollution control efforts and localized $PM_{2.5}$ sources may have contributed to this growing variability within the central range of exposures.

Although the decline in average $PM_{2.5}$ concentrations and reduced variability in extreme values highlight the success of air quality interventions, 2018 saw a significant spike in $PM_{2.5}$ levels, primarily due to unprecedented wildfire activity. Major events such as the Camp Fire in Northern California and the Woolsey Fire in Southern California released large quantities of fine particulate matter, severely degrading air quality across the state. These extreme wildfire events underscore the growing impact of climate change on air pollution patterns, even as regulatory policies continue to reduce emissions from traditional sources. The increasing IQR also highlights the need for more localized, targeted efforts to address disparities in mid-range pollution exposures and mitigate community-level health risks.

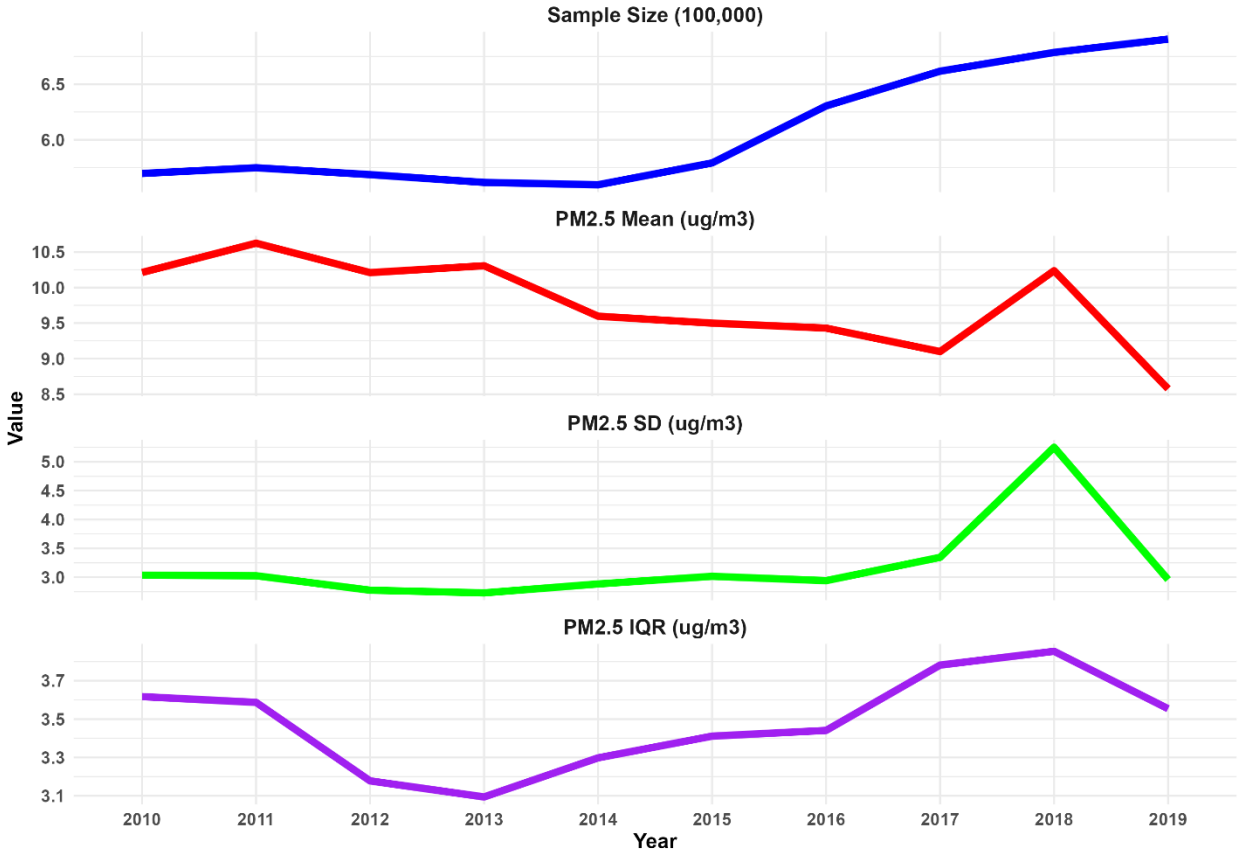

Fig. 3. The temporal trend of the population in California diagnosed with diabetes and $PM_{2.5}$ exposure from 2010 to 2019.

The association between $PM_{2.5}$ exposure and hospitalization reveals a distinct temporal pattern: a positive effect in 2011, a decline in effect estimates from 2012 to 2015, and a renewed increase

from 2015 to 2019 (Fig. 4). Relatively low $PM_{2.5}$ levels may explain the initially negative association observed in 2010. The broader implementation of the Affordable Care Act (ACA) by 2014 significantly shaped this trend, expanding access to healthcare through Medicaid for low-income individuals and Medicare Part B for older adults. Enhanced access likely promoted better disease management and preventive care, which reduced reliance on hospital services for acute conditions. Consequently, the health impacts of environmental exposures, including $PM_{2.5}$, declined during 2012–2015.

However, the upward trend in $PM_{2.5}$-related health effects observed after 2015 may reflect shifts in exposure dynamics and rising population vulnerability. Despite overall declines in average $PM_{2.5}$ levels, there was a noticeable increase in mid-range exposures, which may have amplified health risks.

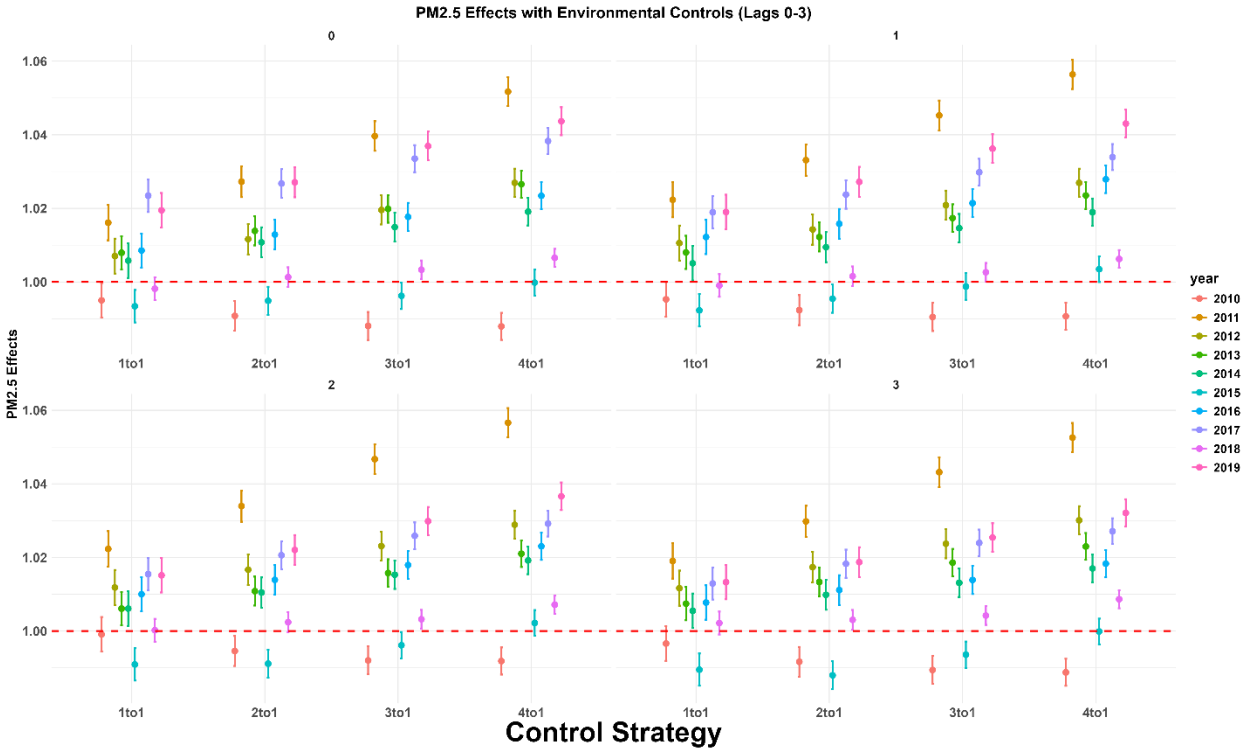

Fig. 4. The association between $PM_{2.5}$ exposure and hospitalization over 0–3 lag days across four control categories, modeled annually from 2010 to 2019.

Interestingly, despite elevated $PM_{2.5}$ levels in 2018, hospitalization remained relatively low at 678,682. Several factors may account for this. Wildfire-related $PM_{2.5}$ tends to occur in short, intense bursts. In contrast, chronic exposure to pollution from traffic and industrial sources has a more established link to sustained health impacts and increased hospital utilization. Additionally, heightened public awareness and protective behaviors—such as using N95 masks, adherence to air quality alerts, and staying indoors—may have reduced acute exposures during wildfire

events. Adaptations like increased use of air purifiers and reduced outdoor activity could have further mitigated immediate health consequences. It is also possible that the health effects of such exposures are delayed and not fully reflected in the same-year hospitalization data. Furthermore, adjustments for wildfire-related $PM_{2.5}$ in the modeling may have overcontrolled for its effects, potentially underestimating its contribution to hospital admissions.

Regarding lagged effects, $PM_{2.5}$ exposure had a relatively stable impact on hospitalization within the 0–2 day period, with a modest reduction in effect by day 3. This indicates that $PM_{2.5}$ predominantly exerts short-term health effects. Comparing different control strategies1-to-1 (one week before the event, versus 4-to-1, four weeks prior revealed a pattern like that seen with NO_2: stronger associations were detected when control periods were further from the event date. This may be due to lower pollution levels during those earlier periods, heightening the apparent contrast and thus the observed effect on the event day.

3.2. Effect on hospitalization stratified by race/ethnicity

From 2010 to 2019, the racial distribution among T2D patients remained relatively stable (Fig. 5). White patients consistently represented the largest group, though their proportion declined slightly from 46.94% to 39.36%. Hispanic patients, the second-largest group, experienced a modest increase from 30.23% to 34.42%. The proportion of Asian patients rose slightly from 9.65% to 9.99%, while Black patients decreased from 11.90% to 10.33%. The "Other" racial category, although the smallest in 2010 (1.26%), grew significantly, reaching 5.87% by 2019. Regarding NO_2 exposure, except for 2010, average NO_2 levels across all racial groups showed a clear downward trend over the study period. For example, mean NO_2 exposure for Black, Hispanic, and Other patients decreased from 12.55 ppb, 12.88 ppb, and 10.50 ppb in 2010 to 9.02 ppb, 9.23 ppb, and 8.32 ppb in 2019, respectively. Similarly, Asian patients experienced a reduction from 12.30 ppb to 8.84 ppb, and White patients from 10.37 ppb to 7.47 ppb over the same period. Hispanic patients had the highest NO_2 exposure, while White patients experienced the lowest. Despite these improvements, the interquartile range (IQR) of NO_2 exposure began to widen after 2016, indicating increased variability within the mid-range of exposures. This suggests that while extreme pollution events became less frequent, exposure disparities persisted or worsened, likely driven by localized pollution sources and regional differences in air quality improvements.

Regarding concentration-response (C-R) functions, the "Other" racial category consistently exhibited the highest NO_2-related health effects. It showed the most pronounced fluctuations, particularly in 2017, when the Effect exceeded 1.18, the largest deviation from the baseline among all groups (Fig. 6). This heightened impact may reflect greater socioeconomic and environmental vulnerabilities, including reduced access to preventive healthcare and increased exposure to local pollution sources. In contrast, the other racial and ethnic groups showed relatively stable C-R patterns with minor fluctuations.

Starting around 2012, the health impacts of NO_2 exposure on hospitalization declined across all racial groups, reaching their lowest levels by 2015. This decline likely reflects the benefits of expanded healthcare access and improved disease management driven by Medicaid expansion and the Affordable Care Act (ACA) reforms. However, after 2015, the effects of NO_2 exposure on hospitalization began to rise again, particularly among patients in the "Other" racial category. This resurgence may be associated with increased susceptibility due to an aging population and a growing burden of chronic conditions within these communities.

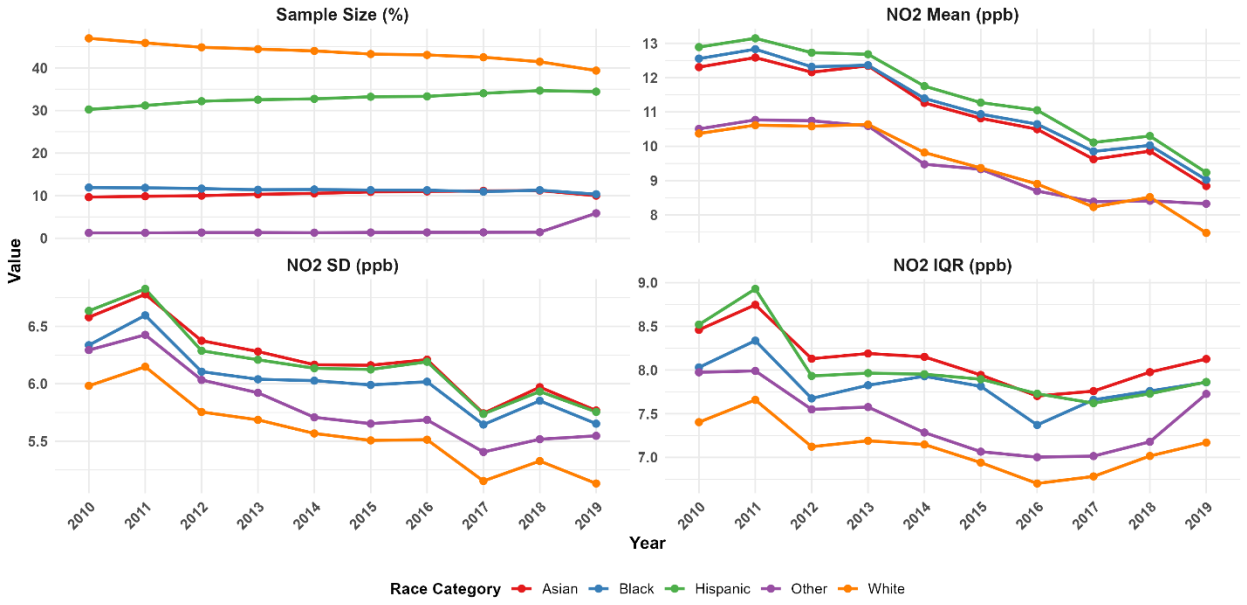

Fig. 5. The temporal trend of the population, categorized by five major races, in California diagnosed with diabetes and NO_2 exposure from 2010 to 2019.

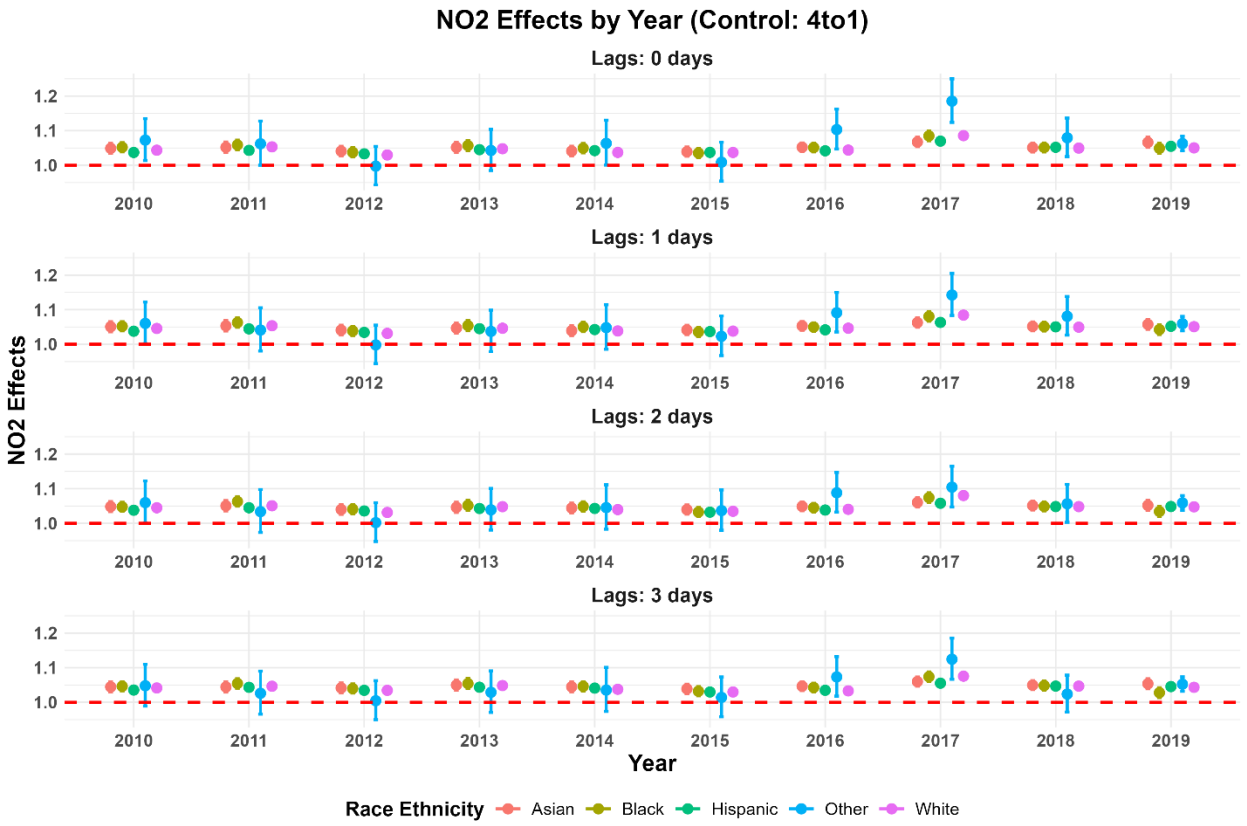

Fig. 6. The associations between NO_2 exposure and hospitalization for diabetic patients across five major race categories in California from 2010 to 2019.

Regarding lag effects, the influence of NO_2 exposure on hospitalization remained relatively stable across 0–2-day lags, with a slight decline by day 3, indicating that the short-term health effects of NO_2 exposure tend to diminish over time. When comparing control periods, larger effect estimates were observed with longer control intervals, such as the four-week control period (Figures S1, S2, S3). This finding highlights the importance of carefully selecting temporal control periods, as variations in seasonal and spatial exposure patterns can significantly affect the observed associations between pollution and health outcomes.

These findings reveal significant associations between NO_2 exposure and hospitalization across all racial groups from 2010 to 2019, underscoring the persistent health burden of air pollution, especially among vulnerable populations. Addressing these disparities through targeted interventions and sustained improvements in air quality is critical to reducing the health impacts of NO_2 exposure and advancing environmental justice for all communities.

$PM_{2.5}$ exposure analysis (Fig.S4) shows average exposure levels declined across all racial and ethnic groups from 2010 to 2019. Specifically, average $PM_{2.5}$ concentrations for Black, Hispanic, and Other individuals decreased from 10.35 $\mu g/m^3$, 10.81 $\mu g/m^3$, and 9.82 $\mu g/m^3$ in 2010 to 8.66

μg/m³, 9.03 μg/m³, and 8.36 μg/m³ in 2019, respectively. Similarly, Asian individuals experienced a reduction from 10.23 μg/m³ to 8.50 μg/m³, and the White population saw levels fall from 9.79 μg/m³ to 8.21 μg/m³ during the same period. Overall, Hispanic and Black patients experienced the highest $PM_{2.5}$ exposures, while White patients consistently had the lowest. Despite the downward trend in average $PM_{2.5}$ levels, 2018 marked a sharp increase in concentrations, accompanied by notable rises in the standard deviation (SD) and interquartile range (IQR). This spike was largely driven by severe wildfire activity that year, which led to widespread and extreme air pollution events. These wildfires not only elevated $PM_{2.5}$ levels but also increased exposure variability across all racial and ethnic groups, contributing to the observed growth in SD and IQR. Regarding concentration-response (C-R) functions, the "Other" category displayed the most pronounced changes. For instance, between 2011 and 2014, effect estimates for this group fell from 1.07 to around 1.0 (Fig.S5).

Between 2012 and 2015, the effects of $PM_{2.5}$ exposure on hospitalization declined across all racial and ethnic groups, reaching their lowest levels during this period. This reduction likely reflects improvements in air quality and expanded access to preventive healthcare services made possible by Medicaid expansion and other initiatives under the Affordable Care Act (ACA).

However, after 2015, the impact of $PM_{2.5}$ exposure on hospitalization began to increase again, particularly among Hispanic and Black populations. This resurgence may indicate increased vulnerability in these communities, potentially due to a higher prevalence of chronic health conditions or other socioeconomic risk factors. Additionally, wider confidence intervals observed for the Asian and "Other" groups suggest smaller sample sizes in these populations, leading to greater uncertainty and variability in the effect estimates.

Examining lagged effects, the "Other" category exhibited notable fluctuations and variability across all lag periods (0 to 3 days), especially during earlier years. Large error bars for this group highlight the uncertainty of these estimates. Furthermore, the choice of control period significantly affected the observed results, with longer control intervals (e.g., four weeks) producing larger estimated effects (Figures S6, S7, S8). This is likely to reflect the lower pollution levels during more distant control periods, which amplify the relative difference compared to exposure levels on the event day.

3.3. Effect on LOS

Between 2010 and 2019, the number of hospitalized Californians with T2D rose from 569,653 to 690,672. This increase (Fig.S9) is primarily driven by an aging and growing obese population, enhanced data reporting, and expanded healthcare access under the Affordable Care Act (ACA). The ACA's implementation improved hospital accessibility through Medi-Cal and subsidized insurance plans, facilitating better identification and documentation of hospitalization cases.

In 2010, NO_2 exposure among Type 2 diabetic patients remained relatively low. A key factor contributing to this was the economic downturn following the Great Recession (2007–2009),

which reduced industrial and transportation emissions, particularly in urban areas where these sources are major contributors to NO_2 and particulate pollution. Additionally, wildfire activity in 2010 was lower than in other years, preventing substantial spikes in pollution from that source. Between 2011 and 2013, NO_2 exposure increased, but from 2014 onward, overall NO_2 concentrations and their standard deviation (SD) showed a steady decline.

This downward trend is likely due to enhanced air quality regulations and the adoption of cleaner technologies, which have helped reduce emissions over time. Policies such as stricter vehicle emissions standards, industrial regulations, and the adoption of cleaner fuels have contributed to an overall decline in emissions, leading to a more consistent reduction in NO_2 levels and fewer extreme pollution events that previously caused high variability. While the mean NO_2 concentrations and standard deviation (SD) continued to decrease, the interquartile range (IQR) of NO_2 exposure began to rise after 2016. This declining SD and an increasing IQR combination suggest that NO_2 values became more concentrated around the mean, yet the middle portion of the data showed greater variability. In other words, while extreme pollution outliers became less common, the spread of NO_2 levels within the central range widened, indicating a more stretched-out distribution of exposure levels over time.

The CR functions between NO_2 exposure and LOS show an upward trend in effect estimates from 2010 to 2012, peaking in 2012. A slight decline followed this in 2013, but the estimates rose again in 2014, indicating some fluctuations. Overall, from 2010 to 2014, the estimates demonstrate a moderate increase. The CR functions between NO_2 exposure and LOS exhibit an upward trend from 2014 to 2016, followed by fluctuations in 2017-2019 (Fig.S10). This trend can be attributed to several key factors. Expanding Medicaid for low-income individuals will likely enhance access to preventive care and disease management, decreasing hospitalizations for acute conditions. With improved healthcare availability, patients may have received earlier interventions and better chronic disease management, reducing the need for emergency hospital admissions. Shifts in population susceptibility may also account for the increased impact of NO_2 after 2014. As the baby boomer generation (born between 1946 and 1964) aged and became more integrated into the healthcare system, their heightened vulnerability to air pollution likely contributed to the observed rise in NO_2-related health effects.

Over all years, lag 2 estimates tend to be slightly higher than lag 0 estimates, suggesting that the impact of NO_2 exposure on LOS increases slightly over the first two days. The most notable increase occurs in 2012, where lag 0 = 1.021 and lag 2 = 1.023, showing a sustained short-term effect of NO_2 exposure. This trend suggests that the Effect of NO_2 exposure may not be immediate but becomes more evident within 1-2 days post-exposure. In most years, lag 3 estimates are slightly lower than lag 2 estimates, indicating that the NO_2 exposure effect starts to decline by day 3. For example, in 2013, the estimate for lag 2 = 1.012 but drops to 1.009 at lag 3, implying that the Effect weakens after two days. This pattern suggests that the influence of NO_2 exposure on hospitalization LOS is strongest within the first 2 days and starts to diminish afterward. NO_2 exposure effect increases from lag 0 to lag 2, suggesting a short-term

accumulation of impact. The Effect declines from lag 2 to lag 3, implying a diminishing influence beyond the initial exposure period. This pattern is consistent across most years, indicating a predictable short-term effect of NO_2 exposure on hospitalization duration.

The impact of NO_2 exposure on LOS remains statistically significant across 2010–2019, considering lags 0–3 days. This finding underscores the robustness of the association between NO_2 exposure and prolonged hospitalization, regardless of temporal considerations. The consistent significance of NO_2's Effect highlights that short-term exposure is a key factor influencing hospitalization duration, emphasizing the importance of air quality monitoring. The persistence of this relationship over nearly a decade reinforces the urgent need for targeted interventions to mitigate NO_2 pollution, particularly in vulnerable populations and high-risk areas where individuals may experience prolonged hospital stays due to air pollution-related complications.

From 2010 to 2019, the number of Californians hospitalized with T2D increased from 569,653 to 690,672 (Fig.S11). The increase in hospitalized cases of T2D from 2010 to 2019 aligns with expanded healthcare access, which improved diabetes screening and diagnosis through Medi-Cal and subsidized insurance programs, likely identifying many previously undiagnosed cases. Several key factors contributed to this trend. California's growing and aging population, particularly the baby boomer generation, played a significant role, as older adults face a higher risk of T2D-related complications requiring hospitalization. Additionally, rising obesity rates, influenced by sedentary lifestyles and unhealthy dietary patterns, further exacerbate the burden of diabetes hospitalizations. Data collection and tracking system improvements also provided a more accurate assessment of diabetes prevalence, ensuring that more cases were documented over time.

Much like NO_2 exposure trends, $PM_{2.5}$ concentrations among individuals with T2D were relatively low in 2010. This pattern likely reflects the economic slowdown following the Great Recession and lower wildfire activity compared to subsequent years. Beginning in 2011, average $PM_{2.5}$ levels experienced slight fluctuations but showed an overall downward trend, indicating gradual improvements in air quality. These improvements were largely attributed to the implementation of more stringent environmental regulations and the widespread adoption of cleaner technologies. A steady decline in the standard deviation (SD) of $PM_{2.5}$ concentrations, particularly after 2013, suggests a reduction in extreme pollution events and more consistent air quality improvements across different regions. This trend points to the positive impact of regulatory measures such as enhanced vehicle emission standards, industrial emission controls, and transitions to cleaner fuel sources in reducing $PM_{2.5}$ variability. However, in 2012, 2016, and 2018, the interquartile range (IQR) of $PM_{2.5}$ exposure was wider, indicating growing variability in moderate pollution levels. This shift may reflect uneven effectiveness in pollution control strategies or localized sources of $PM_{2.5}$ emissions, such as wildfires, urban hotspots, and industrial zones. Although extreme exposure events became less frequent, the increased

variability within the mid-range highlights the need for more geographically targeted interventions to address persistent air quality disparities.

The association between $PM_{2.5}$ exposure and hospitalization reveals a distinct trajectory: a direct relationship in 2010, decreased risk effect estimates in 2011 and 2013, no effects in 2013, and a subsequent rise in 2014- 2018 (Fig.S12). In 2019, higher $PM_{2.5}$ levels were associated with slightly reduced hospitalizations. In 2010, the positive association may be linked to higher overall $PM_{2.5}$ levels. Between 2011 and 2014, the full implementation of the Affordable Care Act (ACA) expanded healthcare access, particularly through Medicaid for low-income populations and Medicare Part B for older adults. The expansion likely enhanced the management of chronic conditions and access to preventive care, leading to decreased dependence on hospital services for acute events triggered by environmental factors such as $PM_{2.5}$. However, the rise in effect estimates after 2014 may reflect shifts in exposure patterns or increased population susceptibility. Interestingly, despite a continued decline in $PM_{2.5}$ concentrations, there was an uptick in mid-range exposure levels, which could have played a role in the observed rebound in health impacts during this time.

The rising association between $PM_{2.5}$ exposure and hospitalizations from 2014 to 2016 may be partly attributed to demographic changes, particularly the aging of the baby boomer generation. As this cohort became more actively engaged with healthcare services, their increased vulnerability to air pollution likely intensified the health effects of $PM_{2.5}$. Interestingly, despite a significant spike in $PM_{2.5}$ levels in 2018 largely due to wildfires, the related increase in hospital admissions was relatively modest. Several factors may account for this pattern. Wildfire-induced $PM_{2.5}$ surges, while intense, tend to be brief compared to chronic exposure from traffic or industrial emissions, which are more consistently linked to long-term health impacts. Moreover, growing public awareness and preventive actions such as air quality alerts, widespread use of N95 masks, and guidance to stay indoors likely helped mitigate exposure during wildfire episodes. Behavioral adaptations, including reduced outdoor activities and greater use of indoor air filtration, may have further limited health risks. Additionally, the effects of acute exposure may have a delayed onset, meaning hospitalizations might not occur immediately. Lastly, including wildfire-specific $PM_{2.5}$ in statistical models may have unintentionally dampened its apparent influence, potentially underestimating the true health burden.

Regarding lagged effects, the relationship between $PM_{2.5}$ exposure and subsequent health outcomes shows a noticeable increase by the third-day post-exposure, suggesting that $PM_{2.5}$ has an acute impact that intensifies over a short period. Between 2010 and 2019, the association between $PM_{2.5}$ and LOS among diabetic patients was generally not statistically significant across most years and lag intervals (0–3 days), with exceptions noted in 2010, 2012, 2014, and 2015. These findings underscore the critical role of short-term $PM_{2.5}$ exposure in precipitating hospitalizations in individuals with diabetes. The recurring pattern over a decade highlights the urgency for targeted public health initiatives and air quality policies, particularly for vulnerable populations and high-risk regions.

3.4. Effect on LOS stratified by race/ethnicity

Between 2010 and 2019, the racial distribution of T2D patients remained generally consistent (Fig.S13). White patients continued to represent the largest group, though their proportion declined slightly from 47% to 39.45%. In contrast, the proportion of Hispanic patients increased moderately, rising from 30.24% to 34.59% over the same period. The percentages of Black and Asian patients showed minimal changes, from 11.84% to 10.02% and 9.65% to 10.16%, respectively. The "Other" racial category, initially the smallest at 1.25% in 2010, saw a notable increase, reaching 5.7% by 2019.

Regarding NO_2 exposure, a consistent decline in average levels was observed across all racial groups from 2010 to 2019, except for 2010. For example, the mean NO_2 exposure among Black, Hispanic, and "Other" populations decreased from 12.72 ppb, 13.03 ppb, and 10.61 ppb in 2010 to 9.15 ppb, 9.39 ppb, and 8.44 ppb in 2019, respectively. Similarly, the Asian population experienced a reduction from 12.46 ppb to 8.97 ppb, and White individuals saw their average exposure fall from 10.46 ppb to 7.56 ppb over the same period. Throughout this timeframe, Hispanic individuals consistently had the highest average NO_2 exposure, while White individuals experienced the lowest. Despite these improvements, the interquartile range (IQR) of NO_2 exposure began widening after 2016, indicating increased variability in exposure levels within the middle range of the distribution. This pattern suggests that although severe pollution events became less common, disparities in exposure may have worsened across neighborhoods or regions, possibly driven by localized pollution sources.

In the concentration-response (C-R) functions, the "Other" racial category consistently exhibited the highest NO_2 effects. It showed the most pronounced fluctuations, particularly in 2011 when its Effect exceeded 1.15, marking the greatest deviation from the baseline across all groups (Fig.S14). This elevated impact may be linked to socioeconomic and environmental vulnerabilities, including reduced access to preventive healthcare services.

In contrast, other racial and ethnic groups displayed relatively stable trends, with only minor variations. Beginning in 2013, the effects of NO_2 exposure on LOS declined steadily across all groups, reaching their lowest point around 2016. This downward trend likely reflects improved healthcare access and disease management following Medicaid expansion and broader reforms introduced under the Affordable Care Act (ACA). However, after 2016, the influence of NO_2 exposure on LOS began to rise again, particularly among individuals in the "Other" category. This resurgence may be attributed to increased vulnerability in these populations, driven by aging demographics and a growing prevalence of chronic health conditions. Concerning lag effects, the impact of NO_2 exposure on LOS remained relatively consistent across lags of 0 to 2 days, with a slight decline by day 3. This pattern suggests that the acute health effects of NO_2 exposure tend to diminish within a few days.

As shown in Fig.S15, average $PM_{2.5}$ exposure levels declined across all racial and ethnic groups between 2010 and 2019. For Black, Hispanic, and "Other" populations, average exposures

dropped from 10.31 μg/m³, 10.76 μg/m³, and 9.78 μg/m³ in 2010 to 8.73 μg/m³, 9.09 μg/m³, and 8.41 μg/m³ in 2019, respectively. Similarly, Asian individuals experienced a reduction from 10.19 μg/m³ to 8.56 μg/m³, while the White population saw exposure levels decline from 9.73 μg/m³ to 8.25 μg/m³ over the same period. Throughout this timeframe, Hispanic and Black individuals consistently experienced the highest $PM_{2.5}$ exposure, while White individuals had the lowest. Despite this downward trend, a significant spike in $PM_{2.5}$ concentrations occurred in 2018, accompanied by notable increases in the standard deviation (SD) and interquartile range (IQR). As discussed earlier, this sharp rise in $PM_{2.5}$ levels and variability was largely driven by the severe and widespread wildfires that year, which led to extreme air pollution events. These conditions contributed to greater fluctuations in $PM_{2.5}$ exposure across all racial and ethnic groups, resulting in increased SD and IQR.

In the concentration-response (C-R) functions, the Asian group demonstrated the most pronounced changes, particularly between 2012 and 2013, when its effect estimate declined from approximately 1.06 to nearly 0.98 (Fig.S16). From 2012 to 2019, the influence of $PM_{2.5}$ exposure on hospitalization consistently decreased across all racial and ethnic groups, reaching its lowest point in 2019. This downward trend likely reflects improved air quality and greater access to preventive healthcare services resulting from Medicaid expansion and other policy reforms under the Affordable Care Act (ACA). However, starting after 2015, the effects of $PM_{2.5}$ exposure on hospitalization began to rise again, most notably among the White and Other populations. This resurgence may indicate increased vulnerability in these groups, possibly driven by a higher prevalence of chronic health conditions or other underlying risk factors. The wider confidence intervals observed for the Asian and Other groups suggest smaller sample sizes in these populations, contributing to greater variability and uncertainty in the effect estimates. Regarding lagged effects, the Other group exhibited persistent fluctuations and variability across all lag periods (0, 1, 2, and 3 days), especially during the earlier years. This group's relatively large error bars further highlight the uncertainty associated with these estimates.

4. Discussion

This study examined the temporal trends and associations between short-term air pollution exposure (NO_2 and $PM_{2.5}$) and hospitalization outcomes including admission rates and length of stay (LOS) among individuals with type 2 diabetes (T2D) in California from 2010 to 2019. Our findings indicate that although average concentrations of NO_2 and $PM_{2.5}$ declined over the study period, their health effects on the diabetic population remained significant and, in some cases, intensified. These patterns are shaped by evolving environmental exposures, population-level susceptibility, healthcare access, and racial/ethnic disparities.

Our analysis revealed a paradox: while absolute concentrations decreased, the concentration-response (C-R) relationships for pollutants and hospital outcomes (admission and LOS) showed complex and non-linear trends. Notably, after initial declines in effect estimates until around

2015, a resurgence in health impacts was observed from 2016 onwards. This may be due to increased mid-range exposure variability (rising IQR) and growing susceptibility within the aging population. Similar findings have been reported, suggesting that air pollution health risks can persist even at lower exposure levels due to chronic disease burden and demographic vulnerability (Di et al., 2017; Pope III & Dockery, 2006).

Between 2012 and 2015, a period marked by substantial ACA implementation and Medicaid expansion, we observed a reduction in the health effects of air pollution. Enhanced healthcare access likely improved disease management among T2D patients, decreasing their reliance on emergency services during pollution episodes. This aligns with prior literature highlighting how increased healthcare access can buffer the acute health impacts of environmental exposures (Sommers et al., 2015). However, after 2015, the growing burden of chronic diseases and aging demographics may have offset these benefits, contributing to a rebound in pollution-related hospitalizations and LOS.

The sharp increase in $PM_{2.5}$ levels in 2018 due to catastrophic wildfires illustrates how climate-driven events are altering the air pollution landscape in California. While these spikes were temporally intense, they did not correspond to proportional increases in hospitalizations or LOS, possibly due to public adaptation behaviors such as mask usage and sheltering indoors. This suggests that the toxicity and duration of exposure (e.g., wildfire vs. traffic-related $PM_{2.5}$) may differentially impact health, a hypothesis supported by emerging literature (Aguilera et al., 2021; Reid et al., 2016). Furthermore, adjustments in statistical models may have overcontrolled for wildfire-related $PM_{2.5}$, potentially underestimating its contribution to health outcomes.

Our findings underscore persistent racial and ethnic disparities in both exposure and vulnerability. Hispanic and Black populations experienced consistently higher average NO_2 and $PM_{2.5}$ levels than White populations. The "Other" racial category, which includes small, often underrepresented subgroups, exhibited the most pronounced and fluctuating health impacts. These disparities likely reflect environmental injustice, neighborhood segregation, healthcare access, and socioeconomic stressors. Previous studies have documented similar patterns of disproportionate exposure and health burden among marginalized communities (Clark et al., 2014; Mikati et al., 2018), highlighting the urgency for targeted interventions in these populations.

Both NO_2 and $PM_{2.5}$ demonstrated significant short-term (0–3 day) associations with T2D-related hospitalization and length of stay (LOS), with the most pronounced effects typically occurring within the first two days of exposure. These patterns underscore the acute health risks posed by these pollutants to vulnerable populations. The variability in effect sizes across lag structures and control periods highlights the importance of rigorous methodological choices in time-series and case-crossover designs, while the consistency of statistical significance across control strategies strengthens the credibility of our findings.

Our results indicate that improvements in overall air quality may not, by themselves, eliminate health disparities unless paired with policies that address underlying population vulnerabilities and healthcare access. Despite California's notable progress in reducing air pollution, the increasing variability in moderate exposure levels and the disproportionate burden observed in specific racial and ethnic groups call for more geographically and demographically tailored interventions. Integrating high-resolution air quality monitoring with chronic disease management particularly for individuals with diabetes could help prevent acute health events and reduce hospital system strain.

Several limitations should be noted. First, exposure estimates relied on ambient pollutant concentrations and did not capture personal exposure variations due to indoor environments or individual behaviors. Second, unmeasured confounding from factors such as diet, smoking, or medication adherence may persist. Third, smaller sample sizes for certain racial/ethnic categories (particularly "Other") produced wider confidence intervals, warranting cautious interpretation. Finally, our analysis focused on short-term exposure, and the impacts of chronic exposure remain an important area for future investigation.

The observed year-to-year fluctuations in effect estimates may reflect the combined influence of changing healthcare access under the Affordable Care Act (ACA) and the episodic nature of wildfire-driven pollution. Notably, disparities in air pollution-related impacts appeared to widen in certain years, underscoring the need for adaptive public health strategies that respond to both environmental variability and shifting policy landscapes.

5. Conclusions and Implications

This study offers a comprehensive assessment of the impact of short-term exposure to air pollutants, specifically nitrogen dioxide (NO_2) and fine particulate matter ($PM_{2.5}$), on hospitalization outcomes among individuals with type 2 diabetes (T2D) in California from 2010 to 2019. Our analysis reveals persistent and significant associations between ambient air pollution and adverse health outcomes in high-risk populations by evaluating hospital admission rates and length of stay (LOS) over a decade of evolving environmental, demographic, and policy landscapes.

Despite measurable improvements in air quality across the state, driven by regulatory interventions and technological advancements, our findings demonstrate that the health burden of air pollution among diabetic patients has not proportionally declined. After a period of reduced effect estimates between 2012 and 2015, likely linked to the implementation of the Affordable Care Act (ACA) and expanded healthcare access, the concentration-response (C-R) functions for both NO_2 and $PM_{2.5}$ began to rise again. This resurgence appears to be associated with increased mid-range exposure variability and growing population vulnerability, particularly due to aging demographics and the cumulative burden of chronic diseases.

Our analysis further highlights the nuanced nature of air pollution impacts, where the average concentration and exposure distribution (e.g., interquartile range and standard deviation) play a critical role in shaping health risks. For instance, while extreme pollution events became less frequent, the widening interquartile ranges after 2016 suggest that mid-level pollution variability increased, potentially sustaining health impacts despite overall air quality improvements.

Another key finding is the role of wildfire-related $PM_{2.5}$ events, particularly in 2018, which led to acute spikes in pollution levels without a corresponding surge in hospitalizations or LOS. This pattern may be explained by protective public behaviors, temporary exposure profiles, and model adjustments that may have underrepresented wildfire-specific health effects. Nonetheless, these events underscore the growing relevance of climate change and environmental extremes in shaping modern pollution dynamics and associated health risks.

Our study also provides strong evidence of racial and ethnic disparities in pollutant exposure and the health effects that result from it. Hispanic and Black populations consistently experienced higher levels of NO_2 and $PM_{2.5}$, and the "Other" racial category likely representing smaller, underrepresented groups showed the most pronounced and variable C-R estimates. These disparities are reflective of broader environmental justice issues, where structural inequities in housing, healthcare access, and neighborhood infrastructure contribute to elevated health burdens among marginalized populations. This reinforces the need for policy approaches that are both environmentally sound and equity-focused.

Lag analyses revealed that the health effects of NO_2 and $PM_{2.5}$ were most pronounced within the first 48 hours post-exposure, consistent with prior evidence that links these pollutants to acute exacerbations of chronic diseases. These short-term dynamics emphasize the urgency of timely public health alerts and interventions, especially during known pollution events or wildfire outbreaks.

Taken together, our findings advocate for a dual-pronged strategy in environmental health policy. On one hand, continued efforts to reduce overall emissions through stricter standards and cleaner technologies remain essential. On the other hand, interventions must also be tailored to address regional disparities, racial/ethnic vulnerabilities, and the unique risks associated with climate-induced pollution spikes such as wildfires. Integrating environmental data with chronic disease management systems, especially within Medicaid and Medicare frameworks, could enhance preventive care delivery and reduce hospital burden.

Environmental factors and healthcare access and utilization patterns significantly shape the relationship between pollution and hospitalization. The observed decrease in health impacts during the ACA expansion years exemplifies the value of healthcare policy as a buffer against environmental stressors. This intersection between public health, healthcare access, and environmental quality represents a crucial frontier for future interdisciplinary research and policymaking.

While this study provides robust and policy-relevant insights, certain limitations must be acknowledged. Ambient pollution estimates do not account for individual-level exposures, indoor air quality, or personal behaviors such as air filters or masks. Additionally, unmeasured confounding variables and small subgroup sizes (especially in the "Other" racial category) may limit the precision of some estimates. Furthermore, this study focused solely on short-term exposures; the cumulative effects of chronic air pollution on diabetes-related morbidity remain an important direction for future investigation.

In conclusion, air pollution remains a significant and inequitable driver of adverse health outcomes among individuals with type 2 diabetes in California, even amid regulatory progress. Short-term exposure to NO_2 and $PM_{2.5}$ is associated with increased hospitalizations and prolonged LOS, with disproportionate effects among racial and ethnic minorities. These findings call for sustained, adaptive, and equity-focused environmental health strategies, particularly in the context of climate change and ongoing demographic shifts. Effective interventions must couple air quality improvements with healthcare accessibility, public education, and targeted support for vulnerable communities to reduce air pollution-related health burdens meaningfully.

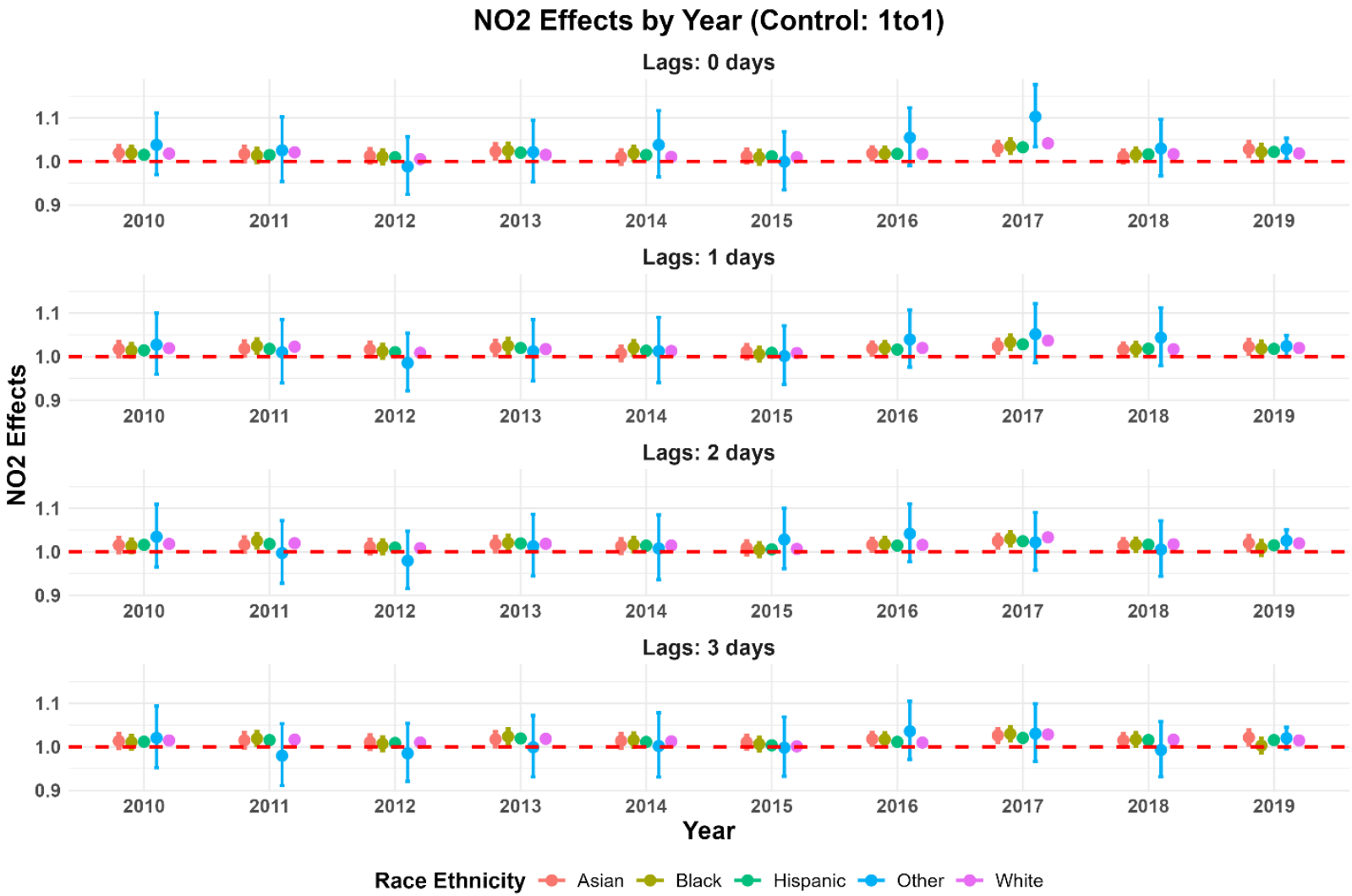

Fig. S1. The associations between NO_2 exposure and hospitalization for diabetic patients across five major race categories in California from 2010 to 2019.

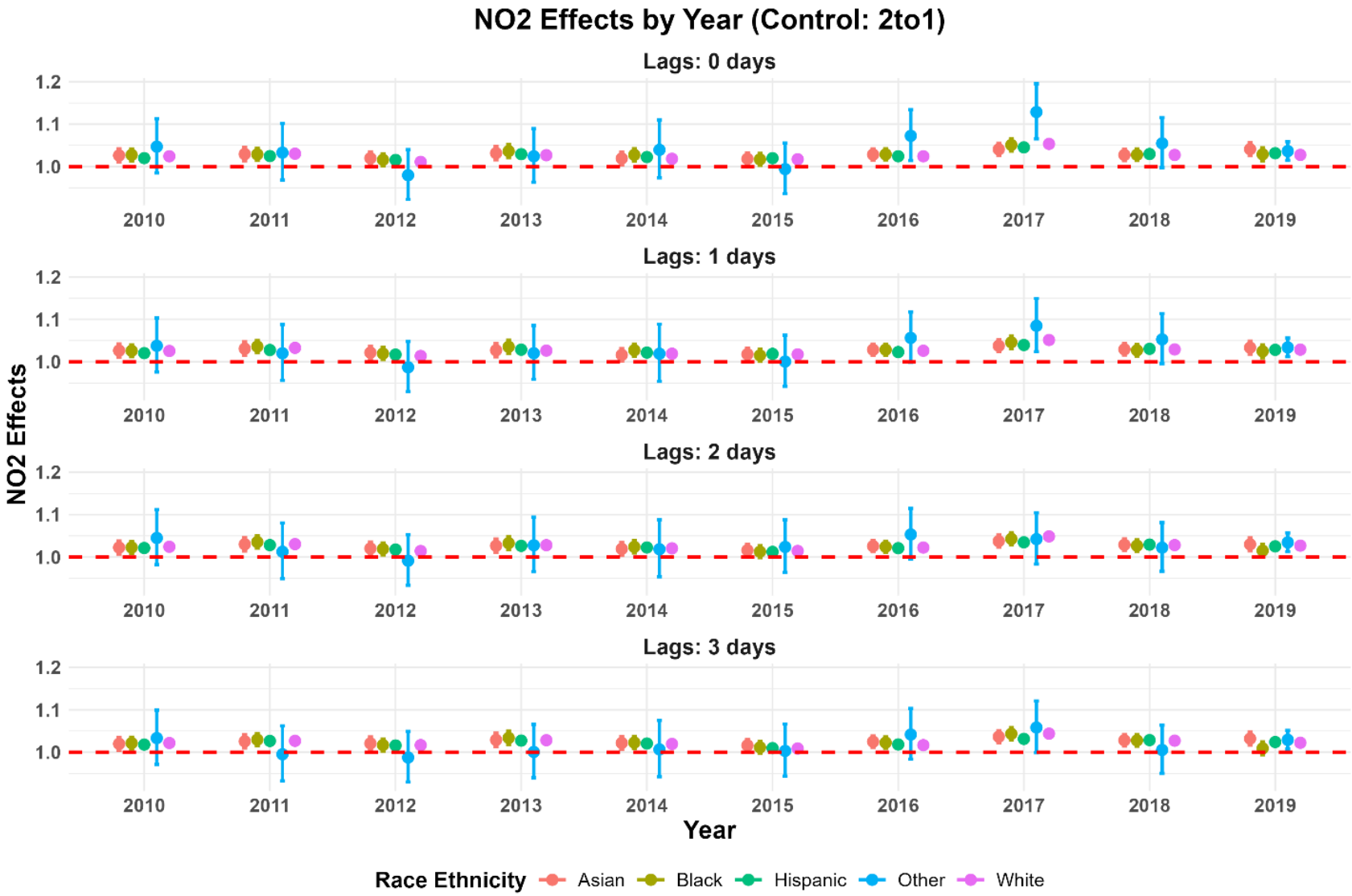

Fig. S2. The associations between NO_2 exposure and hospitalization for diabetic patients across five major race categories in California from 2010 to 2019.

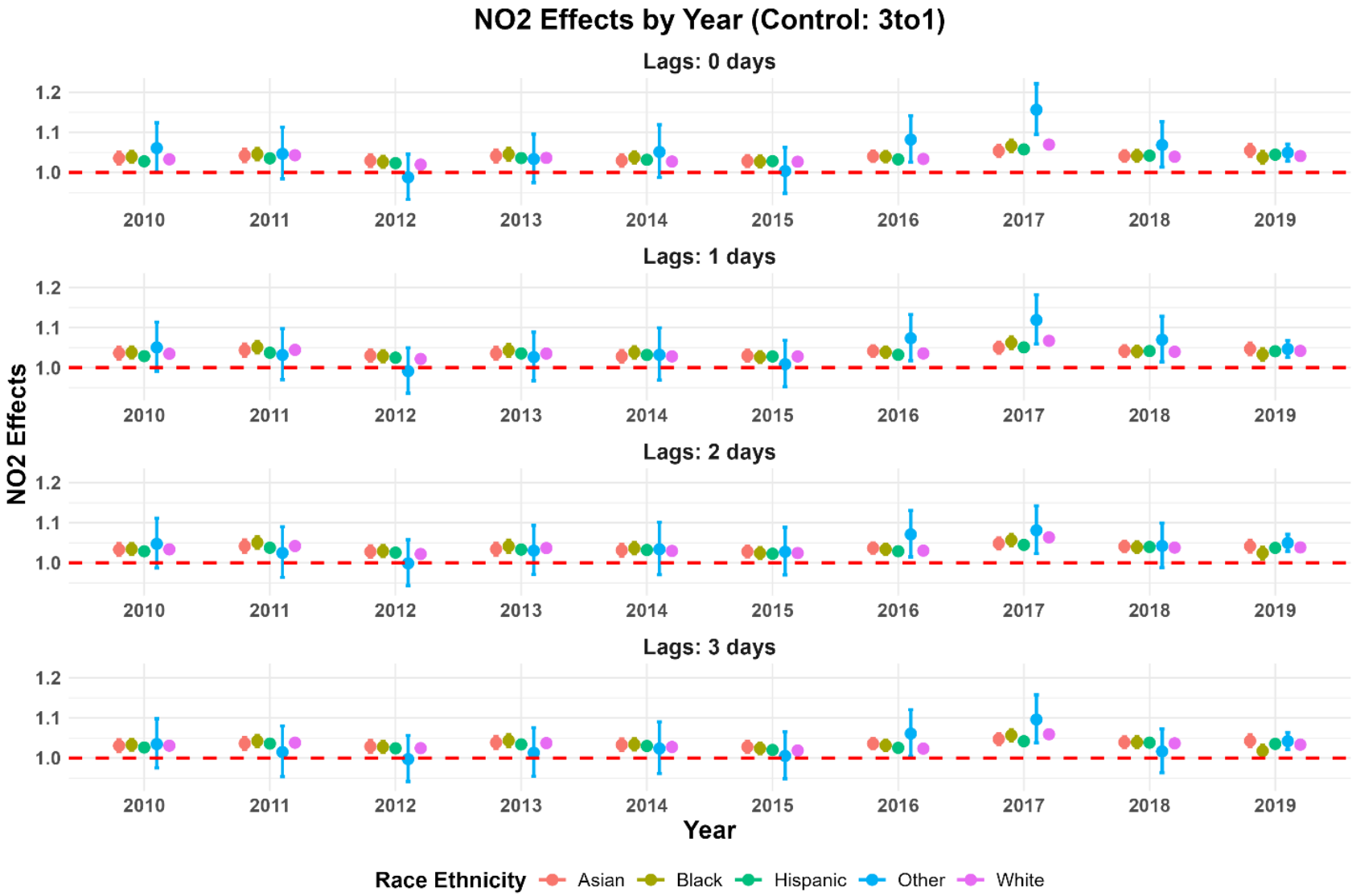

Fig. S3. The associations between NO_2 exposure and hospitalization for diabetic patients across five major race categories in California from 2010 to 2019.

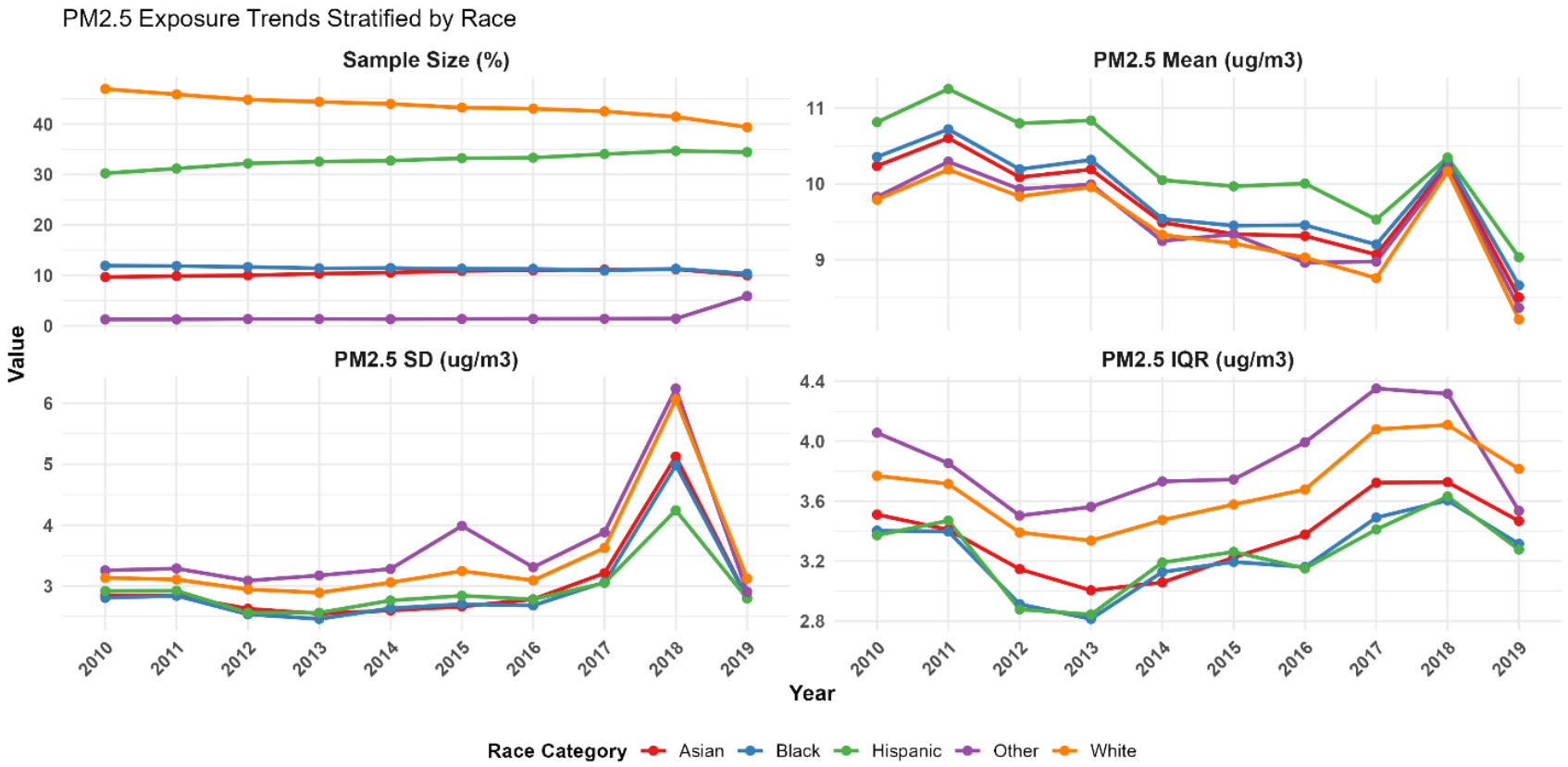

Fig. S4. The temporal trend of the population, categorized by five major races, in California diagnosed with diabetes and $PM_{2.5}$ exposure from 2010 to 2019.

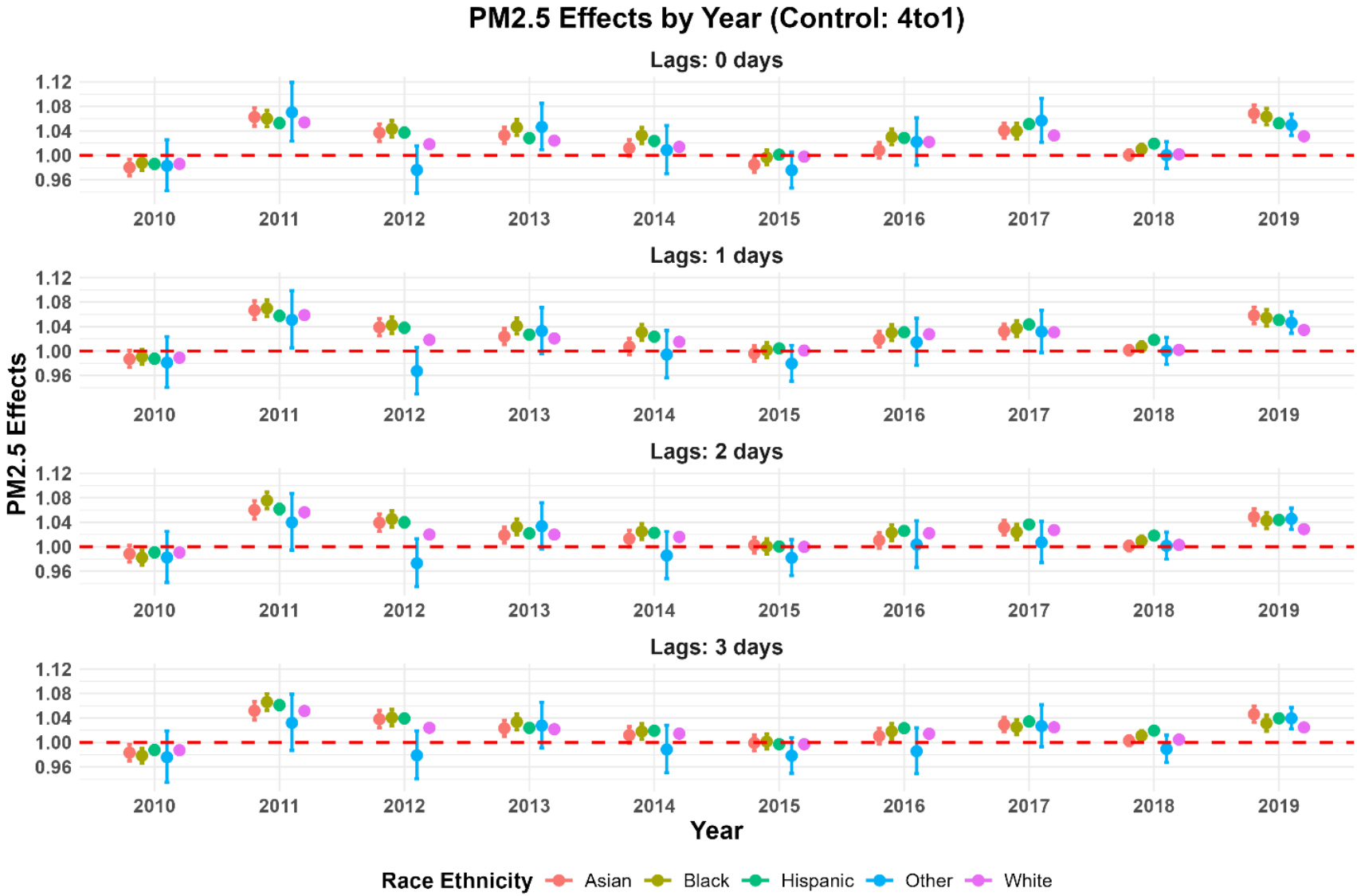

Fig. S5. The associations between $PM_{2.5}$ exposure and hospitalization for diabetic patients across five major race categories in California from 2010 to 2019.

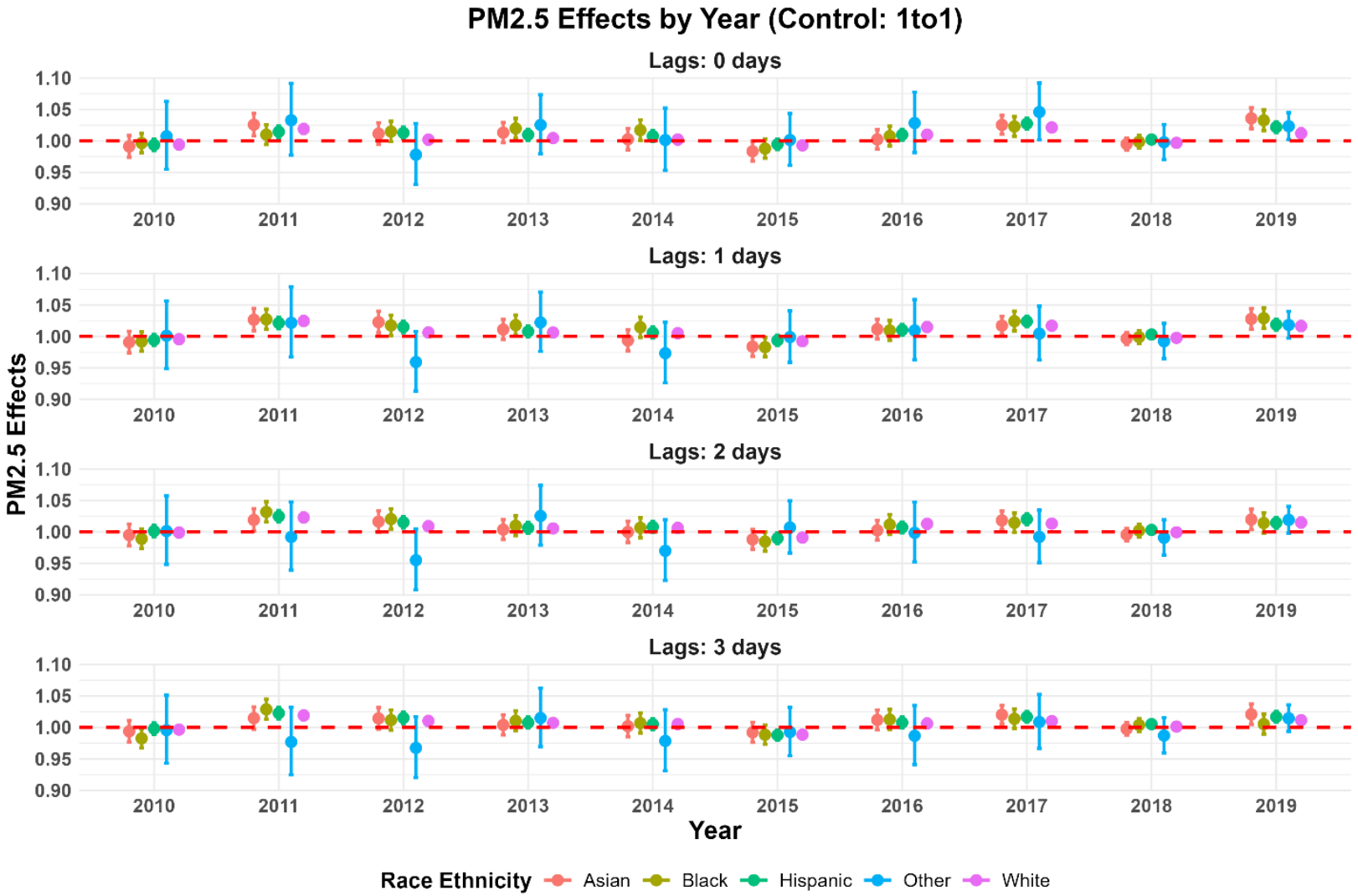

Fig. S6. The associations between $PM_{2.5}$ exposure and hospitalization for diabetic patients across five major race categories in California from 2010 to 2019.

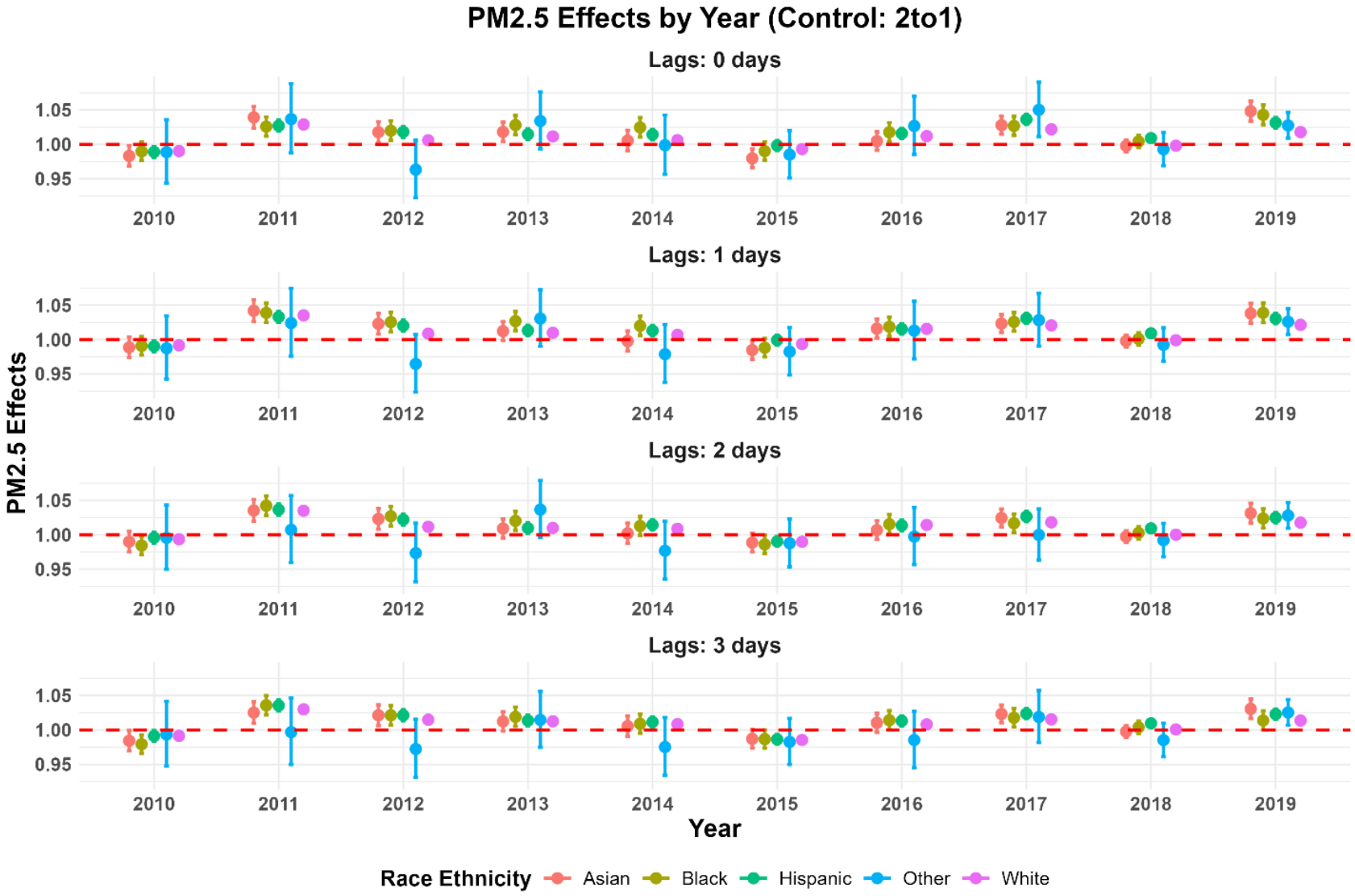

Fig. S7. The associations between $PM_{2.5}$ exposure and hospitalization for diabetic patients across five major race categories in California from 2010 to 2019.

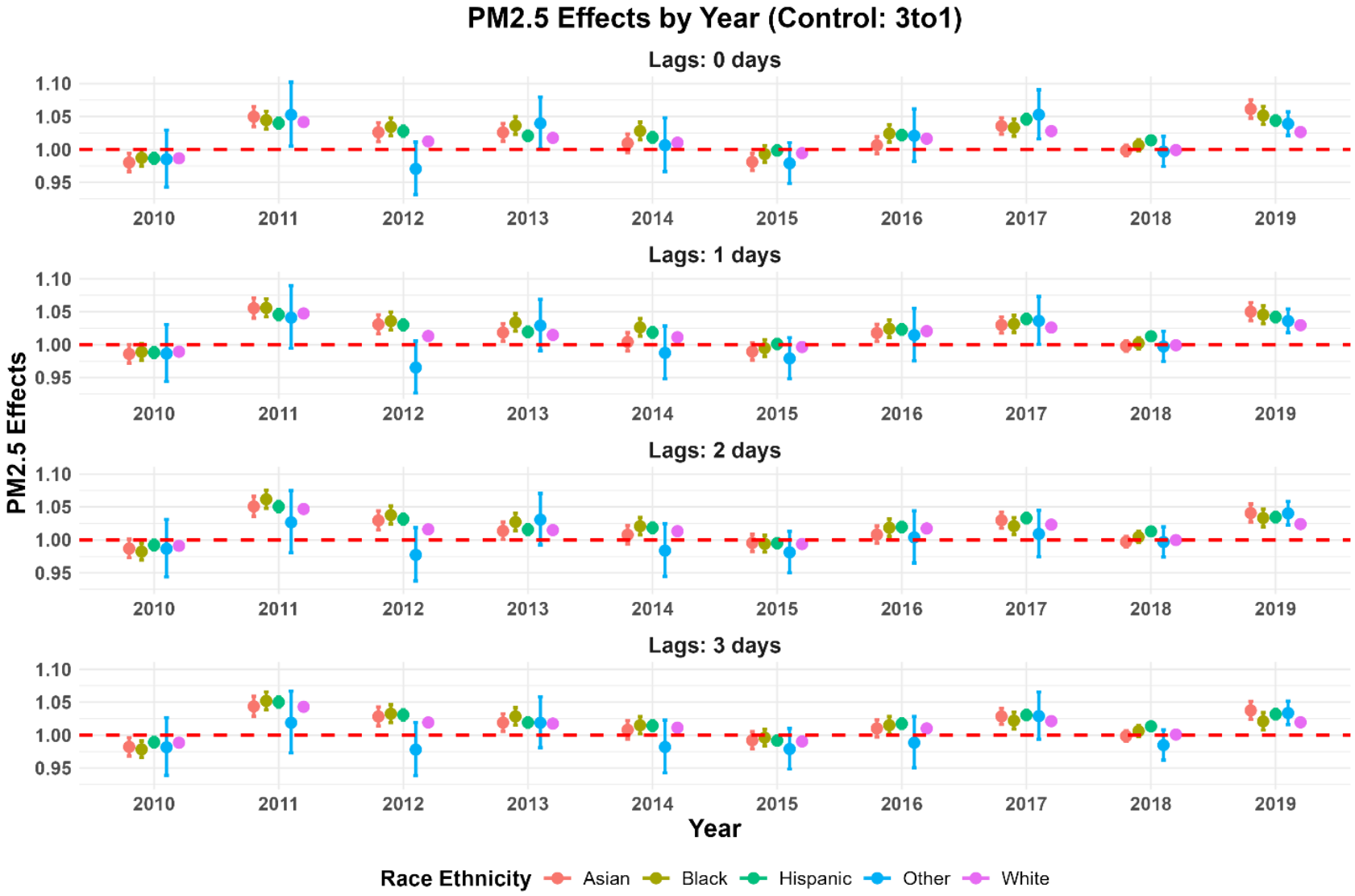

Fig. S8. The associations between $PM_{2.5}$ exposure and hospitalization for diabetic patients across five major race categories in California from 2010 to 2019.

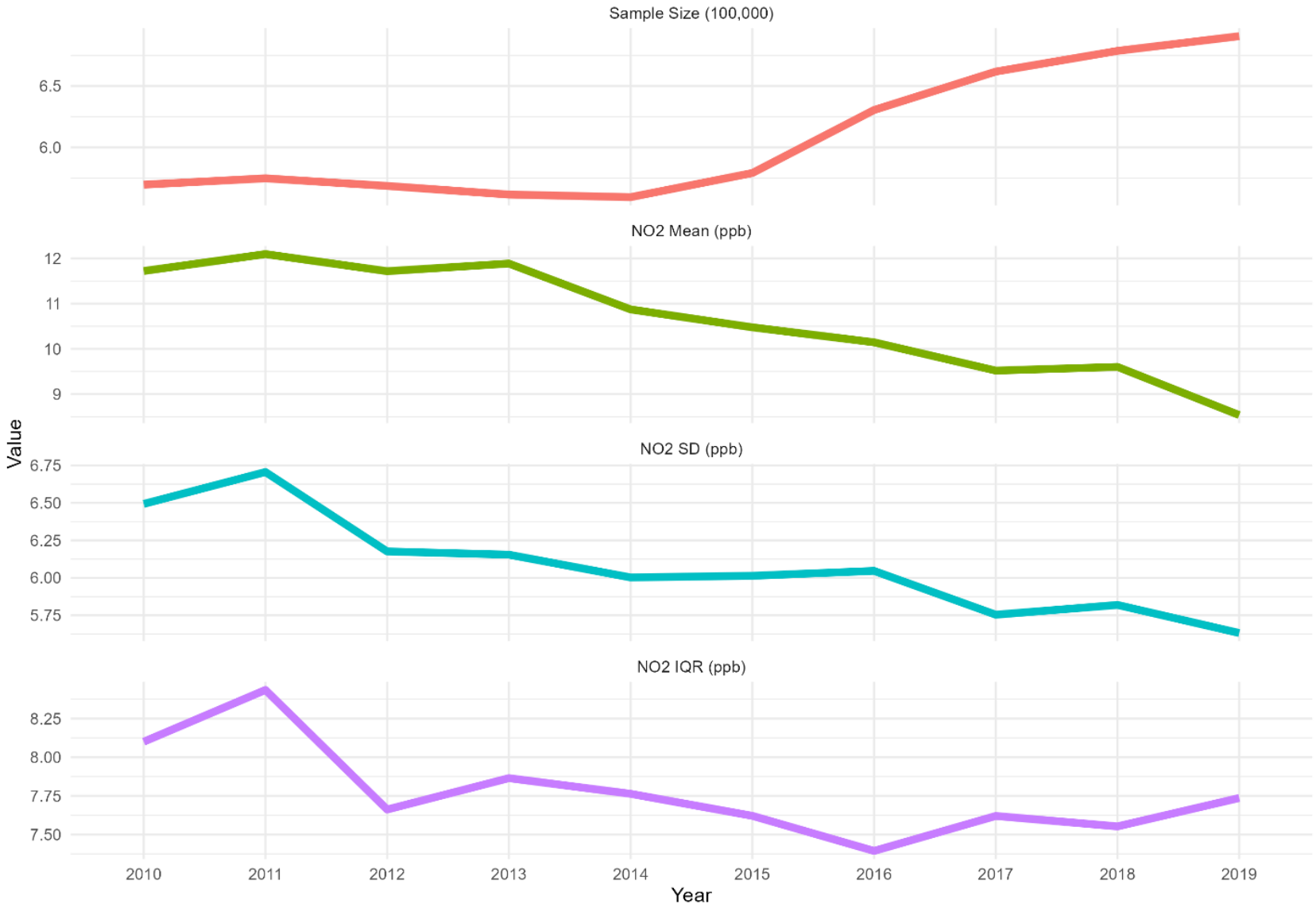

Fig. S9. The temporal trend of the hospitalized population in California diagnosed with diabetes and NO_2 exposure from 2010 to 2019.

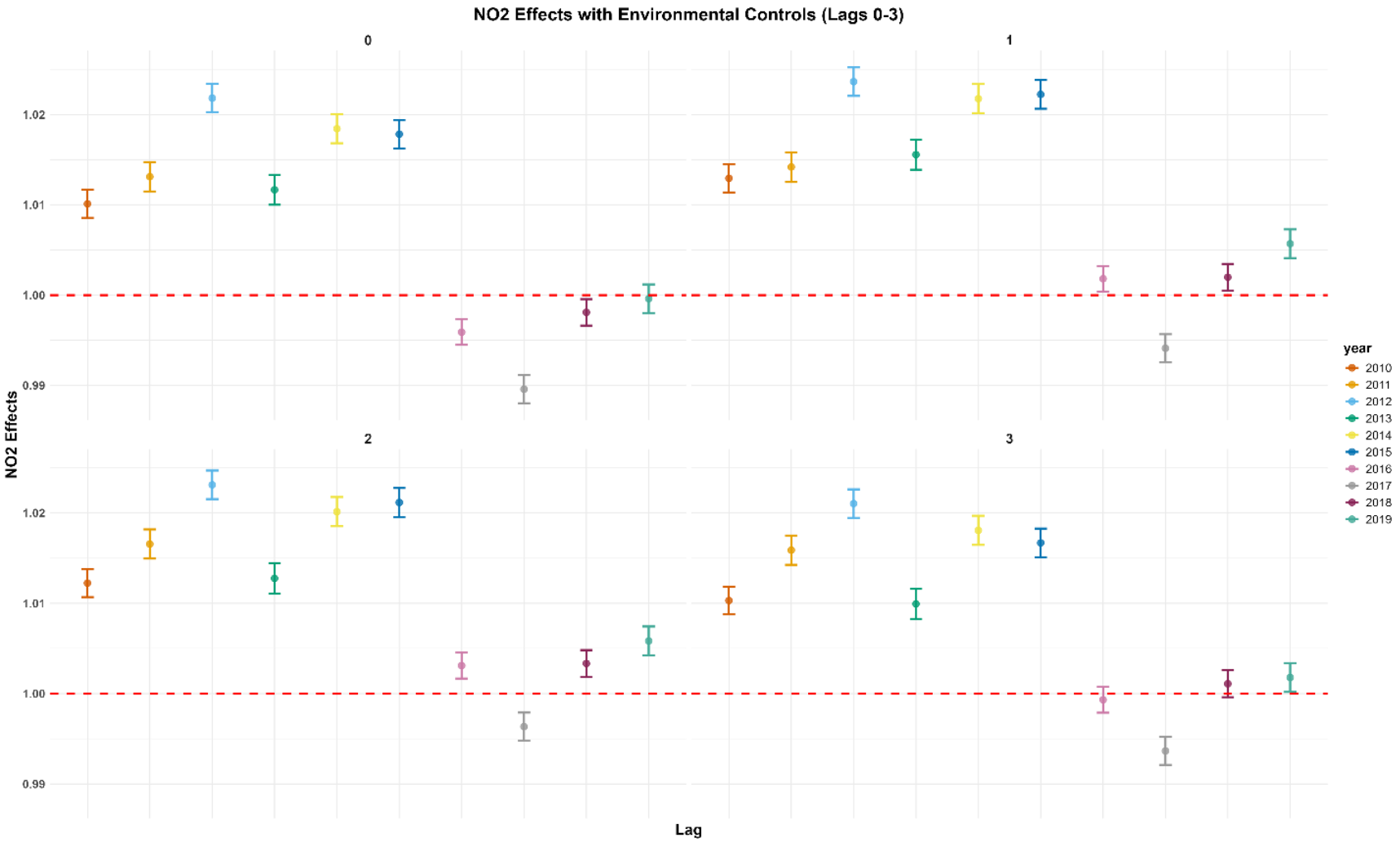

Fig. S10. The association between NO_2 exposure and LOS over 0–3 lag days, modeled annually from 2010 to 2019.

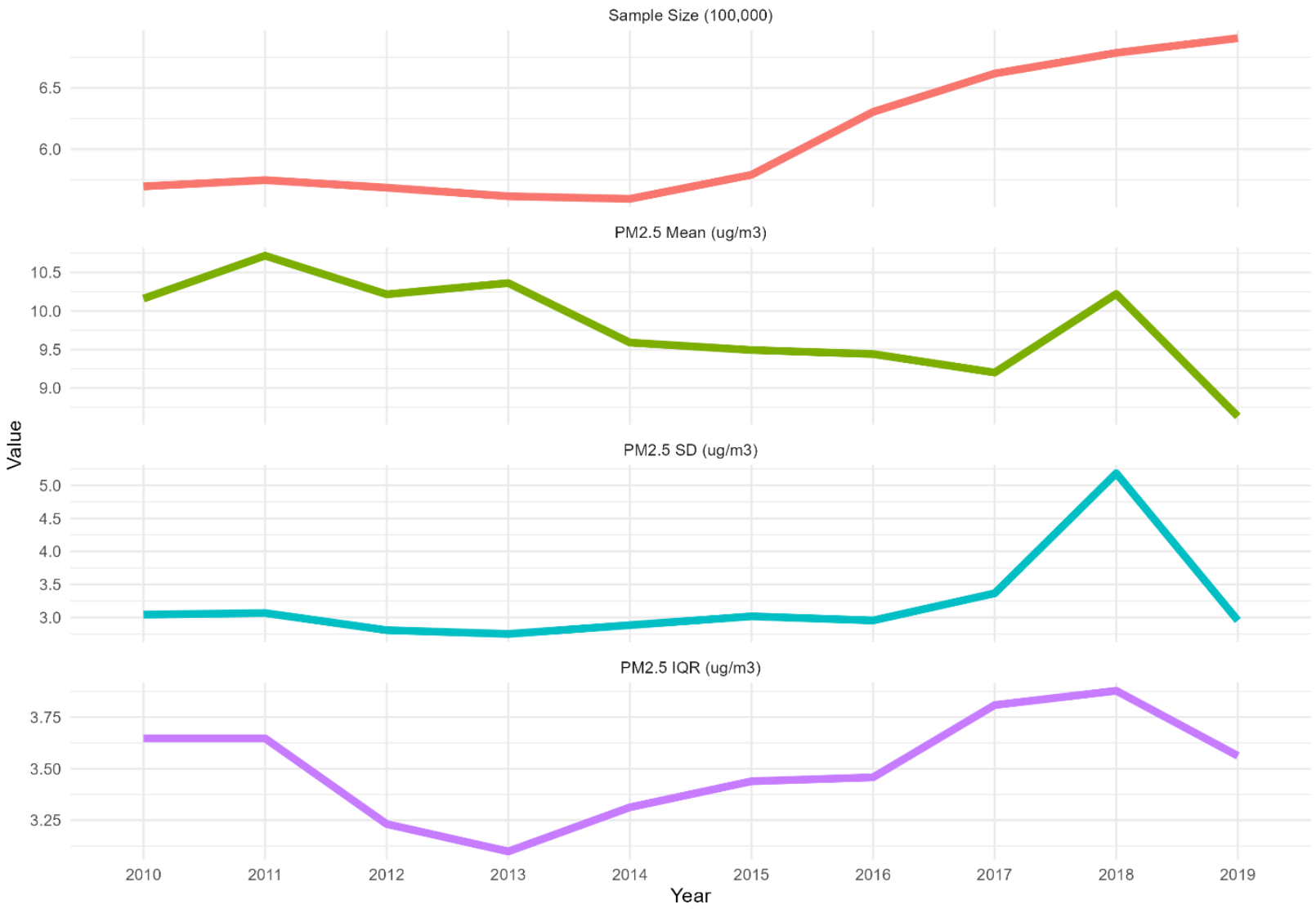

Fig.S11. The temporal trend of the hospitalized population in California diagnosed with diabetes and $PM_{2.5}$ exposure from 2010 to 2019.

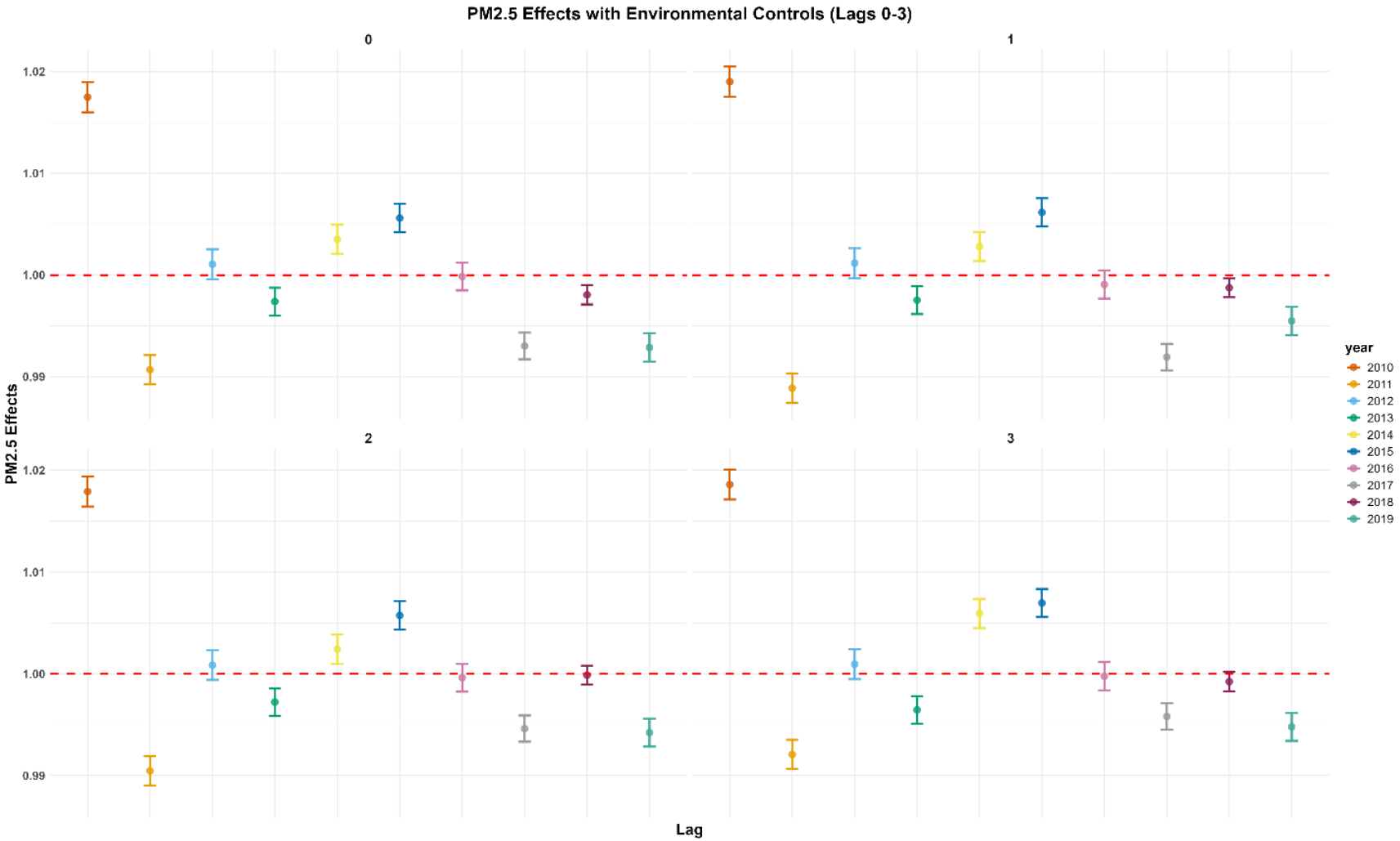

Fig. S12. The association between $PM_{2.5}$ exposure and LOS over 0–3 lag days, modeled annually from 2010 to 2019.

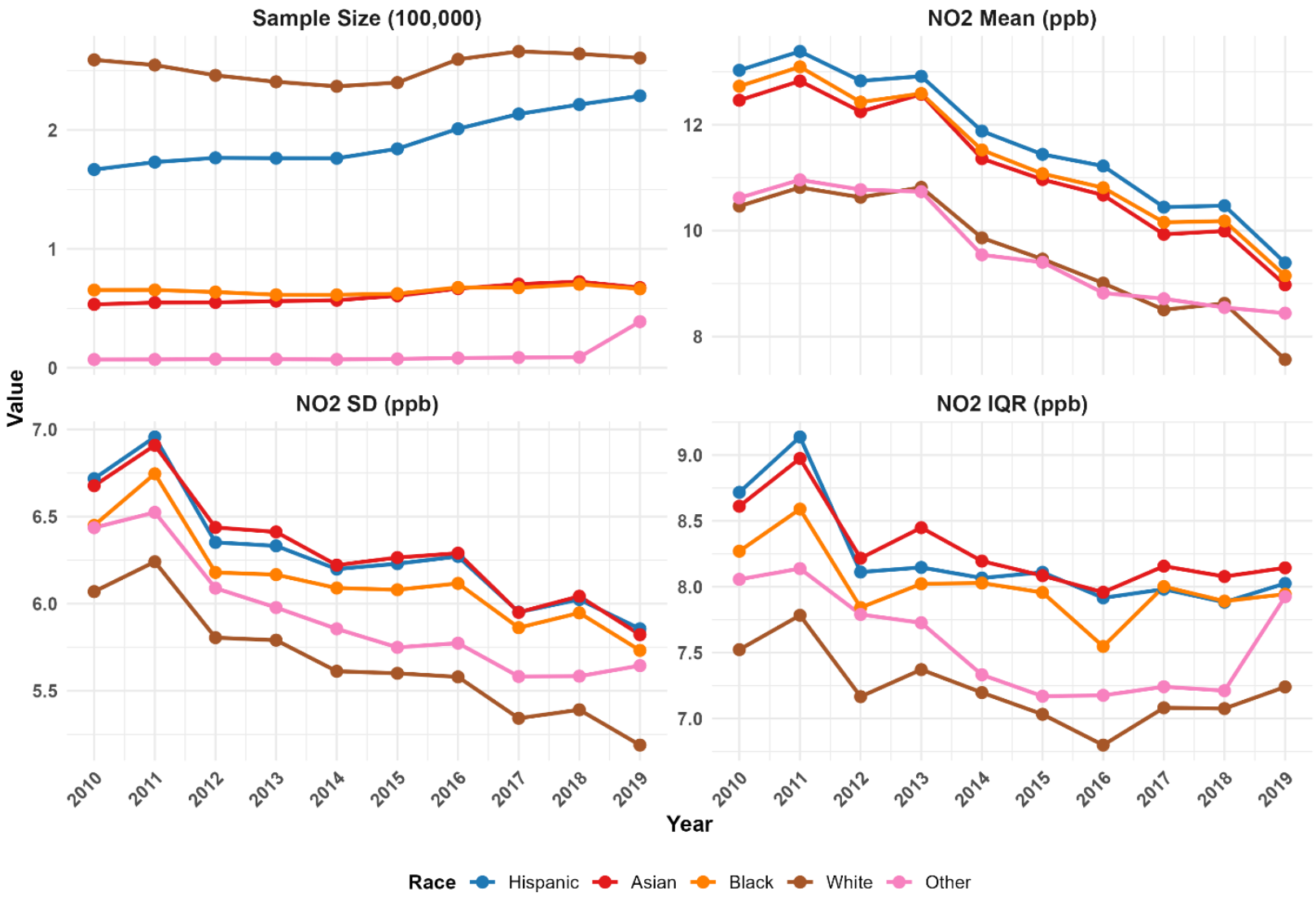

Fig. S13. The temporal trend of the population, categorized by five major races, in California diagnosed with diabetes and NO_2 exposure from 2010 to 2019.

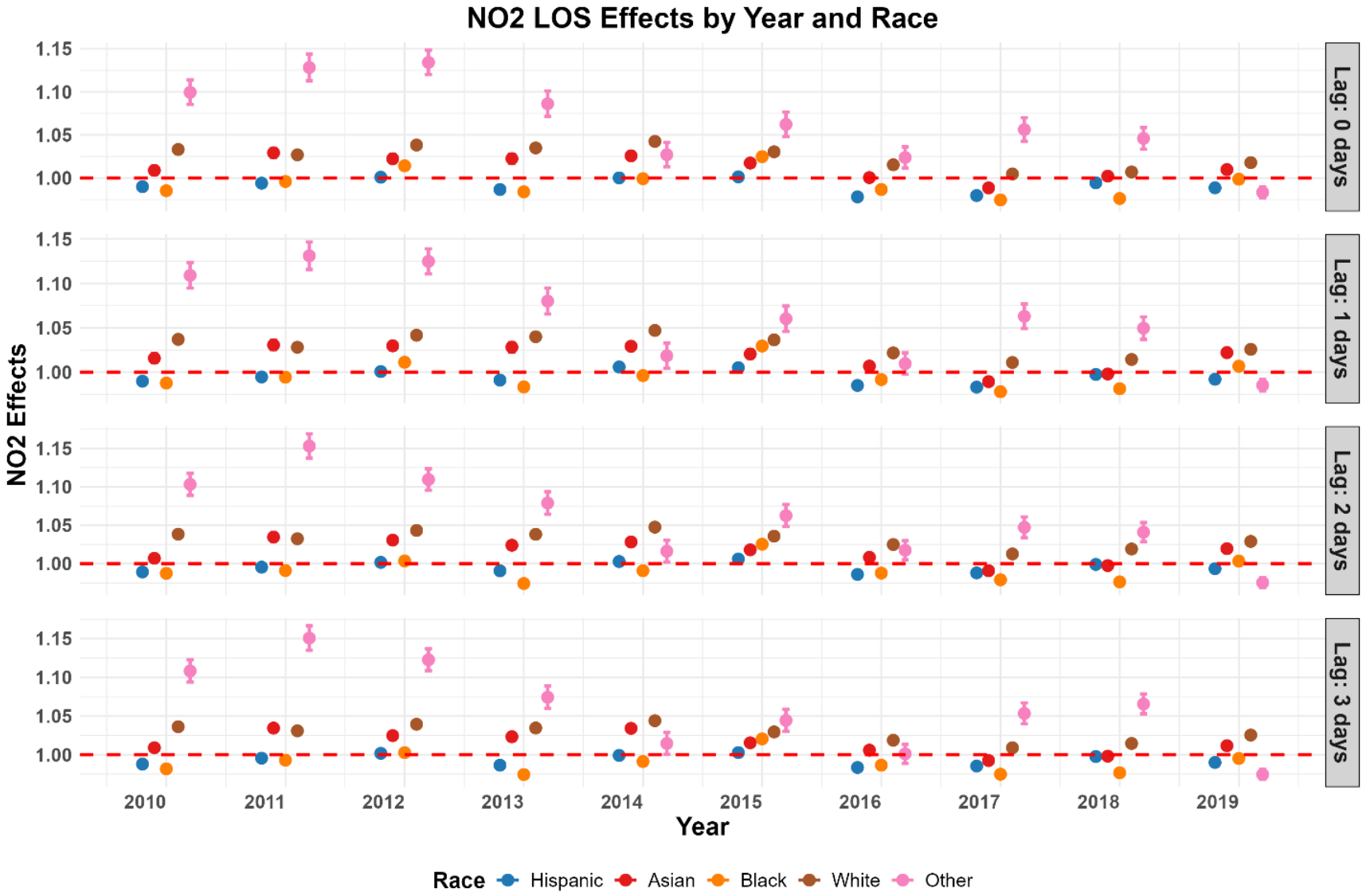

Fig. S14. The associations between NO_2 exposure and LOS for diabetic patients across five major race categories in California from 2010 to 2019.

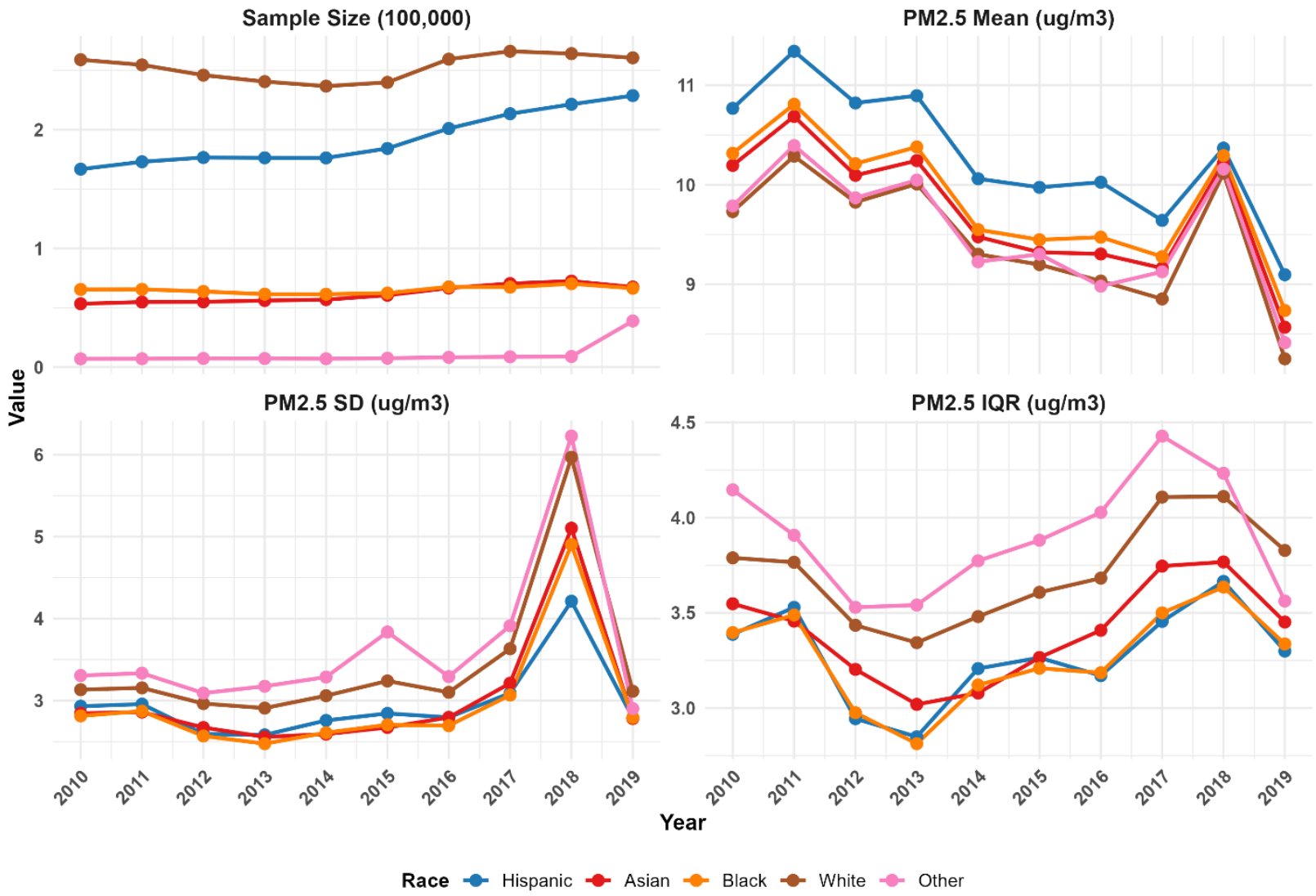

Fig. S15. The temporal trend of the population, categorized by five major races, in California diagnosed with diabetes and $PM_{2.5}$ exposure from 2010 to 2019.

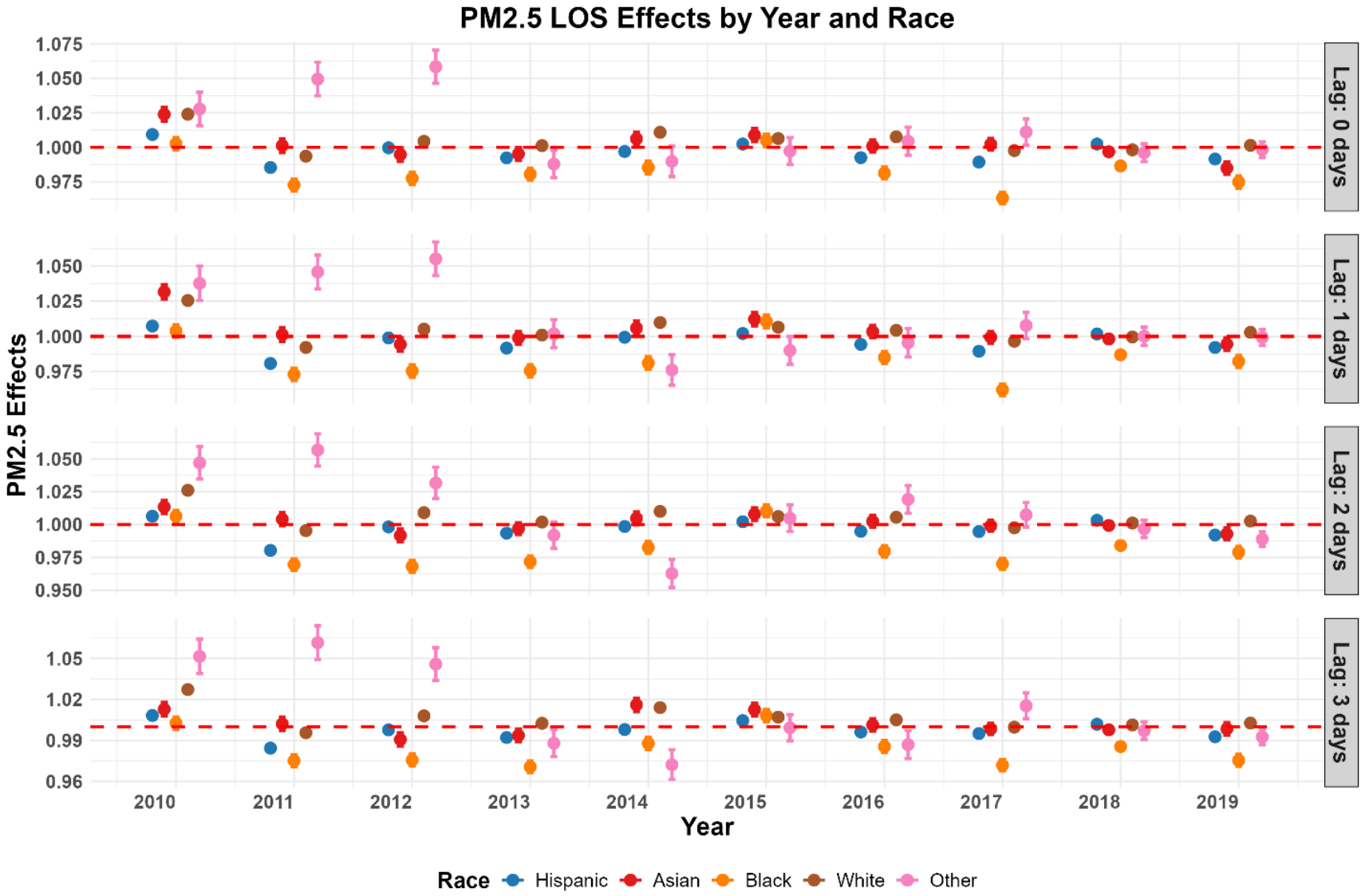

Fig. S16. The associations between $PM_{2.5}$ exposure and LOS for diabetic patients across five major race categories in California from 2010 to 2019.

References

Aguilera, R., Corringham, T., Gershunov, A., & Benmarhnia, T. (2021). Wildfire smoke impacts respiratory health more than fine particles from other sources: observational evidence from Southern California. *Nature communications*, *12*(1), 1493.

Brook, R. D., Rajagopalan, S., Pope III, C. A., Brook, J. R., Bhatnagar, A., Diez-Roux, A. V., Holguin, F., Hong, Y., Luepker, R. V., & Mittleman, M. A. (2010). Particulate matter air pollution and cardiovascular disease: an update to the scientific statement from the American Heart Association. *Circulation*, *121*(21), 2331-2378.

Clark, L. P., Millet, D. B., & Marshall, J. D. (2014). National patterns in environmental injustice and inequality: outdoor NO2 air pollution in the United States. *PloS one*, *9*(4), e94431.

Di, Q., Wang, Y., Zanobetti, A., Wang, Y., Koutrakis, P., Choirat, C., Dominici, F., & Schwartz, J. D. (2017). Air pollution and mortality in the Medicare population. *New England Journal of Medicine*, *376*(26), 2513-2522.

Guo, F., Chen, X., Howland, S., Niu, Z., Zhang, L., Gauderman, W. J., McConnell, R., Pavlovic, N., Lurmann, F., & Bastain, T. M. (2025). Childhood Exposure to Air Pollution, Body Mass Index Trajectories, and Insulin Resistance Among Young Adults. *JAMA Network Open*, *8*(4), e256431-e256431.

Hong, Q., Zhao, Y., Wang, J., Sun, H., Deng, L., Cao, J., & Wang, C. (2025). Correlation of PM2. 5 pollution and daily mortality rate of cardiovascular and cerebrovascular diseases in Northeast China through PM2. 5 sources analysis. *Frigid Zone Medicine*, *4*(4), 193-201.

Hu, M., Hao, X., Zhang, Y., Sun, X., Zhang, M., Zhao, J., & Wang, Q. (2025). Long-term exposure to particulate air pollution associated with the progression of type 2 diabetes mellitus in China: effect size and urban–rural disparities. *BMC Public Health*, *25*(1), 1565.

Liang, H., Zhou, W., Wen, Z., Wei, J., Wang, W., & Li, J. (2025). Short-term exposure to PM2. 5 and its components and type 2 diabetes-related hospital admissions, length of stay, and hospital costs in Shanghai. *International Journal of Environmental Health Research*, 1-14.

Liu, C., Chen, R., Sera, F., Vicedo-Cabrera, A. M., Guo, Y., Tong, S., Coelho, M. S., Saldiva, P. H., Lavigne, E., & Matus, P. (2019). Ambient particulate air pollution and daily mortality in 652 cities. *New England Journal of Medicine*, *381*(8), 705-715.

Mikati, I., Benson, A. F., Luben, T. J., Sacks, J. D., & Richmond-Bryant, J. (2018). Disparities in distribution of particulate matter emission sources by race and poverty status. *American journal of public health*, *108*(4), 480-485.

Pope III, C. A., & Dockery, D. W. (2006). Health effects of fine particulate air pollution: lines that connect. *Journal of the air & waste management association*, *56*(6), 709-742.

R Core Team. (2023). *R: A language and environment for statistical computing [Computer software]. Version 4.3. 1. Vienna, Austria: Foundation for Statistical Computing; 2023*

Rajagopalan, S., & Brook, R. D. (2012). Air pollution and type 2 diabetes: mechanistic insights. *Diabetes*, *61*(12), 3037-3045.

Reid, C. E., Brauer, M., Johnston, F. H., Jerrett, M., Balmes, J. R., & Elliott, C. T. (2016). Critical review of health impacts of wildfire smoke exposure. *Environmental health perspectives*, *124*(9), 1334-1343.

Saeed, R. A. (2025). *Association Between Wildfire-Specific Particulate Matter Exposure and Cardiovascular Disease* University of California, Irvine].

Sommers, B. D., Gunja, M. Z., Finegold, K., & Musco, T. (2015). Changes in self-reported insurance coverage, access to care, and health under the Affordable Care Act. *Jama*, *314*(4), 366-374.

Spinu, M. V., Grolemund, G., & Wickham, H. (2016). Package 'lubridate'. *Recuperado el*.

Su, J. G., Shahriary, E., Sage, E., Jacobsen, J., Park, K., & Mohegh, A. (2024). Development of over 30-years of high spatiotemporal resolution air pollution models and surfaces for California. *Environment International*, *193*, 109100.

Therneau, T. M., & Lumley, T. (2015). Package 'survival'. *R Top Doc*, *128*(10), 28-33.

Wettstein, Z. S., Hoshiko, S., Fahimi, J., Harrison, R. J., Cascio, W. E., & Rappold, A. G. (2018). Cardiovascular and cerebrovascular emergency department visits associated with wildfire smoke exposure in California in 2015. *Journal of the American heart association*, *7*(8), e007492.

Wickham, H. (2015). dplyr: A grammar of data manipulation. *R package version 04.*, *3*, p156.

Wickham, H., Chang, W., & Wickham, M. H. (2016). Package 'ggplot2'. *Create elegant data visualisations using the grammar of graphics. Version*, *2*(1), 1-189.

Wickham, H., & Wickham, M. H. (2017). Package 'tidyr'. *Easily Tidy Data with'spread'and'gather ()' Functions*.

Zhang, J., Chen, J., Nie, J., Shi, Y., Wei, J., Yan, Y., Han, S., Yu, W., Li, X., & Duan, Z. (2025). The Triglyceride–Glucose Index as a Measure of Insulin Resistance, Mediated the Relationship Between Air Pollution and Hypertension in Middle-aged and Older Adults. *The Journals of Gerontology, Series A: Biological Sciences and Medical Sciences*, *80*(7), glaf114.

Supplementary File 3

Ogawa saturation monitoring data

We have collected Ogawa data (NO_2 – nitrogen dioxide and NO_X – nitrogen oxides) for both pre- and post-policy intervention periods for the San Francisco Bay and the LA regions. Table Suppl. 1 displays the date of data collection, pollutants measured and effective sample sizes. To enable us to merge the Ogawa data with the government monitoring data, all the Ogawa data were corrected based on the government monitoring data through collocated sites. Because of differences in vehicle emissions and urban structures, especially for highway roadways, the NO_2 and NO_X data collected through Ogawa were corrected separately for policy periods and regions. We found the agreement (correlation coefficient) for measured pollutant concentrations at the same 14-day period between the collocated government and Ogawa monitors ranged from 0.69 to 0.98 (Table suppl. 1), indicating the overall representativeness of using Ogawa monitors for NO_2 and NO_X monitoring. After consulting with the experts in the Research Triangle Park (North Carolina, USA), the company responsible for providing us the Ogawa samplers and the analysis of the sampled data, we concluded that the reasons for some discrepancy between government monitoring and our Ogawa monitoring were partly because the Ogawa data were calibrated based on the latest lab results, but the government data were rarely calibrated. We also investigated the number of effective hours of data collection for every government site during the same time period when an Ogawa monitor was collocated. We found the number of hours for government monitors ranged from 34 hours to the full range of 14 days. Even though we removed those government monitoring stations with the number of effective hours of measurement being less than 200 in our effort to calibrate the measured Ogawa data, the missing hours might also have contributed to the discrepancy between the two data sources. In some situations, because of our inability to gain access to the exact location of a government monitoring station, the Ogawa samplers were placed on the gate to the building on which the government monitoring station was placed on top. This might also have contributed to the discrepancy between the two data sources.

We further averaged NO_2 and NO_X concentrations for the dry and wet seasons to represent annual concentrations measured at those saturation monitoring sites. This procedure is valid given that measurements for each policy period in each region were selected after reviewing historical long-term government monitoring data with the goal that these two 2-week monitoring would allow us to estimate long-term average concentrations most accurately. Our research did show that the average of dry and wet season concentrations in a sampling period was close to the annual concentrations measured at those sites (Suet al. 2016). Due to lack of NO_X measurements for the pre-policy period for the San Francisco Bay Area, we opted to use NO_2 as a pollutant for our analysis in this paper.

Table Suppl.1. Historical Ogawa samplings conducted in California and agreement with collocated government sites

Region	Policy Period	Year	Month	Pollutants	Sample size	Collocated sites	Correlation coefficient
San Francisco Bay Area	Pre-policy	2004	November	NO2	51	3	0.88
		2005	May	NO2	48	3	0.72
	Post-policy	2012	October	NO2	49	4	0.93
				NOX	49	4	0.98
		2013	March	NO2	49	4	0.69
				NOX	49	4	0.94
Los Angeles Region	Pre-policy	2006	September	NO2	198	10	0.90
				NOX	198	10	0.94
		2007	February	NO2	195	12	0.81
				NOX	195	12	0.97
	Post-policy	2012	October	NO2	70	12	0.91
				NOX	70	12	0.92
		2013	March	NO2	72	8	0.90
				NOX	72	8	0.88

Utilizing location-allocation algorithms for air quality monitoring data from Google Streetcar mobile monitoring

Study area and corridor classification

The study focused on selecting representative road segments for air quality monitoring across four regions in California: San Francisco - San Mateo, Alameda - Contra Costa, Central Valley, and Southern California. Within each region, three corridor types were identified: Goods Movement Corridors, Non-Goods Movement Corridors, and Control Areas (Suet al. 2020). For each corridor type, 50 road segments were selected, leading to a total of 150 segments per region. The goal was to reduce data redundancy by selecting a subset of road segments that best represented the variability in air pollution levels across the regions.

Data preparation

Three key GIS layers were utilized to guide the selection of representative road segments:

1. **Residential land use:** This layer identified residential zones within the study regions. The selection process aimed to include road segments near residential areas to ensure that the air quality data would reflect pollution exposure in these sensitive areas.
2. **Long-term NO_2 pollution surface (Suet al. 2020):** This layer depicted the distribution of NO_2 concentrations across the regions. The selection process prioritized road segments

located in areas with significant NO_2 gradients, ensuring that segments in higher pollution areas were well-represented.

3. **Road network segments:** This layer detailed all road segments within each region. All segments included had more than 100 mobile measurements, and the objective was to select a representative subset, thereby reducing redundancy while maintaining the integrity of the spatial coverage of air pollution monitoring.

Location-allocation algorithm in ArcGIS

The ArcGIS location-allocation algorithm (Kanaroglouet al. 2005) was used to optimize the selection of road segments. The algorithm was configured to balance the need for comprehensive coverage of air pollution variability with the desire to reduce data redundancy. The key steps involved in the algorithm's application included:

- **Objective function:** The algorithm aimed to minimize the sum of squared deviations of air pollution gradient between the selected subset of road segments and the entire set of available data points. This ensured that the selected segments were as representative as possible of the region's air quality conditions.
- **Constraints:** The algorithm was constrained to select 50 road segments for each of the three corridor types per region. The segments were chosen to maximize coverage of residential areas, capture significant NO_2 gradients, and ensure that selected segments were distributed across various road types, including major highways and local streets.
- **Iteration and optimization:** The algorithm iteratively assessed different combinations of road segments, optimizing for representativeness and data reduction. The final selection balanced spatial distribution, pollution variability, and proximity to residential areas.

Results

The above methodology was applied across the four study regions: San Francisco - San Mateo, Alameda - Contra Costa, Central Valley, and Southern California. The selected road segments in each region provided a representative sampling of air pollution levels while significantly reducing data redundancy. In each region, 50 road segments were selected within the Goods Movement Corridors, 50 within the Non-Goods Movement Corridors, and 50 within the Control Areas, totaling 150 road segments per region.

The selection result for the Alameda - Contra Costa region is presented in Figures Suppl 1, which display the spatial distribution of the three input layers and the chosen road segments. These figures illustrate how the selected segments cover key residential areas, capture critical pollution gradients, and reflect the diverse road types present in a study area. The selection process effectively reduced data redundancy while maintaining a robust representation of air quality across the study regions.

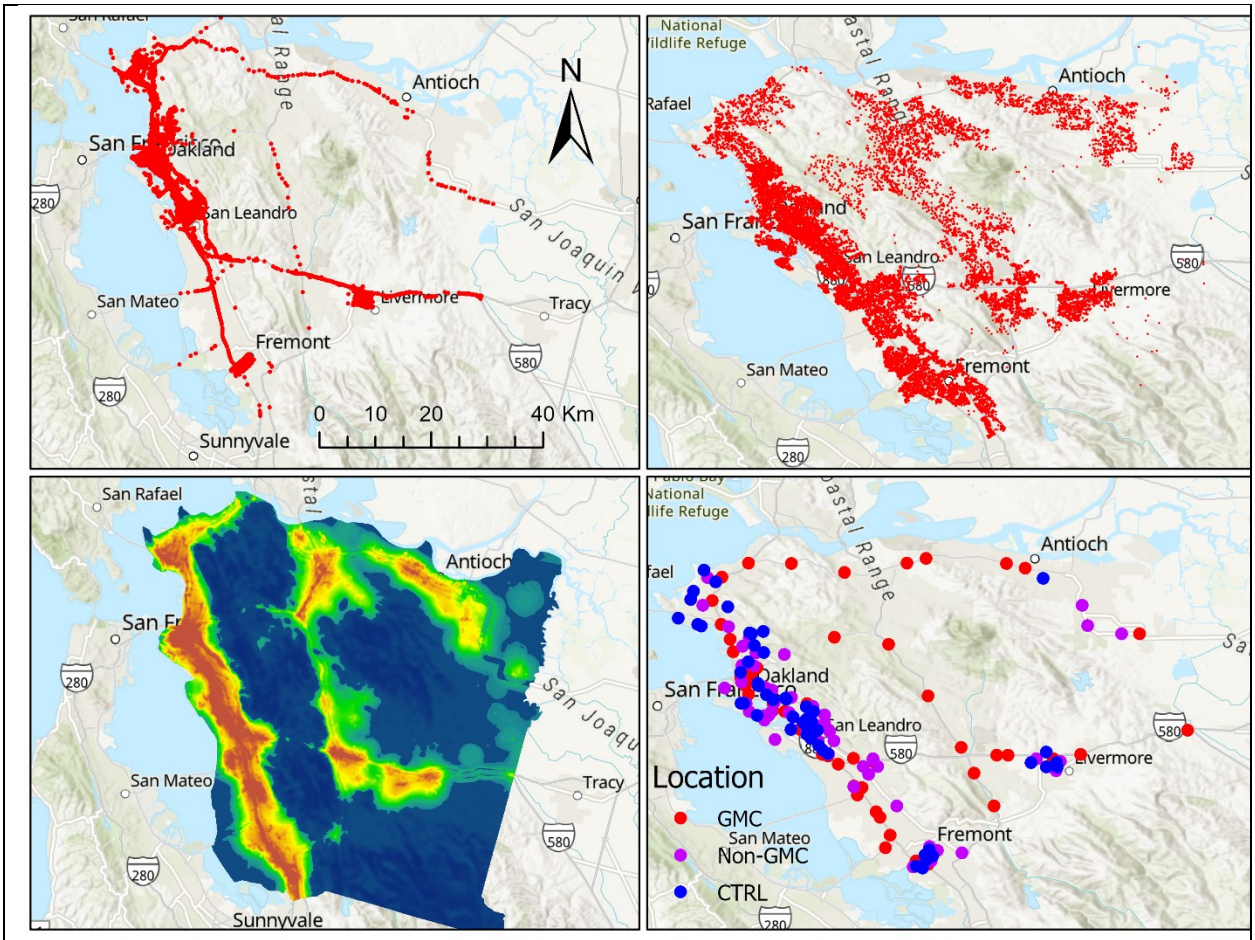

Figure Suppl 1. Location-allocation algorithm selection of Google Streetcar mobile measurement road segments (top left: road segments with at least 100 mobile measurements; top right: residential land use; bottom left: long-term NO2 surface; bottom right: chosen locations of road segments).

Deriving traffic data across the State

Traffic interpolation process

We used the data collected by the California Department of Transportation (Caltrans) Performance Measurement System (PeMS) to derive roadway daily and annual traffic. PeMS data are collected in real-time from nearly 40,000 individual detectors spanning the freeway system across all major metropolitan areas of the State of California and provide an Archived Data User Service that provides over fifteen years of data for historical analysis. The detector measured traffic flow covered ~5 % highway segments and we summed hourly traffic to daily traffic for all the stations across California. The following interconnected steps were then used to derive daily traffic for all the California highways for the observation period (2005-2021):

1. For a road segment with station traffic measure for a day, use all the station traffic measures on that road segment to generate a daily mean traffic for that road segment for that day.
2. For those road segments without traffic measures for a day, assign them using the assigned segments from step 1 by matching route, county, district (Figure Suppl 2), route type and day, and find the one with the smallest distance if having multiple matches. California has 58 counties which are included in one of the 12 air districts. Highways in California are split into at least four different types of systems: Interstate Highways, U.S. Highways, state highways, and county highways.
3. For those road segments without traffic being assigned from steps 1 & 2, assign them using the assigned segments from steps 1 & 2 by matching route, district, route type and day, and find the one with the smallest distance if having multiple matches. In this step county was not used as a restricting factor in daily traffic assignment.
4. For those road segments without traffic being assigned from the above steps, assign them using the above assigned segments by matching route, county, district and route type, plus at most one day difference in data availability and find the one with the smallest distance if having multiple matches.
5. Identify those not assigned and assign them using the assigned segments from above steps by matching county, district, route type and day and find the one with the smallest distance if having multiple matches. Here we removed the restricting factor of route number.
6. Identify those not assigned and assign them using the assigned segments from the above steps by matching district, route type and day and find the one with the smallest distance if having multiple matches. Here we removed the restricting factors of route number and county.

7.1 Identify those not assigned and assign them using the assigned state highway segments from the above steps by matching district and day. Here we removed the restricting factors of route number, route type and county.

7.2 Identify those not assigned and assign them using the assigned U.S. highway segments from the above steps by matching district and day. Here we removed the restricting factors of route number, route type and county.

7.3 Identify those not assigned and assign them using the assigned interstate highway segments from the above steps by matching district and day. Here we removed the restricting factors of route number, route type and county.

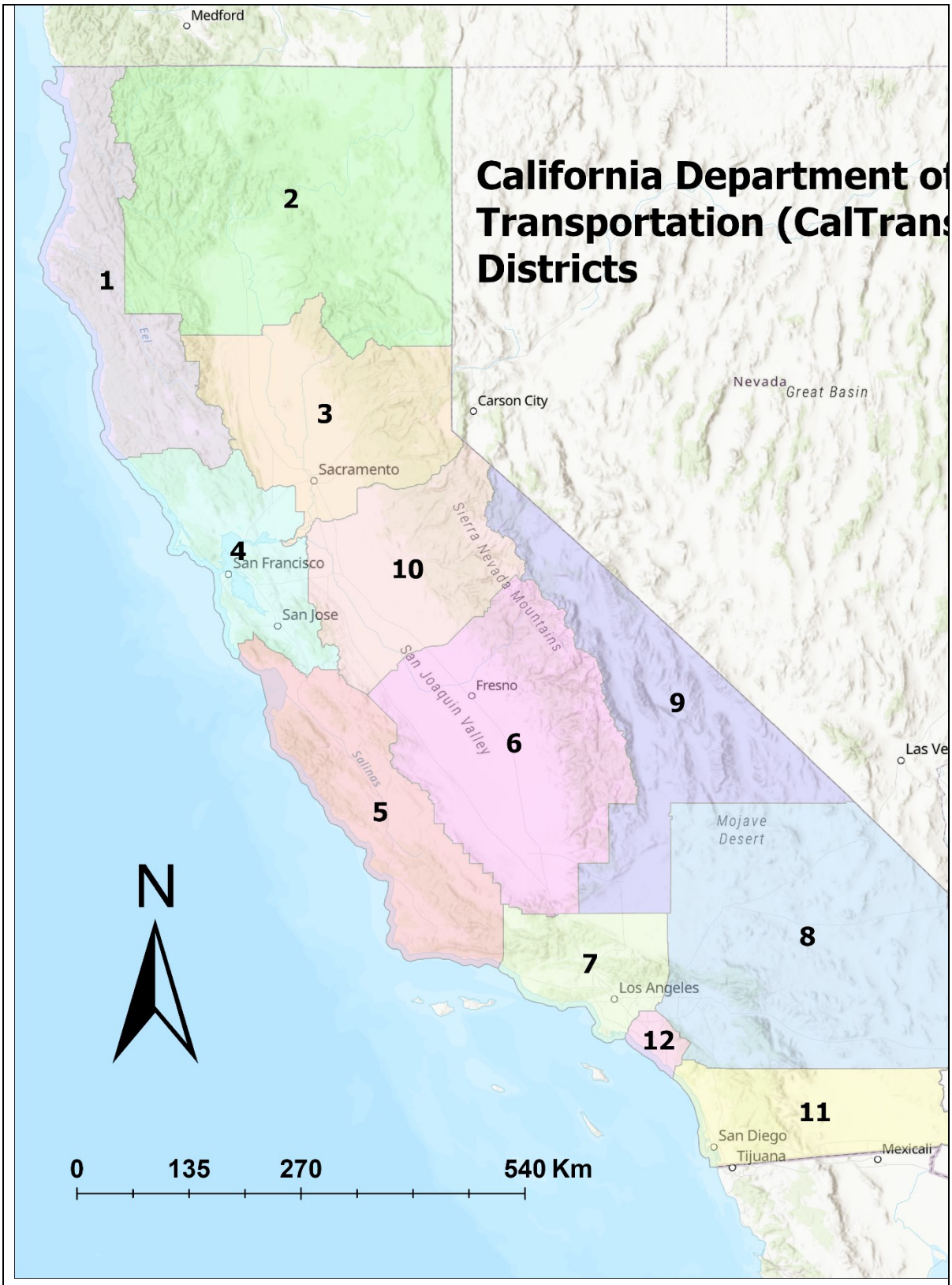

Figure Suppl 2. California Department of Transportation (CalTrans) Districts.

8. Identify those not assigned and assign them using the assigned segments from steps 1-4 by matching district and season to find the one with the smallest distance if having multiple matches. Here route number, county and route type are not required to match.

Traffic assignment results

The road segment (RS) assignment process across the districts shows distinct patterns and stages (Table Suppl 2), with the majority of assignments occurring during Stages 3, 5, and 7.1. Districts 1, 2, and 9, which lacked traffic station measures, were assigned similarly to their neighboring districts 4, 3, and 8, respectively, ensuring consistency in the process.

In District 1, a significant portion of RS assignments (58.91%) took place during Stage 3, with only a small fraction (1.11%) assigned in Stage 7.1. Similarly, District 2 saw the bulk of its RS assignments (72.58%) in Stage 3, with no further assignments after Stage 4. District 3 followed a more spread-out pattern, with key assignments in Stages 5, 6, and 7.1. District 4, on the other hand, concentrated most of its assignments (42.79%) in Stage 5, with an additional 7.69% assigned in Stage 7.1.

District 5 differed slightly, with a significant portion (65.21%) of RS assignments occurring in Stage 6, and only 0.17% in Stage 7.2. District 6 focused its efforts primarily in Stage 5, where 60.60% of assignments were made, followed by 6.53% in Stage 7.1. In District 7, the major assignments were completed early, primarily in Stages 1, 2 and 5, with no assignments in Stage 7. District 8 spread its assignments across various stages, but with 73.34% occurring in Stage 5.

District 9, which started its assignments later, completed the majority (45.95%) in Stage 3 and the remaining 54.05% in Stage 7.1. District 10 concentrated most of its assignments (36.39%) in Stage 5, with minimal activity afterward. In District 11, the assignment process was front-loaded, with 39.65% of RS assignments occurring in Stage 2, and 26.01% in Stage 5. Finally, District 12 saw significant early-stage activity, with most assignments completed by Stage 5 and none beyond that.

This step-by-step process ensured that nearly all RS were accounted for, reflecting the structured and methodical approach taken across the different regions.

Table Suppl 2. Traffic data assignment statistics based on the stages of assignment.

	District #1				District #2				District #3			
Stage	RS (#)	RS (%)	Cum RS (#)	Cum RS (%)	RS (#)	RS (%)	Cum RS (#)	Cum RS (%)	RS (#)	RS (%)	Cum RS (#)	Cum RS (%)
1	34,197	2.93	34,197	2.93	64,284	4.94	64,284	4.94	75,002	4.41	75,002	4.41
2	774	0.07	34,971	3.00	0	0.00	64,284	4.94	142,554	8.38	217,556	12.79
3	686,788	58.91	721,759	61.91	943,806	72.58	1,008,090	77.53	68,950	4.05	286,506	16.85
4	431,122	36.98	1,152,881	98.89	292,200	22.47	1,300,290	100.00	1,548	0.09	288,054	16.94
5	0	0.00	1,152,881	98.89					704,938	41.45	992,992	58.39
6	0	0.00	1,152,881	98.89					503,072	29.58	1,496,064	87.97
7.1	12,997	1.11	1,165,878	100.00					204,540	12.03	1,700,604	100.00
	District #4				District #5				District #6			
Stage	RS (#)	RS (%)	Cum RS (#)	Cum RS (%)	RS (#)	RS (%)	Cum RS (#)	Cum RS (%)	RS (#)	RS (%)	Cum RS (#)	Cum RS (%)
1	360,864	17.08	360,864	17.08	19,666	1.44	19,666	1.44	53,408	3.51	53,408	3.51
2	371,428	17.58	732,292	34.66	83,650	6.14	103,316	7.59	269,068	17.67	322,476	21.18
3	257,311	12.18	989,603	46.84	133,864	9.83	237,180	17.42	107,284	7.05	429,760	28.23
4	2,560	0.12	992,163	46.96	430	0.03	237,610	17.45	552	0.04	430,312	28.27
5	903,900	42.79	1,896,063	89.75	229,642	16.86	467,252	34.32	922,574	60.60	1,352,886	88.87
6	28,870	1.37	1,924,933	91.12	887,904	65.21	1,355,156	99.52	70,128	4.61	1,423,014	93.47
7.1	162,368	7.69	2,087,301	98.8	4,144	0.30	1,359,300	99.83	99,348	6.53	1,522,362	100.00
7.2	0	0.00	2,087,301	98.8	2,352	0.17	1,361,652	100.00				
7.3	0	0.00	2,087,301	98.8								
8	25,305	1.20	2,112,606	100								
	District #7				District #8				District #9			
Stage	RS (#)	RS (%)	Cum RS (#)	Cum RS (%)	RS (#)	RS (%)	Cum RS (#)	Cum RS (%)	RS (#)	RS (%)	Cum RS (#)	Cum RS (%)
1	288,852	25.03	288,852	25.03	68,864	5.82	68,864	5.82	0	0.00	0	0.00
2	315,340	27.32	604,192	52.35	94,562	7.99	163,426	13.81	0	0.00	0	0.00

3	23,360	2.02	627,552	54.37	87,600	7.40	251,026	21.21	198,696	45.95	198,696	45.95
4	466	0.04	628,018	54.41	194	0.02	251,220	21.23	0	0.00	198,696	45.95
5	526,172	45.59	1,154,190	100	867,906	73.34	1,119,126	94.57	0	0.00	198,696	45.95
6					0	0.00	1,119,126	94.57	0	0.00	198,696	45.95
7.1					64,284	5.43	1,183,410	100.00	233,760	54.05	432,456	100.00
	District #10				District #11				District #12			
Stage	RS (#)	RS (%)	Cum RS (#)	Cum RS (%)	RS (#)	RS (%)	Cum RS (#)	Cum RS (%)	RS (#)	RS (%)	Cum RS (#)	Cum RS (%)
1	146,644	9.80	146,644	9.80	241,134	23.85	241,134	23.85	160,898	38.24	160,898	38.24
2	438,638	29.32	585,282	39.12	400,820	39.65	641,954	63.50	139,650	33.19	300,548	71.43
3	352,216	23.54	937,498	62.66	105,120	10.40	747,074	73.89	0	0.00	300,548	71.43
4	2,288	0.15	939,786	62.82	990	0.10	748,064	73.99	290	0.07	300,838	71.50
5	544,392	36.39	1,484,178	99.21	262,948	26.01	1,011,012	100.00	119,930	28.50	420,768	100.00
6	11,886	0.79	1,496,064	100.00								

Note: RS= road segment; Cum RS=cumulative road segments; District 1, 2 and 9 had no traffic station measures and were treated the same as respectively neighboring districts in 4, 3 and 8.

pollutant	lag	estimate	lower_ci	upper_ci	mean	std	iqr
NO2	0	1.017885	1.016854	1.018917	10.64714	6.217118	8.010617
	1	1.017726	1.016694	1.018759	10.51736	6.221056	8.034553
	2	1.015573	1.01454	1.016607	10.36097	6.22401	8.063132
	3	1.010704	1.009673	1.011736	10.36872	6.220576	8.058235
PM2.5	0	1.008438	1.007591	1.009285	9.800294	3.364875	3.631014
	1	1.007223	1.006377	1.00807	9.797528	3.371929	3.63582
	2	1.004505	1.003658	1.005353	9.792482	3.369079	3.637908
	3	1.005531	1.004683	1.006379	9.792989	3.369946	3.637938
O3	0	1.018056	1.017105	1.019009	38.43722	6.836388	10.25059
	1	0.991131	0.990391	0.991871	38.50702	6.844785	10.26532
	2	0.995518	0.994776	0.996261	38.58592	6.852038	10.27377
	3	0.999382	0.998638	1.000126	38.58128	6.854859	10.26498

Appendix A: Derivation of Potential Impact Fraction Equation

Here we derive

$$PIF = 1 - \frac{1}{OR_{IQR}}$$

where *PIF* is the potential impact fraction and OR_{IQR} is the interquartile odds-ratio from a given conditional logit exposure-response function (ERF) under the assumption that the odds-ratio does not overstate the risk ratio since the outcome is sufficiently rare: $RR_{IQR} \approx OR_{IQR}$. We start with definitions presented in Barendregt and Veerman (BV) (2010). Starting with the distribution shift equation (in our case this would be an interquartile shift) for the *PIF* (BV eq. 5);

$$PIF = \frac{\int_l^h RR(x)P(x)dx - \int_l^h RR(x)P^*(x)dx}{\int_l^h RR(x)P(x)dx}$$

where *h* and *l* are high and low integration boundaries and the *RR* is log-linear (BV eq. 7):

$$RR(x) = \exp\,(a + bx)$$

and *P* is the ZIP code population weight and a counterfactual uniform reduction (Δ) in exposure (interquartile) is represented as

$$P^*(x) = P(x + \Delta).$$

Then we can use BV eq. (5) and eq. (7) to derive our final equation.

Let

$$D = \int_l^h RR(x)P(x)dx$$

where *D* is just to compress this expression for use in later equations. Then the counterfactual integral is the following:

$$\int_l^h RR(x)P^*(x)dx \;=\; \int_l^h RR(x)P(x + \Delta)dx.$$

Substitute $u = x + \Delta$, so $x = u - \Delta$ and $dx = du$:

$$\int_l^h RR(x)P(x + \Delta)dx = \int RR(u - \Delta)P(u)du.$$

.

Then using the log-linear *RR* assumption above (BV eq. 7) and substituting similarly:

$$RR(u - \Delta) = \exp\big(a + b(u - \Delta)\big) = \exp(a + bu)\exp(-b\Delta) = RR(u)\exp\,(-b\Delta).$$

Therefore

$$\int RR(u-\Delta)P(u)du = \exp(=b\Delta)\int RR(u)P(u)du = \exp(-b\Delta)\,D.$$

We then put this back into the earlier *PIF* equation (BV eq. 5):

$$PIF = \frac{D-\exp(-b\Delta)D}{D} = 1-\exp(-b\Delta).$$

Then, since the model is log-linear in exposure, the relative risk for an increase of Δ is as follows:

$$RR_{\Delta} = \exp(b\Delta).$$

Therefore

$$1-\exp(-b\Delta) = 1-\frac{1}{\exp(b\Delta)} = 1-\frac{1}{RR_{\Delta}}$$

If we set $\Delta = IQR$ then

$$PIF = 1-\frac{1}{RR_{IQR}}$$

Then, since we have assumed $RR_{IQR} \approx OR_{IQR}$

$$PIF = 1-\frac{1}{OR_{IQR}}$$

Reference

Barendregt, J. J., & Veerman, J. L. (2010). Categorical versus continuous risk factors and the calculation of potential impact fractions. *J Epidemiol Community Health*, *64*(3), 209–212. https://doi.org/10.1136/jech.2009.090274

Appendix B: Derivation of Standard Errors Using the Delta Method

We start with the odds-ratios and their 95% confidence intervals from the equations listed in the report and mean medical expenditures and their 95% confidence intervals from the IHME data cited in the report. This derivation is adapted from the concepts in Oehlert (1992).

Let $\widehat{OR}$ be OR_{IQR}, with lower and upper 95% confidence intervals (CI): OR_L, OR_U.
Define

$$\hat{\theta}=\log(\widehat{OR})$$

If the reported CI is the usual Wald CI on the log scale, then the standard error of θ

$$SE_\theta \approx \frac{\log(OR_U) - \log(OR_L)}{2\ x\ 1.96}$$

which is the standard inversion of the Wald CI to recover an *SE*.

Similarly, let $\widehat{ME}$ be mean medical expenditures with lower and upper 95% confidence intervals (CI): ME_L, ME_U. If the CI was computed as $\widehat{ME} \pm 1.96\ SE_{ME}$, then

$$SE_{ME} \approx \frac{ME_U - ME_L}{2\ x\ 1.96}$$

using the same inversion approach.

The point estimate for the avoided medical expenditure impact is

$$\widehat{AME} = \widehat{PIF}\ x\ \widehat{ME}$$

We then define a smooth function

$$AME(\theta, ME) = \left(1 - e^{-\theta}\right)ME$$

The multivariate delta method gives

$$Var(AME) \approx \left(\frac{\partial AME}{\partial \theta}\right)^2 Var(\theta) + \left(\frac{\partial AME}{\partial ME}\right)^2 Var(ME) + 2\left(\frac{\partial AME}{\partial \theta}\right)\left(\frac{\partial AME}{\partial ME}\right) Cov(\theta, ME)$$

evaluated at $(\widehat{\theta}, \overline{ME})$

Here the derivatives are as follows:

$$\frac{\partial AME}{\partial \theta} = ME e^{-\theta} = \frac{ME}{OR}, \qquad \frac{\partial AME}{\partial ME} = 1 - e^{-\theta} = PIF$$

Thus,

$$Var(AME) \approx \left(\frac{\widehat{ME}}{\widehat{OR}}\right)^2 SE_\theta^2 + \widehat{PIF}^2 SE_{ME}^2 + 2\left(\frac{\widehat{ME}}{\widehat{OR}}\right)\widehat{PIF}\ Cov(\theta, ME)$$

However, to the extent it is reasonable to assume that our estimation errors are to some extent independent, we can assume that $Cov(\theta, ME) \approx 0$.
Thus,

$$SE_{AME} \approx \sqrt{\left(\frac{\widehat{ME}}{\widehat{OR}}\right)^2 SE_\theta^2 + \widehat{PIF}^2 SE_{ME}^2}$$

and the Wald 95% CI is

$$\widehat{AME} \pm 1.96\ SE_{\widehat{AME}}$$

In the case of a mean calculated across mulitple years of data, we simply sum the relevant estimates and confidence intervals across years and then divide by the number of years. This is valid if we can reasonably assume that the annual estimates are independent.

Annual estimates can be assumed to be independent in repeated cross sections to the extent that samples do not rotate, reuse probability sampling units, or reuse the same individuals across years in a non-negligible manner. Confidence intervals will be biased downward to the extent these assumptions are violated.

Reference

Oehlert, G. W. (1992). A Note on the Delta Method. *The American Statistician*, *46*(1), 27–29. https://doi.org/10.1080/00031305.1992.10475842